

Final Technical Report for

**ENHANCED CHARACTERIZATION AND
REPRESENTATION OF FLOW THROUGH
KARST AQUIFERS — PHASE II
REVISION 1**

SwRI Project 20-11674

Prepared for

**Southwest Florida Water Management District
2379 Broad Street
Brooksville, FL 34604-6899
and
Edwards Aquifer Authority
1615 N. St. Mary's Street
San Antonio, TX 78215**

March 2007



**SOUTHWEST RESEARCH INSTITUTE®
SAN ANTONIO, TEXAS
WASHINGTON, DC**

Final Technical Report for

**ENHANCED CHARACTERIZATION AND
REPRESENTATION OF FLOW THROUGH
KARST AQUIFERS — PHASE II
REVISION 1**

SwRI Project 20-11674

Prepared for

**Southwest Florida Water Management District
2379 Broad Street
Brooksville, FL 34604-6899
and
Edwards Aquifer Authority
1615 N. St. Mary's Street
San Antonio, TX 78215**

Prepared by

**Scott L. Painter
Alexander Sun
Ronald T. Green**

**Geosciences and Engineering Division
Southwest Research Institute®
6220 Culebra Road
San Antonio, Texas 78238-5166**

March 2007

CONTENTS

| | |
|--|------|
| LIST OF TABLES | iv |
| LIST OF FIGURES | v |
| ACKNOWLEDGMENTS | viii |
| EXECUTIVE SUMMARY | ix |
| CHAPTER 1: INTRODUCTION | 1 |
| Background | 1 |
| Objectives | 1 |
| Scope | 2 |
| Project Tasks | 2 |
| Structure of the Technical Report | 4 |
| CHAPTER 2: MODFLOW-DCM VERSION 2.0 | 5 |
| Groundwater Flow Representation in MODFLOW | 5 |
| Dual-Conductivity Model | 6 |
| Conduit Flow Model | 7 |
| Simulation of Dry Cells | 9 |
| Newton-Raphson Solver | 11 |
| Validation Tests | 12 |
| CHAPTER 3: DCM MODEL OF THE BARTON SPRINGS SEGMENT OF THE EDWARDS AQUIFER | 22 |
| Background | 22 |
| Study Area and Hydrogeological Setting | 22 |
| The BSEACD MODFLOW Model | 23 |
| Conduit Representation in the MODFLOW-DCM Model | 24 |
| Steady-state MODFLOW-DCM Model | 24 |
| Transient MODFLOW-DCM Model for the Period 1989–1998 | 25 |
| Sensitivity Analysis for the Transient Model | 27 |
| MODFLOW-DCM Simulations of Drought Periods | 28 |
| CHAPTER 4: DCM MODEL OF THE SANTA FE RIVER SINK/RISE SYSTEM OF THE FLORIDAN AQUIFER | 47 |
| Background | 47 |
| Climate | 47 |
| Geology | 48 |
| Physiography | 48 |
| Recharge | 49 |
| Hydrology | 50 |
| Hydraulic Relationship between the Conduit and the Matrix | 53 |
| Numerical Model | 56 |

| | |
|--|----|
| Conduit-flow Groundwater Flow Model | 56 |
| Transient-state Model | 60 |
| Base Case | 61 |
| Case I: Effect of Recharge Rates | 62 |
| Case II: Effect of Transient Boundary Conditions | 62 |
| Case III: Effect of Matrix/Conduit Exchange Parameter | 62 |
| Conclusions | 63 |
| CHAPTER 5: CONCLUSIONS | 84 |
| Development of Modeling Tool for Karst Aquifers—Phase II | 84 |
| Future Development of Karst Modeling Tools | 89 |
| REFERENCES | 90 |
| APPENDICES | |
| A Input Instructions for the MODFLOW-DCM Package | |

TABLES

| | | |
|-----|--|----|
| 2.1 | Parameters for the dual-conductivity validation test | 15 |
| 2.2 | Parameters for the unconfined flow validation test | 15 |
| 2.3 | Parameters for the turbulent flow validation test..... | 15 |
| 3.1 | Calibrated hydraulic conductivity for conduits in the reference steady state model | 29 |
| 4.1 | Monthly precipitation values (inches) for 2001—2003 and the mean precipitation values for 1948—2005 at High Springs, Florida | 65 |
| 4.2 | Stratigraphic and hydrostratigraphic units of the Santa Fe River Basin..... | 65 |
| 4.3 | Recharge (in) estimated as a percentage (34%) of precipitation measured at High Springs, Florida..... | 65 |
| 4.4 | Calculated and measured steady-state water levels in the wells used for calibration..... | 66 |
| 4.5 | Stress periods used in transient simulation | 66 |
| 4.6 | Stress periods and timesteps used in transient simulation | 66 |
| 4.7 | Averaged water levels measured during the University of Florida study..... | 67 |

FIGURES

| | | |
|-----|---|----|
| 2.1 | Hypothetical cross sections illustrating the range of applicability of MODFLOW-DCM. MODFLOW-DCM will model a single-layer aquifer containing a single-level conduit system, as in (a). MODFLOW-DCM will not model a multilevel conduit system like that shown in (b), or a multiple layer aquifer similar to the ones shown in (c). | 16 |
| 2.2 | Configuration for the dual-conductivity validation test..... | 17 |
| 2.3 | Results of the dual-conductivity validation test at $t=20$ minutes. The benchmark results are shown as solid lines and the DCM results as individual data points..... | 18 |
| 2.4 | Results of the unconfined flow validation test (Test 2) at $t = 1, 10,$ and 60 minutes. The hydraulic heads in the conduit as calculated by the standard MODFLOW LPF package are shown as solid lines and the DCM results as individual data points..... | 19 |
| 2.5 | Steady-state results for the unconfined flow validation test (Test 2a). This simulation was used to verify that water balance is properly maintained in the DCM package | 20 |
| 2.6 | Results of the turbulent flow validation test (Test 3) at $t=5, 10,$ and 20 minutes for critical gradient of 0.01 (a) and 0.1 (b). Benchmark results are shown as solid lines and results of MODFLOW-DCM Version 2.0 are shown as individual data points | 21 |
| 3.1 | Study area for the Barton Springs model. The model domain is illustrated within the black box in the insert..... | 30 |
| 3.2 | Diffuse layer bottom elevation and thickness..... | 31 |
| 3.3 | Conduit locations inferred from tracer test results (Hunt <i>et al.</i> , 2006)..... | 32 |
| 3.4 | Locations of modeled conduits in the DCM model of Barton Springs..... | 33 |
| 3.5 | Bottom elevation for the conduit layer | 34 |
| 3.6 | Recharge locations and steady-state recharge values for the Barton Springs model..... | 35 |
| 3.7 | Pumping locations for the Barton Springs model..... | 36 |
| 3.8 | Locations of steady-state hydraulic head observations for calibrating the Barton Springs steady-state model are denoted with dots | 36 |

| | | |
|------|--|----|
| 3.9 | Crossplot of observed and simulated hydraulic heads for the Barton Springs steady-state model..... | 37 |
| 3.10 | Diffuse and conduit hydraulic heads in the Barton Springs steady-state model..... | 38 |
| 3.11 | Recharge at selected locations for the period 1989—1998 | 39 |
| 3.12 | Pumping for the period 1989—1998 | 40 |
| 3.13 | Water level at three selected times..... | 41 |
| 3.14 | Barton Springs discharge versus time..... | 42 |
| 3.15 | Groundwater elevation hydrographs for three wells..... | 43 |
| 3.16 | Barton Springs discharge for the period 1989 to 1998 for three values of the critical gradient | 44 |
| 3.17 | Barton Springs discharge for the period 1989 to 1998 for two different values of the exchange parameter..... | 45 |
| 3.18 | Revised conduit bottom elevation used in the drought-condition simulations | 46 |
| 3.19 | Barton Springs simulated discharge hydrographs for hypothetical drought conditions | 46 |
| 4.1 | Study area of the Santa Fe River Sink/Rise system..... | 68 |
| 4.2 | Precipitation measured at O’Leno State Park (cm) for the period June 2001 to June 2003 | 69 |
| 4.3 | Estimates of monthly potential evapotranspiration (cm) versus precipitation (cm) for the period of April 2002 to May 2003..... | 70 |
| 4.4 | Estimates of monthly recharge (cm) for the period of April 2002 to May 2003 | 70 |
| 4.5 | Model extent of the Santa Fe River Sink/Rise system..... | 71 |
| 4.6 | Water elevations (ft, msl) measured at the River Sink and River Rise, and at the Tower, and 4, and High Springs wells, and at Sweetwater Lake from December 2002 through March 2003..... | 72 |
| 4.7 | Water elevations (ft, msl) measured in the Santa Fe River at the Highway 441 Bridge and at the Well S081703 during the period of December 13, 2002, to March 31, 2003 | 73 |

| | | |
|------|---|----|
| 4.8 | Water-level elevations (ft, msl) measured in the Santa Fe River at the Highway 441 Bridge and at Well 081703 from March 10, 2003, to March 20, 2003 | 74 |
| 4.9 | Calcite saturation index and river discharge measurements for the Santa Fe River at Worthington, Florida, and High Springs, Florida | 75 |
| 4.10 | Water-level elevations at the River Sink and River Rise (after Martin, 2003)..... | 76 |
| 4.11 | Steady-state base case diffuse continuum hydraulic head distribution..... | 77 |
| 4.12 | Transient base case diffuse continuum hydraulic head distribution during peak discharge | 78 |
| 4.13 | Transient River Sink (a) and River Rise (b) elevation for days after start of stress periods (January 22, 2003)..... | 79 |
| 4.14 | River Rise discharge after start of stress periods (January 22, 2003) for the transient base case simulation..... | 80 |
| 4.15 | Transient base case: simulated versus measured heads (ft) in the calibration wells | 81 |
| 4.16 | Case III. Contour map of the transient head distribution during peak discharge in the diffuse continuum with a reduction in the matrix/conduit exchange parameter α_0 from 1.0 to 0.01 | 82 |
| 4.17 | Case III. Simulated versus measured heads (ft) in the calibration wells for reduction in the matrix/conduit exchange parameter α_0 from 1.0 to 0.01 | 83 |

ACKNOWLEDGMENTS

The authors of this report thank Edwards Aquifer Authority and Southwest Florida Water Management District for supporting this work. The authors acknowledge Dr. Philippe Dubreuilh and Dr. David Ferrill for careful reviews of the report. The authors are also grateful to Ms. Lauren Mulverhill for editing and to Ms. Cheryl Patton for formatting the report. The authors gratefully acknowledge review comments by Ms. Melissa Hill, Mr. Angel Martin, and Mr. David DeWitt with the Southwest Florida Water Management District and Mr. Steve Johnson and Mr. Geary Schindel with the Edwards Aquifer Authority that were incorporated in Revision 1 of the Final Report.

The authors gratefully acknowledge the generous support by Dr. Brian Smith, Mr. Brian Hunt, and Mr. Joe Beery with the Barton Springs—Edwards Aquifer Conservation District and Mr. Nico Hauwert with the City of Austin for providing data and technical assistance with the Barton Springs Segment of the Edwards Aquifer.

The authors gratefully acknowledge the generous support by Dr. Liz Screaton and Dr. Jon Martin with the University of Florida and Ms. Megan Wetherington and Mr. John Good with the Suwannee River Water Management District for providing data and technical assistance with the Santa Fe River Sink/Rise system. The authors also gratefully acknowledge Mr. Michael Poucher for providing valuable survey data from numerous cave mapping expeditions of the Santa Fe River Sink/Rise System. Discussions with Drs. Sam Upchurch and Jim Schneider of SDII-Global were very helpful in understanding the regional and local Floridan Aquifer flow systems. Mr. Paul Bertetti is gratefully acknowledged for his assistance with the water quality and calcite saturation analyses of Santa Fe River Sink/Rise system water.

This report is an independent product of the Geosciences and Engineering Division (GED) of Southwest Research Institute® and does not necessarily reflect the views or positions of the funding organizations.

QUALITY ASSURANCE STATEMENT

No GED-generated original data are contained in this report. The analyses contained in this report are documented according to GED quality assurance procedures in Scientific Notebooks SN660E and SN634E.

EXECUTIVE SUMMARY

In 2003, Southwest Research Institute[®] (SwRI) initiated a long-term project to develop new modeling approaches and tools to address applications involving karst aquifers with significant conduit flow. Phase I of the project identified key considerations for modeling karst aquifers, evaluated existing modeling approaches, and selected an approach for detailed investigation and development. To meet the modeling needs, DCM Version 1.0, a dual-conductivity model for MODFLOW, was developed. The first application using DCM enhanced an existing MODFLOW model for the Barton Springs segment of the Edwards Aquifer. Reasonable replication of the conduit/matrix flow system was achieved in terms of matching hydraulic heads and spring discharge.

Phase II of the karst modeling project was commissioned by the Edwards Aquifer Authority and the Southwest Florida Water Management District and initiated in mid-2005. The objective of Phase II was to enhance the karst modeling approach that was developed during Phase I and assess the capability and limitations of DCM by applying it to two karst aquifers that exhibit contrasting hydrogeologic characteristics: the Barton Springs segment of the Edwards Aquifer in south-central Texas and the Santa Fe River Sink/Rise system of the Floridan Aquifer in north-central Florida.

Continued modeling of the Barton Springs segment using DCM revealed poor numerical performance and even convergence failures when the large topographic relief of the recharge zone was incorporated into the model. During Phase II, it was discovered that the current solver routines in the standard MODFLOW package are inadequate to support the DCM approach. A new solver capable of solving the highly nonlinear systems associated with the conduit/matrix flow regime under confined/unconfined conditions was developed. The new solver is based on the Newton-Raphson method and requires derivative information from active MODFLOW packages. The derivative information is beyond that currently provided by the MODFLOW groundwater flow packages. Because of this new data requirement, the resulting dual-conductivity model could not be implemented as a self-contained package, and it was necessary to modify multiple packages. Therefore, a new MODFLOW variant, MODFLOW-DCM Version 2.0, was created.

Additional enhanced attributes in MODFLOW-DCM Version 2.0 include the ability to transition between turbulent and laminar flow and a new algorithm for simulating dry cells. MODFLOW-DCM is appropriate for two-dimensional karst aquifers, although information in the vertical dimension, namely aquifer and conduit top and bottom elevations, is incorporated.

The Barton Springs model was completely revised in Phase II by incorporating site-specific groundwater hydraulic data and more detailed conduit characterization information. The model was successfully calibrated to hydraulic head and spring flows for steady and transient conditions. Sensitivities to major parameters were identified. MODFLOW-DCM successfully simulated the drying and rewetting of cells in the unconfined recharge zone of the Barton Springs model.

Sensitivity analyses were performed to test the laminar/turbulent flow transition and the sensitivity to the MODFLOW-DCM matrix/conduit exchange parameter. Sensitivity analysis indicated that the addition of the turbulence model resulted in an improved match to the dynamic spring hydrograph for Barton Springs and that the matrix/conduit exchange parameter can be tuned to allow for a better match of dynamic spring flow. Model results also highlighted the sensitivity of spring discharge to conduit elevation relative to matrix elevation. This important outcome confirms that conduit elevations influence flow during low-flow conditions because some conduits can become de-watered when water levels are sufficiently lowered. This feature enables the conduit elevations to be determined by model calibration during low-flow periods. The MODFLOW-DCM simulation of drought conditions appeared to better match hydraulic head and spring discharge rates than existing models that are predicated on porous media flow concepts.

MODFLOW-DCM was applied to the Santa Fe River Sink/Rise system in the Floridan Aquifer to test the ability of MODFLOW-DCM to simulate large flow karst systems with relatively high matrix permeability. Although the Santa Fe River Sink/Rise system was selected because there is extensive data on site characterization, it was necessary to develop a new MODFLOW model because the scale and resolution of existing models were inappropriate to test the ability of MODFLOW-DCM to match the dynamic hydraulics of the Santa Fe River Sink/Rise system. A relatively well-documented recharge event in March 2003 was used as the model target period. By virtue of the relatively short duration of the simulation period, model boundaries were prescribed as constant head. This assumption is clearly inappropriate for the long-term simulation of the modeled area, but was justified by the relatively short duration of the target recharge event and because there was inadequate information on the groundwater system.

The Floridan Aquifer model reasonably captured the basic hydraulic dynamics of the Santa Fe River Sink/Rise system in terms of water elevations at the River Sink and River Rise, discharge at the River Rise, and hydraulic head values at four calibration wells. Sensitivity analyses indicated that reductions in conduit conductivity and diffuse continuum conductivity did not have a significant effect on model performance, but that a reduction in the matrix/conduit exchange parameter produced a marked change in head values particularly in the diffuse continuum near the focused point of recharge in the model, the River Sink. Lack of head data from a calibration well in this area, however prevented definitive determination of the most appropriate value for this parameter in the Floridan Aquifer model. Better general agreement in head values indicated that a larger value (i.e., $\alpha_0=1.0$) for the matrix/conduit exchange parameter is probably more representative of the modeled system than a smaller value (i.e., $\alpha_0=0.01$).

The MODFLOW-DCM variant is completed and promises to provide significant improvements in modeling groundwater flow through conduits located within porous media. Interest has shifted from model development to model calibration and parameter estimation. It is clear that the efficient and effective application of MODFLOW-DCM to karst aquifers will hinge on using better methods to calibrate karst aquifer models and

estimate parameter values. Calibration is expected to be important for determining conduit properties such as conduit hydraulic conductivity, matrix/conduit exchange parameters, and the top and bottom elevations of conduits. Development of advanced calibration and parameter estimation tools and techniques will allow for quicker and better focused karst aquifer characterization.

CHAPTER 1

INTRODUCTION

BACKGROUND

It is estimated that the potable water needs of 25% of the world's population are mostly supplied by karst aquifers (Ford and Williams, 1989). In the United States, approximately 40% of the groundwater used for drinking comes from karst aquifers (Quinlan and Ewers, 1989). In spite of this large reliance on karst aquifers for water resources, water resource assessment tools appropriate for karst aquifers are inadequate and vastly inferior when compared with similar tools developed for porous media-type aquifers, such as sand and gravel deposits or sandstone reservoirs. In particular, groundwater modeling tools developed for porous media-type aquifers cannot accommodate both the rapid flow of groundwater through conduits and the slow flow and storage of groundwater in the matrix of karst aquifers.

To address this lack of combined matrix- and conduit-flow modeling tools, Southwest Research Institute[®] (SwRI) conducted a project in 2004 to develop tools to enhance characterization and representation of flow through karst aquifers. The project, referred to as the karst modeling project, was funded by the Awwa Research Foundation, the Southwest Florida Water Management District (SWFWMD), and the Edwards Aquifer Authority (EAA). Major activities of the project were completed in December 2004, and the final report was published in 2006 (Painter et al., 2006). The main product of the karst modeling project was the development of DCM Version 1.0, a MODFLOW package that simulates coupled conduit/diffuse flow systems. DCM denotes that the model was developed using a dual conductivity conceptualization. At the conclusion of the project, it was recognized that additional refinement and demonstration of the DCM package were required before making the module available for use by the technical community.

In 2005, the SWFWMD and EAA commissioned SwRI to enter a second phase of the karst modeling project to complete the necessary model refinements to DCM and perform demonstration activities to test the performance of the conduit modeling package. This report documents the progress of the second phase of the karst modeling project. Additional phases to development of tools for enhanced characterization and representation of flow through karst aquifers had not been identified at the time of the conclusion of the second phase.

OBJECTIVES

The long-term objective of the karst modeling project is to develop new modeling approaches and tools to address applications involving karst aquifers with significant conduit flow. The objective of the second phase is to enhance the karst modeling approach that was developed during the first phase of the project. The capability and limitations of the module are assessed by applying the module to two karst aquifers that exhibit contrasting hydrogeologic characteristics.

SCOPE

Following are the specific tasks of Phase II of the karst modeling project:

- Incorporate modeling enhancements into the two-dimensional version of DCM. Enhancements include the capability for laminar-turbulent flow transition and adaptive timestepping.
- Develop a user's manual that describes the usage and input/output elements of DCM that differ from standard MODFLOW (Banta, 2000).
- Complete the Barton Springs demonstration simulations using MODFLOW with the DCM package. The Barton Springs segment of the Edwards Aquifer is a karst aquifer with a relatively well-characterized conduit system.
- Perform Floridan Aquifer demonstration simulations. The Floridan Aquifer is a karst aquifer with relatively high matrix permeability when compared with the Edwards Aquifer.
- Collaborate with Environmental Simulations International to prepare a graphical user interface (GUI).
- Evaluate the need and feasibility for a three-dimensional version of DCM.
- Transfer technology to the funding agencies through technical interactions and workshops.

PROJECT TASKS

The project scope and task descriptions for Phase II were identified at the conclusion of Phase I. However, the scope and tasks were slightly modified during the execution of the project to overcome technical challenges. A summary of the task description modifications and accomplishments follows.

Task 1. Code Refinement. During the execution of this task, it was discovered that the current solver routines in the standard MODFLOW (Banta, 2000) package are inadequate to support the DCM approach. A new solver capable of solving the highly nonlinear systems associated with the conduit/matrix flow regime under confined/unconfined conditions was developed. The new solver is based on the Newton-Raphson method and requires information beyond that currently provided by the MODFLOW groundwater flow packages. Because of this additional information requirement, it was not possible to keep DCM as a self-contained MODFLOW package. Instead, a new MODFLOW variant, MODFLOW-DCM Version 2.0, was created. MODFLOW-DCM Version 2.0 is extremely robust – no convergence failures were encountered in extensive testing. This improved robustness of the new solver made it unnecessary to consider adaptive timestepping, which was originally in the project plan. In addition to the new solver and more robust formulation, MODFLOW-DCM Version 2.0 also represents the transition between turbulent and laminar flow. DCM Version 1.0 could only accommodate one flow regime or the other without providing for a transition between the two.

A User's Manual, consistent with the standard MODFLOW User's Manual, was developed to describe data input and entry. This report, in particular, Chapter 2: MODFLOW-DCM Version 2.0, provides detailed discussions on how the model variant operates. The User's Manual is included as an Appendix to this report.

Task 2. Barton Springs Demonstration Simulations. The application of DCM to the Barton Springs segment of the Edwards Aquifer was initiated during the first phase of the karst modeling project. The Barton Springs model was completely revised in Phase II by incorporating site-specific groundwater hydraulic data and more detailed conduit characterization information. The model was successfully calibrated to hydraulic head and spring flows in steady and transient conditions. Sensitivities to major parameters were identified.

Task 3. Floridan Aquifer Demonstration Simulations. MODFLOW-DCM was applied to a site in the Floridan Aquifer to test the ability of MODFLOW-DCM to simulate large flow karst systems with relatively high matrix permeability. The Santa Fe River Sink/Rise Spring system was selected as the Floridan Aquifer model site because there was an existing MODFLOW model and extensive data on tracer tests and hydraulic testing were available. Although the scope of this task was predicated on the assumption that there was a viable MODFLOW model for the Floridan Aquifer Demonstration Site, it became apparent that the scale and resolution of existing MODFLOW models were inappropriate to evaluate MODFLOW-DCM. It was decided to retain the Santa Fe River Sink/Rise system as the Floridan Aquifer test site and develop a new MODFLOW model, however, because of the extensive hydrogeological information available. Similar to the Barton Springs demonstration simulation, matching of model results to the physical system was evaluated in terms of hydraulic head, recharge rates, and spring and river flow.

Task 4. Subtask 4.1 — Preparation of a GUI With Environmental Simulations International; Subtask 4.2 — Evaluation of the Costs and Benefits of Developing a Three-Dimensional MODFLOW-DCM. This task consisted of two subtasks, with priority placed on Subtask 4.1, the preparation of a GUI in cooperation with Environmental Simulations International. Subtask 4.2 evaluated the development of a three-dimensional conduit flow model.

Subtask 4.1. This task coordinated the addition of a GUI for MODFLOW-DCM to Groundwater Vistas (ESI). SwRI provided specifications for the additional input data sets required for MODFLOW-DCM to Environmental Simulations International. Input for MODFLOW-DCM is identical to that of standard MODFLOW except that the standard MODFLOW solver packages are not relevant and a new DCM groundwater flow package must be active. Input to the DCM package is very similar to the LPF package. The DCM package takes no input relating to vertical flow or rewetting algorithms. Two new parameters describing conduit-diffuse exchange and turbulent flow are required. Because of the necessity to develop a solver routine external to the standard MODFLOW package, it was not possible to strictly adhere to U.S. Geological Survey guidance standards that seek to retain all modifications to singular packages. The final

product is a MODFLOW variant that includes modifications to all packages that incorporated nonlinear dependence on hydraulic head.

Subtask 4.2. The potential future development of a three-dimensional version of MODFLOW-DCM was considered and discussed during the project. Development of a three-dimensional version of a conduit model was not initiated during this phase of the karst modeling effort.

Task 5. Technical Exchanges, Reporting, and Meetings. There were two technical exchange meetings convened during the project. This comprehensive technical report documenting the project results was prepared at the conclusion of the project.

STRUCTURE OF THE TECHNICAL REPORT

This report is a summary of Phase II of the karst modeling project. Chapter 2 discusses the technical/mathematical basis for MODFLOW-DCM Version 2.0, including a description of the solver and software validation tests. The MODFLOW-DCM variant is applied to the Barton Springs Segment of the Edwards Aquifer and to the Santa Fe River Sink/Rise system in the Floridan Aquifer in Chapter 3 and 4, respectively. Chapter 5 provides conclusions to the project and a discussion of future research needs.

CHAPTER 2

MODFLOW-DCM VERSION 2.0

DCM Version 1.0, a dual-conductivity module for MODFLOW, was developed in Phase I of the karst modeling project. Version 1.0 was implemented as a self-contained module (“package” in the MODFLOW terminology). Numerical experiments undertaken as part of Phase I revealed poor numerical performance and even convergence failures for DCM Version 1.0. The numerical performance issue was resolved during the current phase of the project by the addition of a new solver for MODFLOW. The new solver, NR1, is based on the Newton-Raphson method and requires derivative information from active MODFLOW packages. Because of this new data requirement from the packages, NR1 could not be implemented as a self-contained package, and it was necessary to modify multiple packages. The result is a new MODFLOW variant denoted MODFLOW-DCM Version 2.0.

Input for MODFLOW-DCM follows the standard MODFLOW formats. To use MODFLOW-DCM, the user must specify the DCM groundwater flow package in the name file. Other groundwater flow packages (BCF, LPF, etc.) must not be specified. Required inputs for the DCM groundwater flow packages include conduit and diffuse system parameters, a matrix/conduit exchange parameter, and, optionally, one parameter required for the turbulence model. Conduits are defined by activating relevant MODFLOW cells and assigning hydraulic conductivity and storage parameters to each conduit cell. The NR1 solver is automatically activated. The user must not activate other solver packages.

Note that MODFLOW-DCM Version 2.0 is currently limited to single-layer aquifers. Thus, the software will model the situation shown in Figure 2.1(a), but not the multilevel configuration shown in Figure 2.1(b). To model the configuration shown in Figure 2.1(b) or an aquifer with multiple layers with disparate properties [Figure 2.1(c)], a three-dimensional version of the MODFLOW-DCM would be required.

This chapter summarizes the technical basis for MODFLOW-DCM Version 2.0. A review of the groundwater flow representation in MODFLOW is provided first. Subsequent sections describe the dual-conductivity representation, conduit flow model, simulation of dry cells, basis for the new solver, and software validation activities. Input formats for the DCM package and NR1 solver are provided in Appendix A.

GROUNDWATER FLOW REPRESENTATION IN MODFLOW

In MODFLOW, flow is conceptualized as occurring in an aquifer with multiple layers that may be stacked one upon the other. For a single layer using principal coordinates, the groundwater flow equations can be written

$$S(h)\frac{\partial h}{\partial t} = \frac{\partial}{\partial x}\left[T_x(h)\frac{\partial h}{\partial x}\right] + \frac{\partial}{\partial y}\left[T_y(h)\frac{\partial h}{\partial y}\right] + Q \quad h \in \Omega \quad (2-1)$$

where h [L] is hydraulic head, T_x (T_y) [L^2] is transmissivity in the x (y) direction, S [unitless] is a storage term, and Q [L/T] is the volumetric source term per unit area of the aquifer. Equation (2-1) applies for both confined and unconfined aquifers with appropriate definitions of the head-dependent parameters T and S . Specifically, let $Z^{top}(x, y)$ denote the elevation of the top of the aquifer and $Z^{bot}(x, y)$ the bottom elevation. The x -direction transmissivity is then written

$$\begin{aligned} T_x &= 0 & h &\leq Z^{bot} \\ T_x &= K_x(h - Z^{bot}) & Z^{bot} < h < Z^{top} \\ T_x &= K_x(Z^{top} - Z^{bot}) & h &\geq Z^{top} \end{aligned} \quad (2-2)$$

where K_x [L/T] is the x -direction hydraulic conductivity. The y -direction transmissivity is written similarly. For the storage term, the corresponding equation is

$$\begin{aligned} S &= 0 & h &\leq Z^{bot} \\ S &= S_Y & Z^{bot} < h < Z^{top} \\ S &= S_S(Z^{top} - Z^{bot}) & h &\geq Z^{top} \end{aligned} \quad (2-3)$$

where S_Y [unitless] is the specific yield and S_S [L^{-1}] is the specific storage.

DUAL-CONDUCTIVITY MODEL

In the conventional MODFLOW software, Equation (2-1) is solved over a specified region, Ω . For the dual-conductivity model, it is necessary to keep track of two hydraulic heads: one for the conduit and one for the diffuse system. Hydraulic head in the diffuse system is defined over the entire region, Ω , as in the single conductivity case. The conduit hydraulic head is defined only for those spatial locations that correspond to a conduit. To be more specific, consider a system of n conduits, and let Ψ_i denote the spatial region occupied by the i^{th} conduit. Let the subscript c denote the conduit system, so that the hydraulic head of the conduit system becomes h_c . Similarly, let a subscript m denote the diffuse, or matrix, system. The flow equations then become

$$S_m(h_m) \frac{\partial h_m}{\partial t} = \frac{\partial}{\partial x} \left[T_{mx}(h_m) \frac{\partial h_m}{\partial x} \right] + \frac{\partial}{\partial y} \left[T_{my}(h_m) \frac{\partial h_m}{\partial y} \right] + Q_m + \alpha(h_c, h_m)[h_c - h_m] \quad h_m \in \Omega \quad (2-4a)$$

$$S_c(h_c) \frac{\partial h_c}{\partial t} = - \frac{\partial}{\partial x} [q_{cx}] - \frac{\partial}{\partial y} [q_{cy}] + Q_c - \alpha(h_c, h_m)[h_c - h_m] \quad h_c \in \Psi \quad (2-4b)$$

where Ψ is the entire region occupied by all conduits $\Psi = \Psi_1 \cup \Psi_2 \cup \Psi_3 \dots \cup \Psi_n$. Note that while h_m is defined for the entire spatial region, Ω , h_c is defined only for region

Ψ , which is a subset of Ω . If Ω and Ψ correspond, the system of Equations (2-4a,b) is the dual-continuum model that is widely used in fractured rock modeling. For karst systems, the conduit network is generally not well represented as a continuum at the scale of interest, and the system of Equations (2-4a,b) represents a sparse network of conduits coupled to a continuum diffuse system. The transmissivity and storage terms in Equations (2-4a,b) are defined as in Equations (2-2) and (2-3), except that distinct top and bottom elevations may be used for the two flow systems: $Z_c^{top} \leq Z_m^{top}$ and $Z_c^{bot} \geq Z_m^{bot}$. The conduit flow terms q_{cx} and q_{cy} have been left in symbolic form in Equations (2-4a,b). These terms are defined in the next section of this report.

The final term in each equation in Equations (2-4a,b) represents the movement of fluid between the two systems, with α quantifying the strength of the linear exchange. If α is 0, the conduit and diffuse systems decouple, and flow in each system is independent. If the conduit is filled with water, α is simply a number, independent of the head. If the conduit is only partially filled, this value needs to be decreased to account for the fact that only a fraction of the conduit surface area is available to transmit water. Thus, to model unconfined aquifers, α should be dependent on the hydraulic head. The situation is further complicated because flow can be either from the conduit to the diffuse or vice versa, and the surface area available to transmit water depends on the flow direction. The simplest condition incorporating all of these constraints is the linear upwind or upstream condition

$$\alpha = \alpha_0 \left[\frac{\min(Z_c^{top}, \max(h_m, h_c, Z_c^{bot})) - Z_c^{bot}}{Z_c^{top} - Z_c^{bot}} \right] \quad (2-5)$$

The term in brackets is unity if the conduit is completely filled with water and zero if both the conduit head and the diffuse head drop below the conduit base elevation. The parameter α_0 [T^{-1}] is the linear exchange coefficient for a conduit filled with water. It is a property of the conduit and, in general, will be spatially variable. Theoretically, α_0 should be proportional to the product of the conduit surface area and diffuse hydraulic conductivity. In practice, it is a property of the system that is to be determined by calibration.

CONDUIT FLOW MODEL

In mature karst aquifers, conduit flow is often in the turbulent regime. For example, Halihan *et al.* (2000) estimate 95–99% of conduits in the Edwards Aquifer have Reynolds numbers greater than 2,000, which represents the approximate threshold for onset of turbulent behavior. Based on this analysis, all conduits with diameters greater than a few centimeters, which presumably dominate flow, would be in the turbulent regime.

For turbulent flow, the familiar linear relationship between Darcy velocity and hydraulic gradient is not valid and is replaced by a nonlinear flow law. By analogy with flow in engineering systems, the Darcy-Weisbach equation is typically assumed for flow

in pipes. The Darcy-Weisbach equation relates the macroscopic head loss, Δh , in a straight section of pipe to the flow velocity

$$\Delta h = ff \frac{L}{D_H} \frac{\bar{v}^2}{2g} \quad (2-6)$$

where L is the length of the pipe, D_H is the mean hydraulic diameter, \bar{v} is the mean velocity in the pipe, g is acceleration due to gravity, and ff is the friction factor. For straight pipes, ff depends on the relative roughness ε of the pipe and on the Reynolds number Re . Graphical representations of this dependence can be found in standard engineering handbooks. For Reynolds numbers greater than about 4,000, the dependencies are also well represented by the implicit Colebrook equation (e.g. Murdoch, 1996).

$$\frac{1}{\sqrt{ff}} = -2 \log \left[\frac{\varepsilon}{3.7} + \frac{2.51}{Re \sqrt{ff}} \right] \quad (2-7)$$

Gale (1984) and Halihan *et al.* (2000) used similar Reynolds-number-dependent models for friction factors in natural conduits.

For rough pipes, the friction factor becomes independent of Reynolds number; this appears to be appropriate for conduits which are naturally rough-walled.

Springer (2004) pointed out that real conduit passages are rarely well approximated as straight pipes, but instead have bends, constrictions, expansions, and contractions. In engineering systems, the head loss caused by such arrangements of components is usually estimated by summing empirically determined values for each component (e.g., Murdoch, 1996):

$$\Delta h = ff \frac{L}{D_H} \frac{\bar{v}^2}{2g} + C_{bends} \frac{\bar{v}^2}{2g} + C_{ec} \frac{\bar{v}^2}{2g} \quad (2-8)$$

where C_{bends} is an empirically determined coefficient accounting for head loss in all bends, and C_{ec} is a similar coefficient for cross-sectional expansions/contractions. Springer (2004) used detailed conduit geometry, flow-loss coefficients from engineering handbooks, and Equation (2-8) to calculate head losses in a segment of the Buckeye Creek Cave in West Virginia. The model was then used to estimate discharge for a flood with known head loss estimated from high water marks recorded as silt lines. Independent estimates of the discharge were not available for verification.

In most applications, detailed conduit geometry is not available, and direct calculation of head losses from conduit geometry is impractical. Instead, a lumped parameter that can be inferred or calibrated to match spring flows is needed. To this end, note each term in Equation (2-8) has identical dependence on velocity. Thus, the effects of the various bends and cross-sectional variations can be grouped into an effective friction factor

$$\Delta h = ff_e \frac{L}{D_H} \frac{\bar{v}^2}{2g} \quad (2-9)$$

An analogous form is more convenient for use in distributed groundwater models

$$q = -\frac{k_c}{\sqrt{\|\nabla h\|}} \nabla h \quad (2-10)$$

where q is the Darcy velocity, and k_c is an effective conductivity for the conduit. Jeannin (2001) used this form in modeling flow in the Holloch cave in Muotatal, Switzerland, and calibrated values of k_c to match observed discharges. Jeannin (2001) also converted effective friction factors reported by several authors to an equivalent k_c and showed that conductivity estimates for eight different studies clustered in the range 1–10 m/s.

Equation (2-10) is the preferred equation for modeling turbulent flow in conduits because it concisely accommodates friction and conduit geometry in the hydraulic conductivity term. However, groundwater modeling codes are typically based on the Darcy equation. It should be recognized that a Darcy model can always be calibrated to match a turbulent model in steady state. Specifically, an effective conductivity can be selected as $k_{eff} = k_c / \sqrt{\|\nabla h\|}$, which yields the same flow as the turbulent model in steady state. In transient conditions, however, the hydraulic gradient will necessarily deviate from the value used in calibration, and the two flow models will diverge. Painter *et al.* (2006) used numerical experiments to demonstrate the potential error introduced by applying a Darcy model to karst aquifers with turbulent flow.

The DCM turbulent flow model for conduits can be written

$$q_{cx} = -T_{cx}(h_c) i_{crit}^{1/2} \left| \frac{\partial h_c}{\partial x} \right|^{-1/2} \frac{\partial h_c}{\partial x} \quad \left| \frac{\partial h_c}{\partial x} \right| > i_{crit} \quad (2-11a)$$

$$q_{cx} = -T_{cx}(h_c) \frac{\partial h_c}{\partial x} \quad \left| \frac{\partial h_c}{\partial x} \right| \leq i_{crit} \quad (2-11b)$$

with analogous expressions for the y-components of flux. The parameter i_{crit} is the critical gradient for the onset of turbulence. It is regarded here as a calibration parameter similar to aquifer transmissivity. The turbulent flow equation (Equation 2-11a) will be invoked when the hydraulic gradient exceeds the critical gradient i_{crit} and the laminar flow equation (Equation 2-11b) will be invoked when the hydraulic gradient is less than i_{crit} .

SIMULATION OF DRY CELLS

When the conventional MODFLOW software calculates a water level that is below the base elevation of a computational cell, that cell is declared to be dry and removed (temporarily or permanently) from the calculation. This dry-cell simulation

algorithm may prevent the MODFLOW outer iteration scheme from converging (McDonald *et al.*, 1991). Moreover, if the dry cell has a specified recharge or pumping rate, then making it inactive causes a nonphysical change in the global water balance. These problems with the MODFLOW system are well known and long standing.

A new algorithm for simulation of dry cells was developed for DCM Version 1.0 and further refined in MODFLOW-DCM Version 2.0. The algorithm combines a new updating procedure for potentially dry cells with an upstream-weighted calculation of intercell conductances. Upstream weighting uses the saturated thickness in the upstream cell to calculate the intercell conductance for a pair of cells.

In the new updating procedure, the hydraulic head is never allowed to drop below the bottom elevation of a cell. If an outer iteration calculates a hydraulic head that is below the bottom elevation of a cell, the updated head for that cell is set equal to the arithmetic average of the previous head and the cell bottom. This procedure allows the head in a cell to become arbitrarily close to the cell bottom over the course of several iterations. However, the head will always be greater than the cell bottom, thus allowing the cell to remain active in the calculation.

The upstream weighting for the intercell conductance prevents flow from leaving a nearly dry cell while allowing flow to return to a nearly dry cell if the neighboring heads are higher than the cell in question. To express the upstream weighting in a compact form, a simplified, albeit nonstandard, notation is useful. First, suppress the c and m subscripts; the upstream weighting algorithm applies similarly to both conduit and diffuse system. Let h_{j+} denote the hydraulic head in cell $j+1, i, k$, and let h denote the head in cell j, i, k . Similarly, let CR_+ denote the row conductance between cells j, i, k and $j+1, i, k$. In standard MODFLOW notation, that row conductance is denoted $CR_{j+1/2, i, k}$. In the notation used here, the row conductance is then expressed as

$$CR_+ = CR_+^0 \frac{\min(Z_{j+}^{top}, \max(h_{j+}, h)) - Z_{j+}^{bot}}{Z_{j+}^{top} - Z_{j+}^{bot}} \quad (2-12)$$

where CR_+^0 is the branch conductance under fully saturated conditions as obtained by harmonic averaging of the hydraulic conductivity. In Equation (2-12), Z_{j+}^{top} and Z_{j+}^{bot} are intercell averages for top and bottom elevations. To prevent flow from leaving a dry cell, the following definition for Z_{j+}^{bot} is needed

$$Z_{j+}^{bot} = \max(Z_{j, i, k}^{bot}, Z_{j+1, i, k}^{bot}) \quad (2-13)$$

We have more flexibility in the definition of the Z_{j+}^{top} parameter, and the following is used in MODFLOW-DCM

$$Z_j^{top} = (Z_{j,i,k}^{top} + Z_{j,i+1,k}^{top}) / 2 \quad (2-14)$$

With the new handling of dry cells, all initially active cells remain active throughout the simulation. Thus, water balance issues related to drying cells are completely avoided. The algorithm requires no control parameters as input; parameters that controlled rewetting in conventional MODFLOW are not required and are not recognized by the DCM package.

NEWTON-RAPHSON SOLVER

For unconfined aquifers, the groundwater flow equations solved by MODFLOW are nonlinear because the branch conductances depend on saturated thickness and thus the dependent variable (hydraulic head). The turbulence model of MODFLOW-DCM introduces additional nonlinearities; with the turbulence model activated, the equations solved by MODFLOW-DCM are nonlinear for both unconfined and confined conditions.

The conventional MODFLOW system uses a Picard iteration strategy to resolve the nonlinear terms. With Picard iterations, the branch conductances are calculated using the hydraulic head from the previous iteration. The branch conductances are then held fixed while the head is updated by solving the resulting linear system. This iterative process is repeated until the head changes very little between subsequent iterations. The solution to the linear system itself may also be accomplished by an iterative process. Iterations to solve the linearized system are typically referred to as “inner iterations” and the process of iteratively updating the head and branch conductances as “outer iterations”. All nonproprietary solver packages in the conventional MODFLOW system use a variant on the Picard iteration strategy for the outer iterations.

Picard iteration is generally adequate for mildly nonlinear systems, but may fail to converge or require an excessive number of iterations for more strongly nonlinear systems. Numerical tests with the DCM Version 1.0 package revealed that the large contrast in branch conductances between conduit and diffuse-system cells often leads to convergence failures. In some cases, nearly dry cells also caused convergence failures.

A new Newton-Raphson solver, NR1, was developed for MODFLOW-DCM Version 2.0 to replace the Picard iteration scheme. The Newton-Raphson method for solving nonlinear equations is more robust than the Picard scheme because it uses derivative information in the iterations. The Newton-Raphson method is, however, more difficult to implement than the Picard iteration scheme and requires more information from the groundwater flow packages.

The groundwater flow equations system, discretized with respect to space and time, can be written in symbolic form as

$$\mathbf{R}(\mathbf{h}) = \mathbf{0} \quad (2-15)$$

where \mathbf{R} is the residual vector representing cell-by-cell errors in water balance and \mathbf{h} is the head vector. Let \mathbf{h}^m and \mathbf{R}^m denote the head approximation and resulting residual vector at iteration m . In the Newton-Raphson method, the next iteration of the head is obtained as $\mathbf{h}^{m+1} = \mathbf{h}^m + \mathbf{\Delta}^m$ where $\mathbf{\Delta}^m$ is the solution to the linear system

$$\mathbf{J}^m \mathbf{\Delta}^m = -\mathbf{R}^m \quad (2-16)$$

Here \mathbf{J}^m is the Jacobian matrix. The entry J_{pq} in the p^{th} row and q^{th} column of that matrix is the derivative of the p^{th} residual with respect to the q^{th} hydraulic head,

$$J_{pq} = \frac{\partial R_p}{\partial h_q}.$$

The NR1 solver implements a slight variation on the classical Newton-Raphson method by employing an adaptive damping strategy. The adaptive damping algorithm is a slight modification to Cooley's method (1983). The algorithm monitors for oscillations in the iteration procedure and applies damping if oscillations are detected.

The linear system given by Equation (2-16) is solved in the NR1 solver by a preconditioned conjugate gradient algorithm. Incomplete lower-upper (ILU) decomposition with a fixed level of fill is used for the preconditioner. Iteration acceleration is by the biconjugate gradient stabilized (BCGSTAB) method. The algorithms for solving the linear system are described in detail by Saad (2003).

VALIDATION TESTS

Test 1: Dual-Conductivity Confined System

A validation simulation is designed to test the MODFLOW-DCM representation of dual-conductivity flow in a confined system. The configuration is shown in Figure 2.2. The Darcy flow law is used. The system has translational symmetry in the y -direction and can be modeled as a one-dimensional system. However, it was implemented as a two-dimensional system, and symmetry in the y -direction was checked as part of the validation. In addition, the results of the numerical simulation were compared with an independent numerical solution. The system is initially in steady state with a hydraulic head of 0 ft. At $t = 0$, the head in the conduit system on the left boundary is increased from 0 to 5 ft. The simulation then proceeds for 100 minutes. Input parameters are listed in Table 2-1.

For a one-dimensional confined system and presuming Darcy flow, the groundwater flow equations become

$$S_m \frac{\partial h_m}{\partial t} = \frac{\partial}{\partial x} \left[T_{mx} \frac{\partial h_m}{\partial x} \right] + \alpha_0 [h_c - h_m] \quad (2-17a)$$

$$S_c \frac{\partial h_c}{\partial t} = \frac{\partial}{\partial x} \left[T_{cx} \frac{\partial h_c}{\partial x} \right] - \alpha_0 [h_c - h_m] \quad (2-17b)$$

where the S , T , and α_0 parameters are all independent of head. These equations were solved using the *NDSolve* routine of the commercial software Mathematica™ (Wolfram Research Inc., 2005). The *NDSolve* routine uses sophisticated adaptive algorithms for one-dimensional systems of partial differential equations, and the resulting solutions are highly accurate.

Hydraulic heads calculated by MODFLOW-DCM are compared to the benchmark solutions at $t = 20$ minutes in Figure 2.3. The benchmark solutions are shown as curves and the DCM results as individual data points. The agreement is excellent. The maximum absolute difference between the simulated and benchmark hydraulic head in the conduit is less than 0.05 ft, or less than 1% of the 5 ft head drop in the system. The maximum deviation in the diffuse head is even smaller.

Test 2: Unconfined System

These validation simulations are designed to test the MODFLOW-DCM representation of flow in an unconfined system and to provide some information on the consequences of the new averaging scheme in addition to verifying that the equations are implemented correctly. The configuration is the same as in Figure 2.2. The base of the conduit and the diffuse system are specified at 0 ft elevation, while the top of the conduit is at 3 ft, and the top of the diffuse system at 10 ft. The system is initially at steady state, with hydraulic head of 0 ft. At $t = 0$, the head in the conduit system on the left boundary is increased to 5 ft. Input parameters are listed in Table 2.2.

Two variants are considered, depending on the value of the exchange parameter. In the first variant, Test 2, the matrix/conduit exchange parameter is set to zero, and the simulation proceeds for 120 minutes. With no exchange, the conduit head is governed by the standard single-conductivity model, and the results of the DCM simulation can be compared with the results of the standard MODFLOW using the LPF package. Note, however that MODFLOW-DCM and the LPF package use different techniques for averaging the saturated thickness between two grid cells. Specifically, LPF uses simple arithmetic averaging of the saturated thickness and DCM uses the upstream weighting method. Thus, DCM and LPF may not produce identical results, although they should be similar. Results of Test 2 are shown in Figure 2.4 for $t = 1, 10,$ and 60 minutes. The agreement is good. The small deviations near the leading edge of the water pulse are due to the different averaging schemes and are to be expected.

In the second variant, Test 2a, the exchange term is set to 10^{-4} minute⁻¹, and the simulation proceeds until steady state is reached. Once steady state is reached, the calculated hydraulic heads can be used to verify on a cell-by-cell basis that the water balance is maintained. Steady-state results are shown in Figure 2.5. Hand calculations verify that the water balance is correct. For example, for a cell located about 90 ft from the outlet, the water balance is correct to one part in 10^5 .

Test 3: Turbulent Flow

This validation simulation is designed to test the DCM representation of turbulent flow. The configuration is similar to that of Figure 2.2. The system is confined, and there is no coupling between the conduit and diffuse system in this test. The system is initially at steady state, with a hydraulic head of 0 m. At the beginning of the simulation, the head in the conduit system on the left boundary is increased to 1.5 ft. Input parameters are listed in Table 2-3.

In 1-D with no conduit/diffuse interaction, the equation governing evolution of the hydraulic head in the conduit is

$$\begin{aligned}
 S_c \frac{\partial h_c}{\partial t} &= -\frac{\partial}{\partial x} [q_{cx}] \\
 q_{cx} &= -T_{cx}^0 i_{crit}^{1/2} \left| \frac{\partial h_c}{\partial x} \right|^{-1/2} \frac{\partial h_c}{\partial x} \quad \left| \frac{\partial h_c}{\partial x} \right| > i_{crit} \\
 q_{cx} &= -T_{cx}^0 \frac{\partial h_c}{\partial x} \quad \left| \frac{\partial h_c}{\partial x} \right| \leq i_{crit}
 \end{aligned} \tag{2-18}$$

where T_c^1 is the effective transmissivity at unit gradient and all other parameters have been defined previously. This equation was solved using the *NDSolve* routine of the commercial software Mathematica, as in Test 1.

Two variants of the test were executed. The first variant used a critical gradient of $i_{crit} = 0.01$, while the second used $i_{crit} = 0.1$. Results of both tests are shown in Figure 2.6 for $t = 5, 10,$ and 20 minutes. In each plot, the solid curves represent the target solution and the individual data points are the results from MODFLOW-DCM Version 2.0. The target and MODFLOW-DCM results overplot each other over the entire range. The maximum error is approximately 1.6% of the 5 ft head drop and occurs at $t = 5$ minutes, when the head gradient (and thus the discretization error) is largest.

Table 2.1 Parameters for the dual-conductivity validation test.

| Parameter | Value | Units |
|-------------------------------|------------------|----------------------|
| Conduit Transmissivity | 1 | ft ² /min |
| Diffuse Transmissivity | 1 | ft ² /min |
| Conduit-Diffuse Exchange Term | 10 ⁻⁴ | min ⁻¹ |
| Conduit Storativity | 0.001 | dimensionless |
| Diffuse Storativity | 0.001 | dimensionless |

Table 2.2 Parameters for the unconfined flow validation test.

| Parameter | Value | Units |
|-------------------------------|-----------------------|----------------------|
| Conduit Transmissivity | 1 | ft ² /min |
| Diffuse Transmissivity | 1 | ft ² /min |
| Conduit-Diffuse Exchange Term | 0 or 10 ⁻⁴ | min ⁻¹ |
| Conduit Storativity | 0.001 | dimensionless |
| Diffuse Storativity | 0.001 | dimensionless |
| Conduit Specific Yield | 0.1 | dimensionless |
| Conduit Specific Yield | 0.1 | dimensionless |

Table 2.3 Parameters for the turbulent flow validation test.

| Parameter | Value | Units |
|--|-------|----------------------|
| Conduit Transmissivity at Unit Head Gradient | 0.25 | ft ² /min |
| Diffuse Transmissivity | 1 | ft ² /min |
| Conduit-Diffuse Exchange Term | 0 | min ⁻¹ |
| Conduit Storativity | 0.001 | dimensionless |
| Diffuse Storativity | 0.001 | dimensionless |

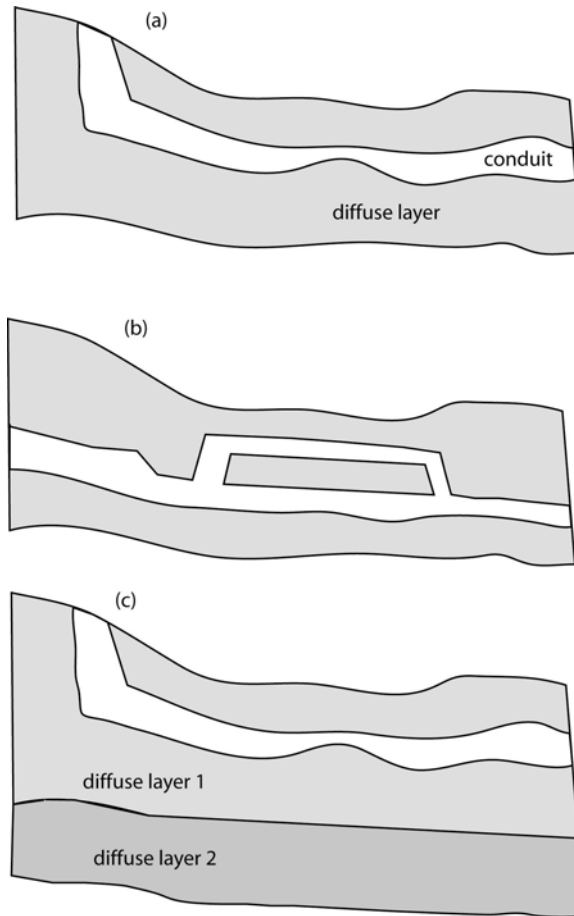


Figure 2.1 Hypothetical cross sections illustrating the range of applicability of MODFLOW-DCM. MODFLOW-DCM will model a single-layer aquifer containing a single-level conduit system, as in (a). MODFLOW-DCM will not model a multilevel conduit system like that shown in (b) or a multiple-layer aquifer similar to the ones shown in (c).

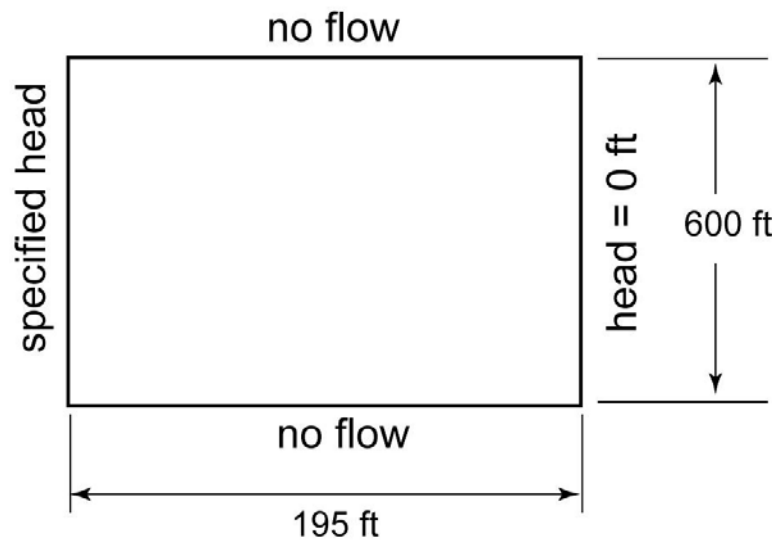


Figure 2.2 Configuration for the dual-conductivity validation test. Figure is not to scale.

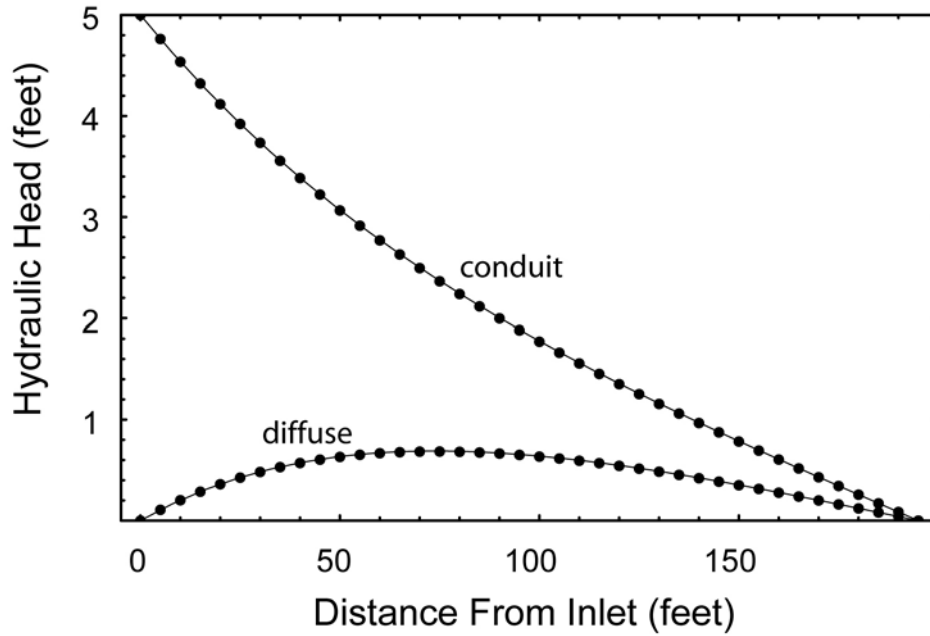


Figure 2.3 Results of the dual-conductivity validation test at $t = 20$ minutes. The benchmark results are shown as solid lines and the DCM results as individual data points. The upper set represents the hydraulic head in the conduit system and the lower set represents the hydraulic head in the matrix system.

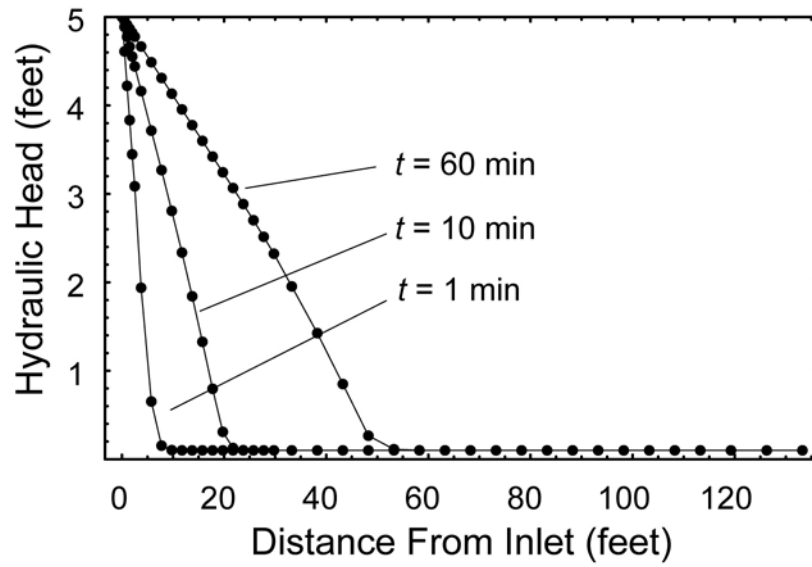


Figure 2.4 Results of the unconfined flow validation test (Test 2) at $t = 1, 10,$ and 60 minutes. The hydraulic heads in the conduit as calculated by the standard MODFLOW LPF package are shown as solid lines and the DCM results as individual data points.

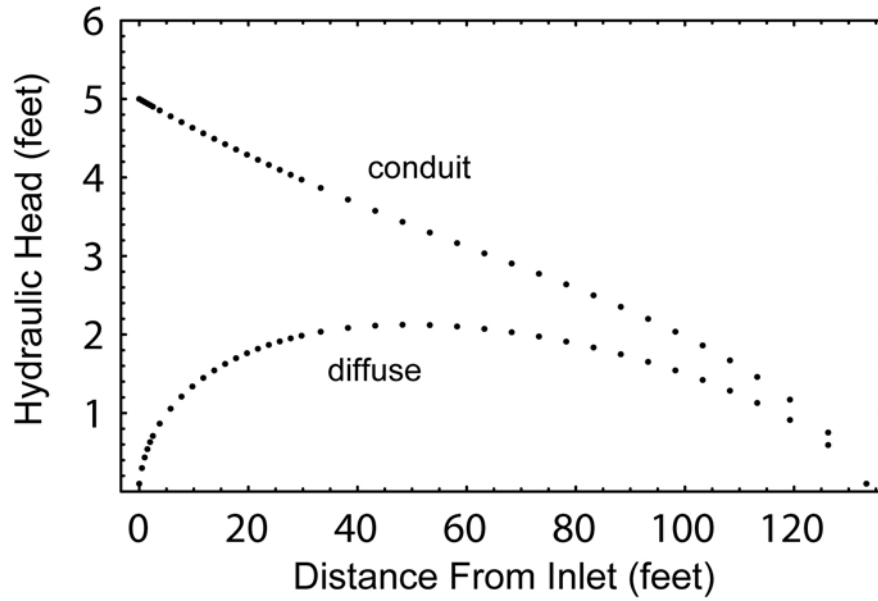


Figure 2.5 Steady-state results for the unconfined flow validation test (Test 2a). This simulation was used to verify that water balance is properly maintained in the DCM package.

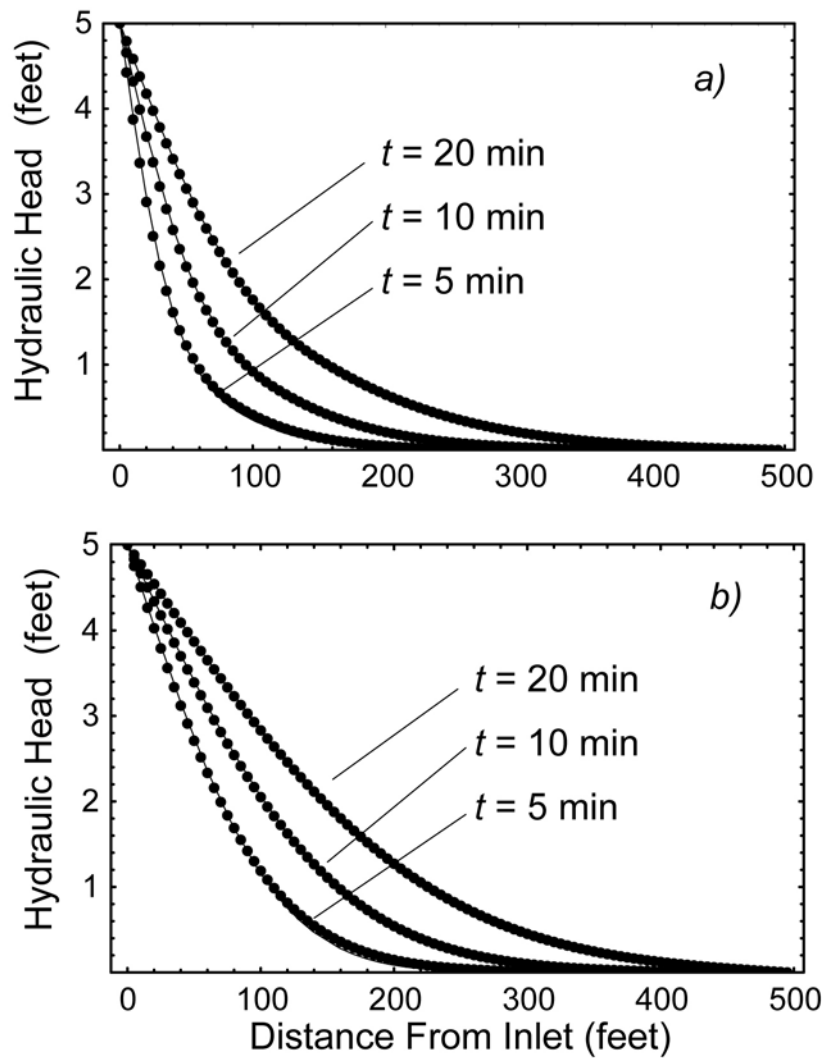


Figure 2.6 Results of the turbulent flow validation test (Test 3) at $t = 5$, 10, and 20 minutes for critical gradient of 0.01 (a) and 0.1 (b). Benchmark results are shown as solid lines and results of MODFLOW-DCM Version 2.0 are shown as individual data points.

CHAPTER 3

DCM MODEL OF THE BARTON SPRINGS SEGMENT OF THE EDWARDS AQUIFER

BACKGROUND

In Phase I of this project, a preliminary model of the Barton Springs segment of the Edwards Aquifer in south-central Texas was implemented using Version 1.0 of the DCM package (Painter *et al.*, 2006). In that work, an existing MODFLOW-96 model (Scanlon *et al.*, 2001, 2003) developed by the Barton Springs Edwards Aquifer Conservation District (BSEACD) was converted to a MODFLOW-DCM model. The objectives of the Phase I Barton Springs modeling task were to test the stability and numerical performance of the DCM code, to identify any shortcomings, and to gain some experience with calibrating an explicit conduit model to spring and water-level hydrographs. Poor numerical performance identified as part of that work led directly to the MODFLOW-DCM Version 2.0 changes described in Chapter 2.

This chapter describes a revised model of the Barton Spring segment that was constructed using the new MODFLOW-DCM Version 2.0 software. This new model is intended to further demonstrate the use of MODFLOW-DCM in complex real-world applications. The previous BSEACD model was used as a starting point in constructing the MODFLOW-DCM model, as in the Phase I work.

STUDY AREA AND HYDROGEOLOGICAL SETTING

The Barton Springs segment is a subsection of the Edwards Aquifer located in south-central Texas (Figure 3.1). The Edwards Aquifer is a Cretaceous age limestone aquifer which exhibits well-developed karstic features — such as caves, sinkholes, and swallets — and associated rapid karst flow. Rapid groundwater velocities, indicative of karst aquifers, have been measured in the Edwards Aquifer using results from dye tracer tests (Hauwert *et al.*, 2002).

The Edwards Aquifer is divided into three subsections: the Southern segment, the Barton Springs segment, and the Northern segment. The Barton Springs segment is terminated by a groundwater divide near Buda on the west end and the Barton Springs along the Colorado River at the eastern downgradient end. In general, the Edwards Aquifer is structurally controlled by the uplift of the Edwards Plateau along the Balcones Fault Zone. This faulting has developed three zones associated with the Edwards Aquifer: the contributing zone, the recharge zone, and the confined zone. Normal faulting along *en echelon* faults and grabens associated with the uplift of the Edwards Plateau have resulted in exposure of the underlying Glen Rose Formation to the north and northwest of the Edwards Aquifer. This region is referred to as the contributing zone to the Edwards Aquifer. Continued faulting to the south and southeast has exposed the Edwards Aquifer at the surface. This region is referred to as the recharge zone. Farther to the south and southeast, younger, less permeable units overlay the Edwards Aquifer, causing the aquifer to be confined. The southern and southeastern extent of the Edwards Aquifer is

defined by the transition from fresh to saline water, commonly designated as water with total dissolved solids in excess of 1,000 ppm.

The Barton Springs segment, including the contributing zone, is approximately 25 mi long and 12.5 mi wide. The recharge zone of the Barton Springs segment covers 100 mi². Along this segment, the Edwards Aquifer has an approximate thickness of 100—600 ft, with thickness greatest on the down-dip side. Most fault orientation is coincident with the Balcones Fault Zone orientation, which tends to be northeast-southwest in the Barton Springs segment. Also oriented coincident with the Balcones Fault Zone orientation are the main groundwater karst conduits whose location and orientation have been inferred using results from tracer tests (Hauwert *et al.*, 2002; Hunt *et al.*, 2006). Tracer test results have also allowed identification of three principal subbasins within the Barton Springs segment: Cold Springs groundwater basin, Sunset Valley groundwater basin, and Manchaca groundwater basin.

THE BSEACD MODFLOW MODEL

The BSEACD model has a single layer with 7,043 active cells and uses the confined/unconfined mode of MODFLOW. The grid cells are 1000 ft long and 500 ft wide. The grid is aligned with the predominant faults in the Edwards formation and is thus rotated 45% from the east–west direction (see Figure 3.1). The model extends from a presumed groundwater divide near Buda, Texas, in the south to the Colorado River near downtown Austin along the northern boundary. The eastern boundary corresponds to the fresh water/saline water interface, and the western boundary corresponds to the Mount Bonnell fault. The aquifer bottom elevation and aquifer thickness are shown in Figure 3.2. Note the large elevation change in the model region.

All boundaries were modeled as no-flow boundaries. Barton Springs and Cold Springs were modeled as drains with very high conductances. Recharge had two components. Eighty-five percent of the recharge was assumed to be concentrated along losing streams, and the remaining 15% was distributed uniformly across the recharge zone (Puente, 1976, 1978). The aquifer was divided into nine zones for the purpose of assigning transmissivity. Higher transmissivities were assigned to zones aligned with the major flow paths as inferred from tracer tests.

BSEACD constructed a steady-state model and a transient model. The steady-state model used a spatial distribution of recharge averaged for the years 1979—1998. Total recharge and total pumpage were set to 50 cubic feet per second (cfs) and 5 cfs, respectively. Water-level measurements from July and August 1999 were used as calibration targets. Transmissivities in the 9 zones were calibrated to these hydraulic heads. The transient model used monthly recharge and pumping for the 10-year period from 1989 through 1998.

The BSEACD model was constructed to model spring flow during drought periods and aquifer-wide water-level declines due to future increased pumping. From this perspective, the model was successful because it generally reproduces spring flow

histories during the 1989 to 1998 period. However, the model does have some limitations. Simulated recessions in the spring flows tend to be slower than observed. Simulated spring flows during high-flow periods tend to be larger than observed. Water-level hydrographs in monitoring wells appear to fluctuate more strongly to changes in recharge than the observed hydrographs. Simulated heads in the southwest fringe of the model tend to be too high. Most importantly, simulated spring flows during extreme droughts tend to be too large. To address that problem, BSEACD developed an alternative calibration to simulate extreme low-flow periods (Smith and Hunt, 2004).

The limitations of the current BSEACD model may reflect modeling assumptions or inadequate input data, but the more likely limitation to the current model is that there are inherent limitations of using a single-continuum model with a Darcy flow law to model a dynamic karst system.

In this project, the BSEACD model was converted to a MODFLOW-DCM model by (i) adding a conduit layer, (ii) reducing transmissivity in the high transmissivity zones to levels more typical for a diffuse flow system, and (iii) increasing specific storage and specific yield in the diffuse system to values more typical for a diffuse flow system. The latter two steps are necessary because the conduit system is now accounting for the majority of flow and all of the fast flow.

CONDUIT REPRESENTATION IN THE MODFLOW-DCM MODEL

The conduit representation in the MODFLOW-DCM model was developed collaboratively with BSEACD staff. Conduit placement was constrained by locations of major flow paths (Figure 3.3) as inferred from the dye tracer studies of Hauwert *et al.* (2002) and Hunt *et al.* (2006). In addition, conduits were located so that known locations for focused recharge were intercepted by conduits. The conduit network, which is composed of 14 individual conduits, is shown in Figure 3.4. Conduits 2 and 12 are the main flow paths. Conduit 6 also channels significant flow directly to Barton Springs.

The top elevation of the conduit layer was initially assumed to coincide with the top of the Kirshberg member, as suggested by BSEACD staff. After some preliminary numerical experiments, the conduit top elevation was lowered by approximately 50 ft in the recharge zone in Hayes County. Conduit thickness was taken as 30 ft. Conduit top elevation compared to top elevation for the diffuse system is shown in Figure 3.5. It is noted that conduit elevation and conduit thickness are highly uncertain; the elevation in Figure 3.5 and the assumed thickness are considered working hypotheses. Consequences of the conduit elevation specification are examined later in this report in the section “MODFLOW-DCM Simulations of Drought Periods”.

STEADY-STATE MODFLOW-DCM MODEL

Steady-state recharge and pumping data from the BSEACD model were used in a steady-state DCM simulation. Recharge locations and magnitude assigned to each are shown in Figure 3.6. The majority (85%) of the recharge is assigned to the focused

recharge locations per assessments by Puente (1976, 1978). The distributed recharge (15%) was assigned uniformly to the green shaded area in Figure 3.6. Total recharge for the steady-state model is 61 cfs.

Pumping locations are shown in Figure 3.7. The symbols are color coded by pumping magnitude: red symbols indicate pumping rates >0.1 cfs, blue symbols indicate a pumping range $0.01\text{--}0.1$ cfs, and black symbols indicate a pumping rate <0.001 cfs. The aggregate pumping rate is approximately 5 cfs.

Hydraulic head measurements at 74 well locations were available for calibration purposes (Figure 3.8). The total head range in the calibration set is 278 ft. The calibration strategy adopted was to first fix the exchange parameter α_0 and then adjust the transmissivity in the major conduits to achieve a rough calibration. Transmissivities in the secondary conduits and diffuse-layer zones were then varied to improve the calibration. This calibration strategy was successful for a range of α_0 values, indicating that the steady-state calibration is not unique. Automatic calibration using a standard Levenberg-Marquardt minimization was also successfully tested.

Conduit hydraulic conductivity values for a calibrated steady-state model denoted 5SS are shown in Table 3-1. The exchange parameter α_0 is 0.001 day^{-1} for all conduits. Note the very large hydraulic conductivity values for the main conduit (Conduit 2).

A cross plot of observed versus simulated hydraulic head for Model 5SS is shown in Figure 3.9. The solid line has a slope of unity and represents a perfect calibration. Although there is scatter around the target line, the agreement is generally good, and there is little systematic bias in the results (mean residual of 0.05 ft). The root-mean-square (RMS) residual is 16.8 ft, which is about 6% of the total range of observed head.

Figure 3.10 shows calculated hydraulic heads in the conduit and diffuse systems as color density plots. Positions of the conduits are marked in black on the diffuse-head density plot. The hydraulic head increases from 430 ft at Barton Springs to more than 800 ft in the western edge of the recharge zone. Hydraulic gradients are generally low in the confined region due to the influence of the major conduits. Hydraulic gradients are larger in the recharge zone. These features are in general agreement with hydraulic head measured during the July—August 1999 period (Scanlon *et al.*, 2001, 2003).

TRANSIENT MODFLOW-DCM MODEL FOR THE PERIOD 1989—1998

Ten-year transient simulations for the period 1989—1998 were also performed. The simulations used one-month recharge periods. The time histories for recharge and pumping are shown in Figures 3.11 and 3.12, respectively.

The transient simulations also used a one-month timestep, which is significantly larger than the 1—3 day timestep used in Phase I of this project (Painter *et al.*, 2006). Longer timesteps are possible in MODFLOW-DCM Version 2.0 because of the robustness of the new NR1 solver.

Initial conditions were generated by starting with hydraulic head calculated by the steady-state model 5SS and then allowing the simulation to proceed 3—5 months (depending on the parameter combination) using the January 1989 pumping and recharge values. This procedure ensured an approximate match between the simulated and observed spring discharge for January 1989.

Parameters for the reference case transient simulation are identical to those of the reference case steady-state model except for two values. First, the hydraulic conductivity of Conduit 12 was increased to 15,000 ft/day in the transient simulation during the calibration process. This change had little effect on the steady-state head distribution. Second, the turbulence model with a critical gradient i_{crit} of 0.01 ft/ft was used in the transient model as opposed to the laminar flow model in the steady-state model. This change also had little effect during steady-state or low-flow conditions, as will be explored later in this report. The specific storage and specific yield for the diffuse and conduit systems were adjusted during the transient calibrations. The calibrated values for storage parameters are 10^{-5} for specific storage in conduits, 3×10^{-5} for specific storage in the diffuse system, 10^{-3} for specific yield in conduits, and 3×10^{-3} for specific yield in the diffuse system.

Color density plots of the calculated diffuse-system hydraulic heads at three times are shown in Figure 3.13. These three head maps illustrate the range of conduit-diffuse exchange expected for different recharge conditions.

The hydraulic head map for February 1992, a month of high recharge that followed a period of relatively average recharge, shows groundwater mounding near the recharge point in Bear Creek (Conduit 4). Groundwater ridges aligned with Conduit 6 and Conduit 3 are also apparent. These groundwater mounds and ridges in the diffuse system are caused by flow from the conduits to the diffuse system during the period of increased recharge.

The hydraulic heads for October 1992, a period of average recharge that followed a nine-month period of intense recharge, are significantly higher than average in the upstream parts of the model. The elevated hydraulic heads represent storage of water following the period of intense recharge. No significant groundwater mounds or ridges are apparent.

January 1997 was at the end of a one-year drought. The hydraulic heads are significantly lower than typical throughout the model region. Conduit 2 is acting to drain the diffuse system, resulting in a large groundwater trough aligned with that conduit.

Measured and simulated spring-flow hydrographs are shown in Figure 3.14. The solid line represents the simulated Barton Springs discharge hydrograph, and the individual data points are measured discharge. The measured discharge for the first half of 1992 is uncertain and likely underestimates the true discharge because water

overtopped the dam at Barton Springs during this period, which interfered with the discharge measurements (Scanlon *et al.*, 2003).

The agreement between the simulated and measured hydrographs is generally good. The major discrepancy occurs at the end of 1992, where the simulation results are somewhat lower than those measured. The cause of the discrepancy during this period is not known. The quality of the match between the simulated and measured hydrographs is similar to that obtained with the previous BSEACD MODFLOW model. The previous model matched the measured values better than MODFLOW-DCM during the late 1992 and early 1993 period. However, the MODFLOW-DCM model produces significantly lower discharge and better matches to the measured discharge during the peak discharge events in 1992, 1997, and 1998. The significantly lower peaks during the periods of high recharge are caused by the turbulence model.

As can be seen from Figure 3.14, spring flow responds very quickly to changes in recharge. In the previous BSEACD MODFLOW model, this rapid spring response time was reproduced by decreasing specific yield and specific storage in the system. Although this strategy was successful in matching spring-flow hydrographs, it resulted in water-level hydrographs that are overly responsive. This can be easily seen in Figure 3.15, where the simulated water-level hydrographs from the original BSEACD model (Scanlon *et al.* 2001, 2003) are compared with measured hydrographs and results from the MODFLOW-DCM simulations. Clearly, the conventional MODFLOW model used by Scanlon *et al.* (2001, 2003) produces unrealistic excursions in hydraulic head at Well 58-58-101. The discrepancy is as large as 250 ft during 1992. Significant differences are also seen for Well 58-58-801. The MODFLOW-DCM model produces a much more subdued water-level hydrograph that better matches the observed water level. This ability to match both the rapid spring response and the more subdued water-level hydrographs demonstrates the inherent flexibility in the MODFLOW-DCM model to match both low base flow and large spring discharges. Because most of the flow and all of the fast flow is in the conduit system, rapid spring response can be achieved by assigning small values to the conduit storage parameters. The storage parameters for the diffuse system are then free to be adjusted to match the relatively subdued water-level hydrographs.

SENSITIVITY ANALYSIS FOR THE TRANSIENT MODEL

Sensitivity to the critical gradient for onset of turbulence i_{crit} is shown in Figure 3.16. The three cases correspond to critical gradients of 0.01 ft/ft (calibrated value), 0.005 ft/ft, and infinity (no turbulence). During periods of low flow, the turbulence model has only a minor effect on the simulated discharge. In periods of high discharge, the turbulence model reduces the peak discharge significantly. Specifically, the three peaks in 1992, 1997, and 1998 are higher without the turbulence model. The dips following the peaks are also slightly lower without the turbulence model. Comparison with Figure 3.14 reveals that the addition of the turbulence model results in an improved match to the dynamic spring hydrograph for Barton Springs.

Sensitivity to the exchange parameter α_0 was investigated by changing α_0 from the reference value of 0.001 to 0.002 and then recalibrating the steady-state model. In steady-state, the match between measured and observed water levels was similar in both cases. However, the transient model was slightly less responsive for the larger value of α_0 (Figure 3.17). Water-level hydrographs (not shown) were slightly more responsive with the larger value of α_0 . These results demonstrate that the exchange parameter α_0 is an important calibration parameter that can be tuned to match dynamic spring flow responses.

MODFLOW-DCM SIMULATIONS OF DROUGHT PERIODS

Hypothetical drought conditions were simulated by starting with a calibrated steady-state model and then eliminating recharge for a 5-year period. The objectives of these simulations are to investigate the robustness of MODFLOW-DCM on simulations with significant numbers of dry cells and test the hypothesis that spring discharge during dry periods can be affected by conduit elevations in the model.

Three drought-condition simulations were performed. The first simulation used the reference case steady-state parameter combination. In the second simulation, the elevation of the bottom and top of the conduits was raised to force conduits to de-water earlier in the simulation. The revised conduit elevation is shown as a color density map in Figure 3.18. The third simulation also used the revised conduit elevation, but in that simulation, the aggregate pumping rate was increased by a factor of 4 to 20 cfs.

Spring hydrographs for the three drought-condition simulations are shown in Figure 3.19. With the original conduit elevation, spring discharge drops below 10 cfs after 4 years and 9 months of drought. With the revised conduit elevation, the spring discharge is smaller because conduits de-water quicker, thus reducing the capability of the aquifer to transmit water to the springs. For that simulation, the spring discharge drops below 10 cfs after 4 years of drought. The relative sensitivity to the conduit elevation confirms that conduit elevations influence flow during low-flow conditions and suggest that the elevations may be determined by model calibration during low-flow periods.

The spring hydrograph for the third simulation is also shown in Figure 3.19. As expected, the spring discharge is much lower with the increased pumping. After less than 2 years, the spring discharge has dropped below 10 cfs. At the end of 5 years, the springs are still flowing as water is slowly liberated from storage, but the flow rate is less than 2 cfs.

Table 3-1. Calibrated hydraulic conductivity for conduits in the reference steady-state model.

| Conduit Number | Hydraulic Conductivity (ft/day) |
|----------------|---------------------------------|
| 2 | 160000 |
| 3 | 15000 |
| 4 | 10000 |
| 5 | 10000 |
| 6 | 5000 |
| 7 | 35000 |
| 8 | 5000 |
| 9 | 4200 |
| 10 | 5000 |
| 11 | 10000 |
| 12 | 5000 |
| 13 | 100000 |
| 14 | 1000 |

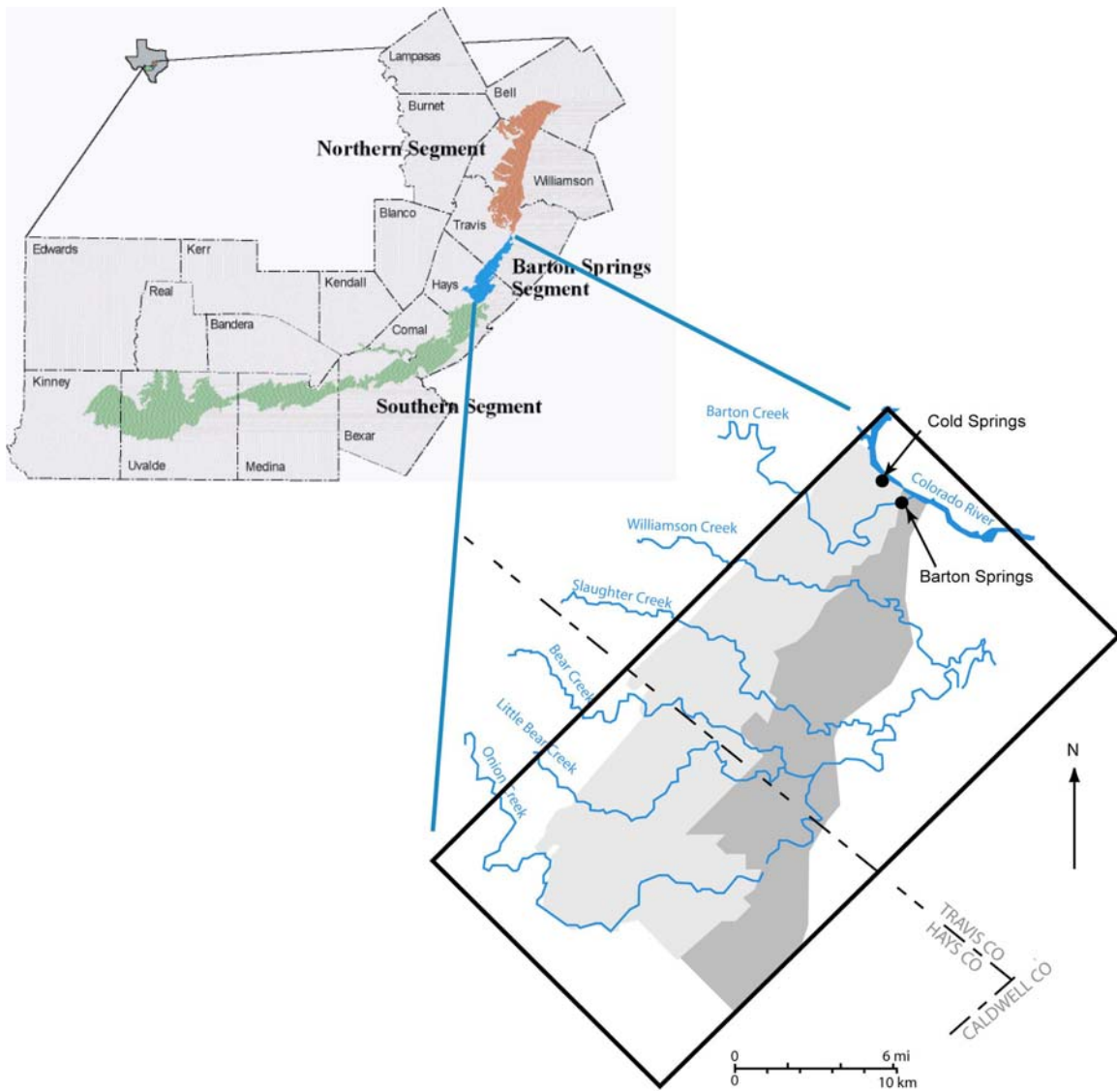


Figure 3.1 Study area for the Barton Springs model. The model domain is illustrated within the black box in the insert.

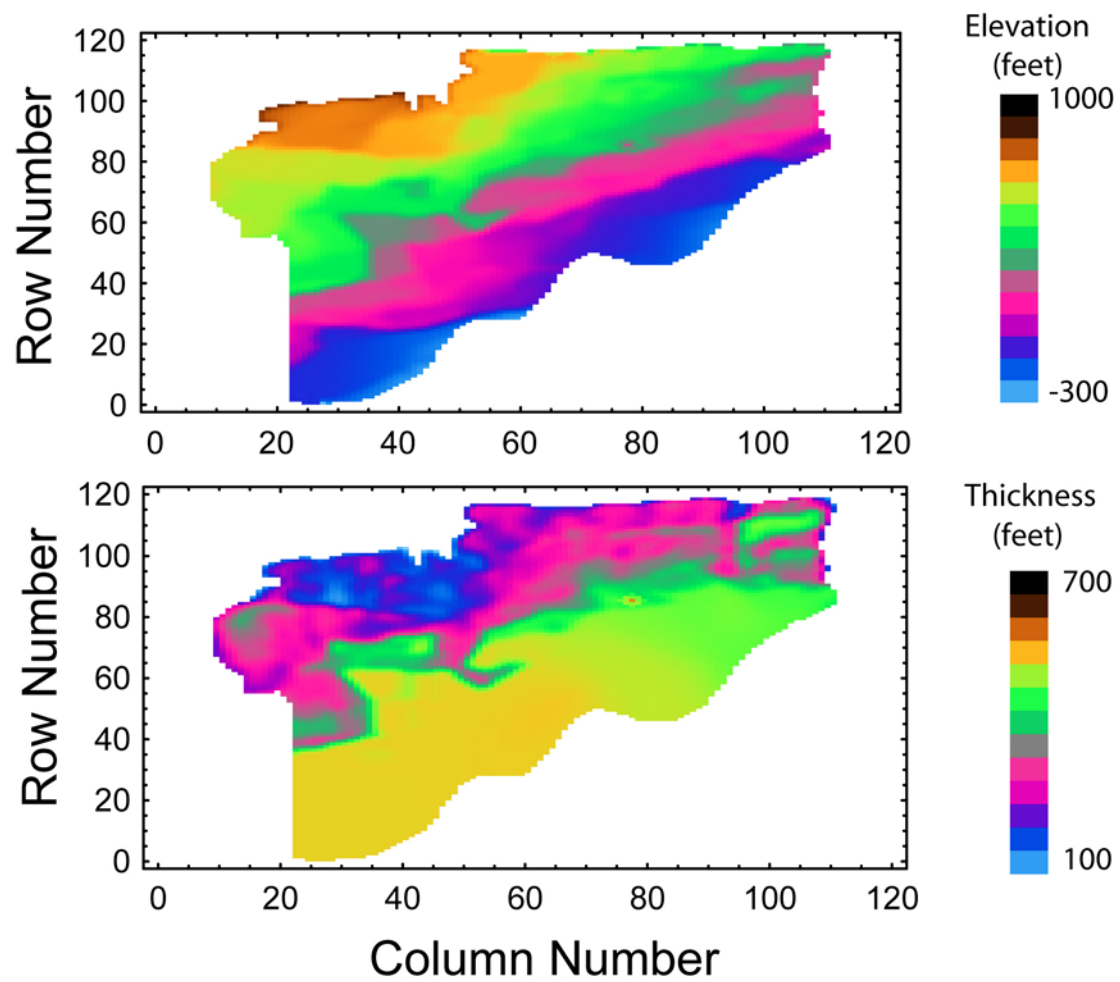


Figure 3.2 Diffuse layer bottom elevation and thickness.

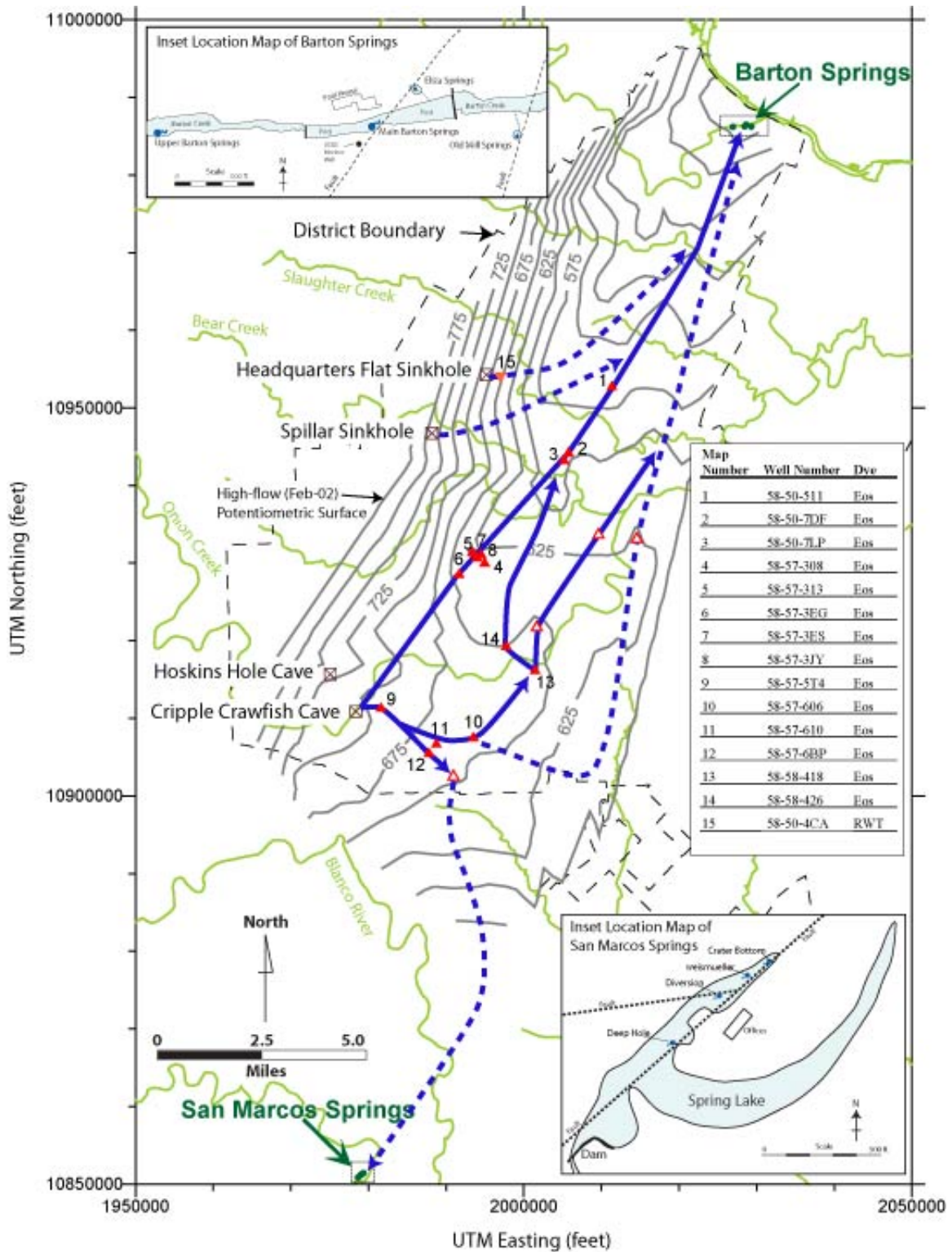


Figure 3.3 Conduit locations inferred from tracer test results (Hunt *et al.*, 2006).

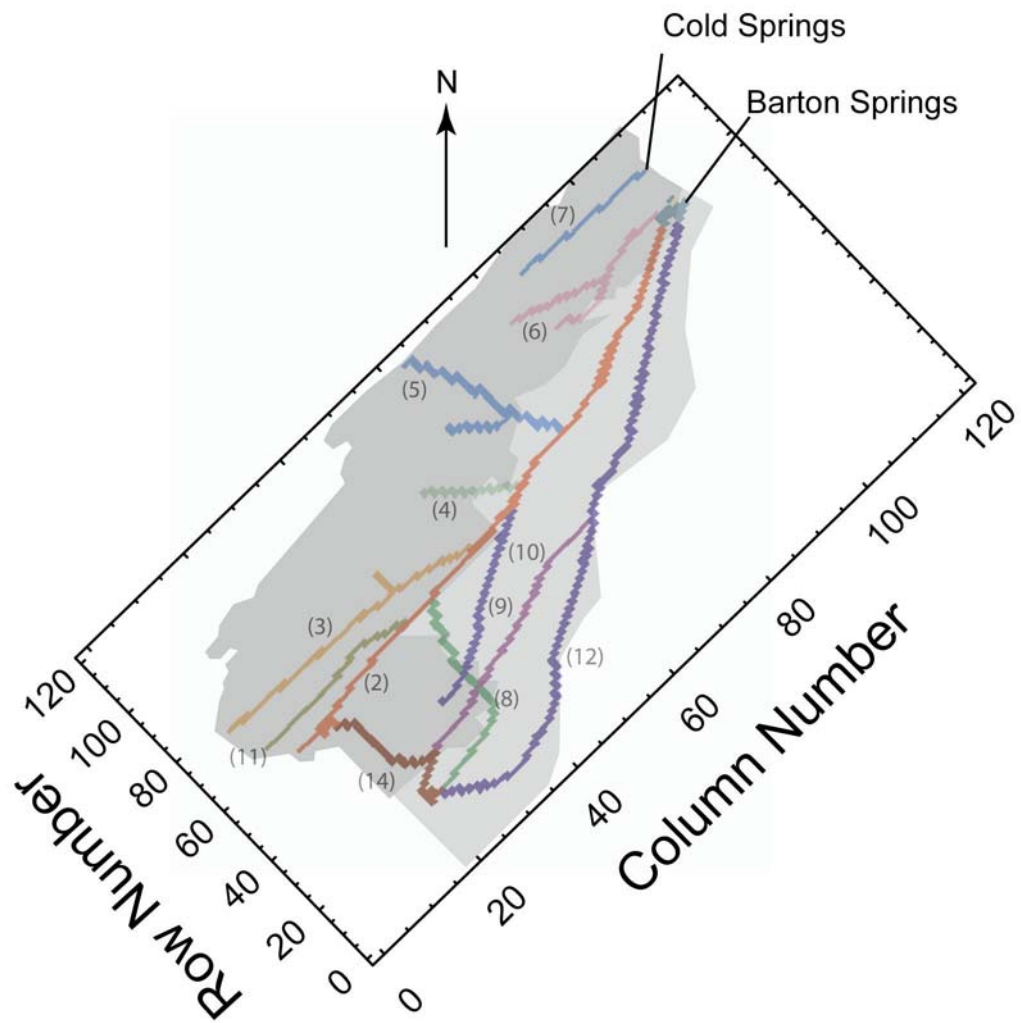


Figure 3.4 Locations of modeled conduits in the DCM model of Barton Springs.

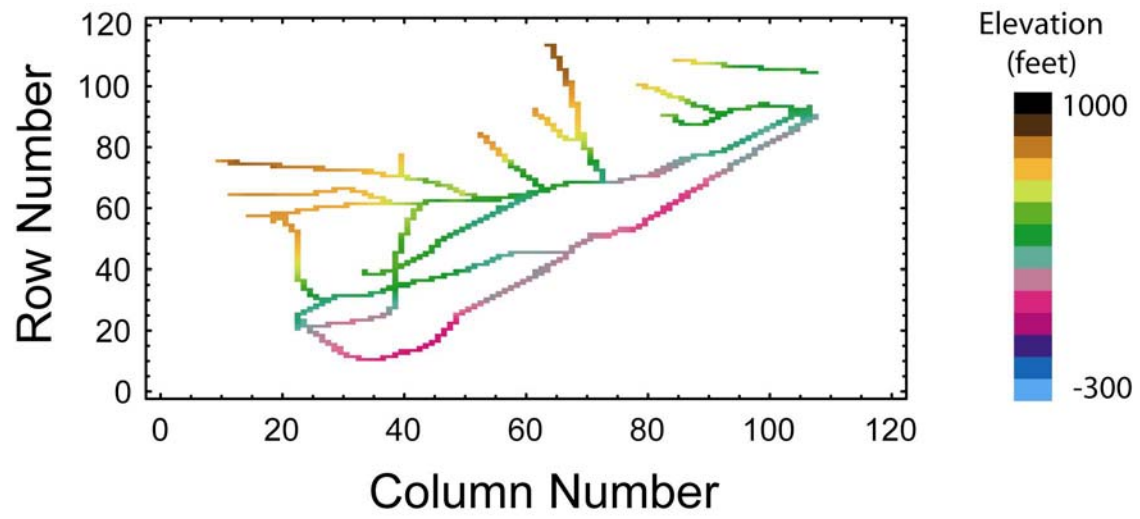


Figure 3.5 Bottom elevation for the conduit layer.

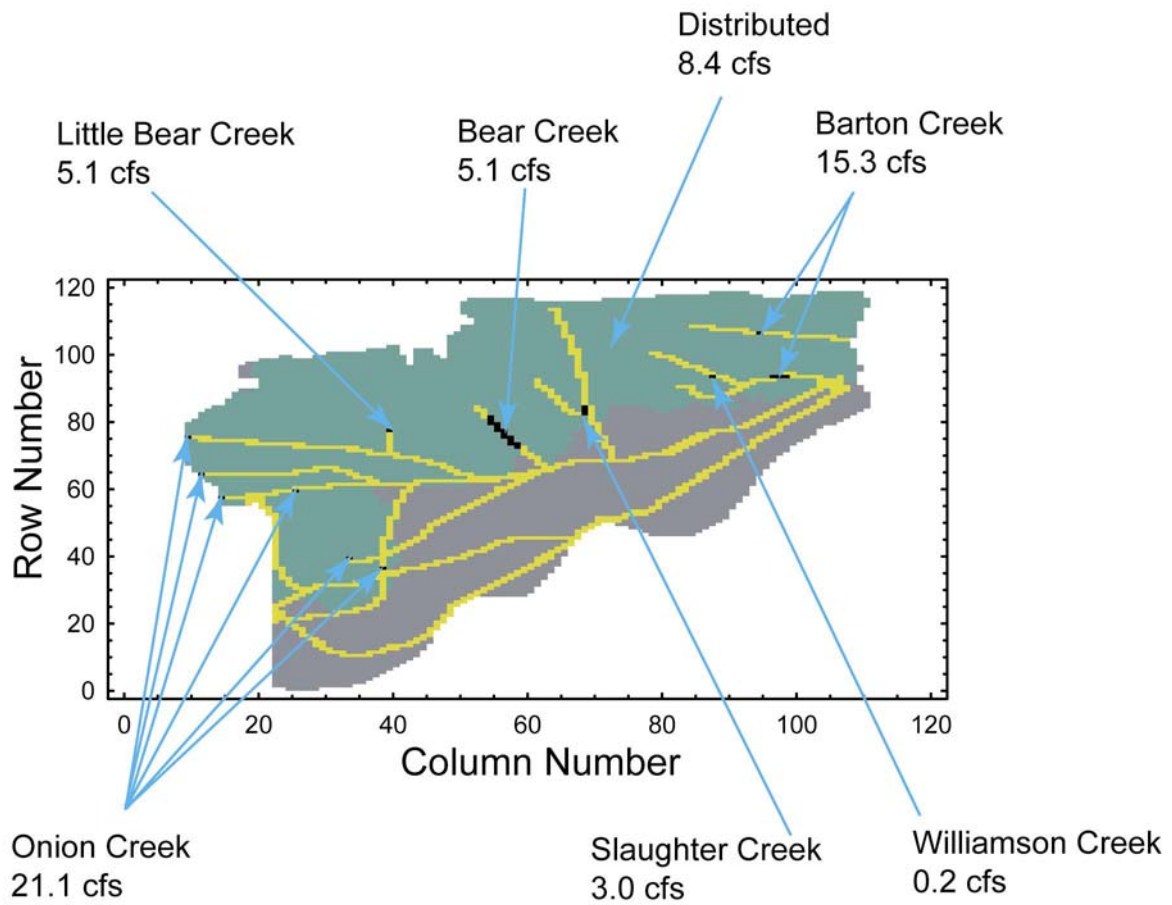


Figure 3.6 Recharge locations and steady-state recharge values for the Barton Springs model.

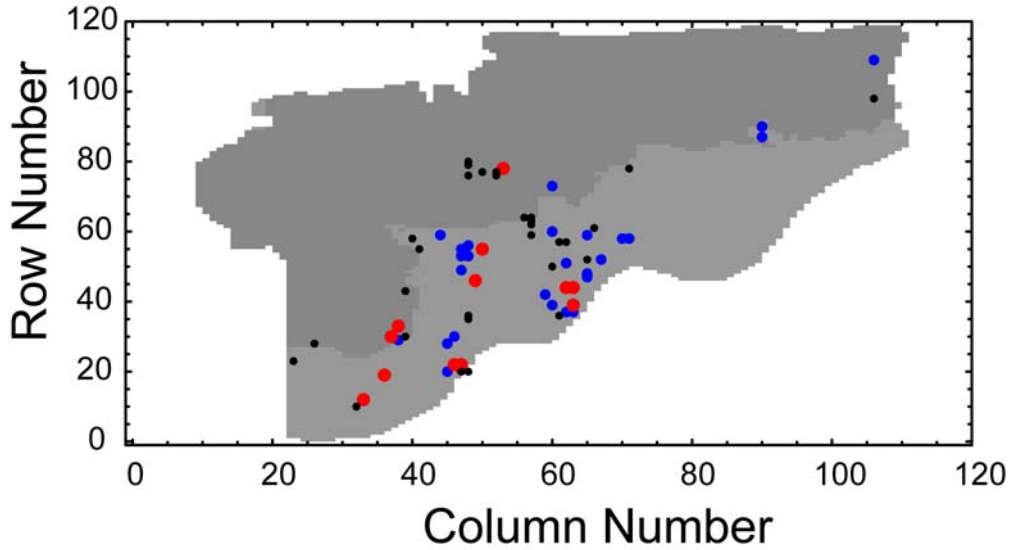


Figure 3.7 Pumping locations for the Barton Springs model. Red dots denote large (>0.1 cfs) pumping centers, blue dots denote moderate (0.01—0.1 cfs) pumping centers, and black dots denote small (<0.01 cfs) pumping centers. Dark shading denotes outcrop zone and light shading denotes confined zone of the Edwards Aquifer.

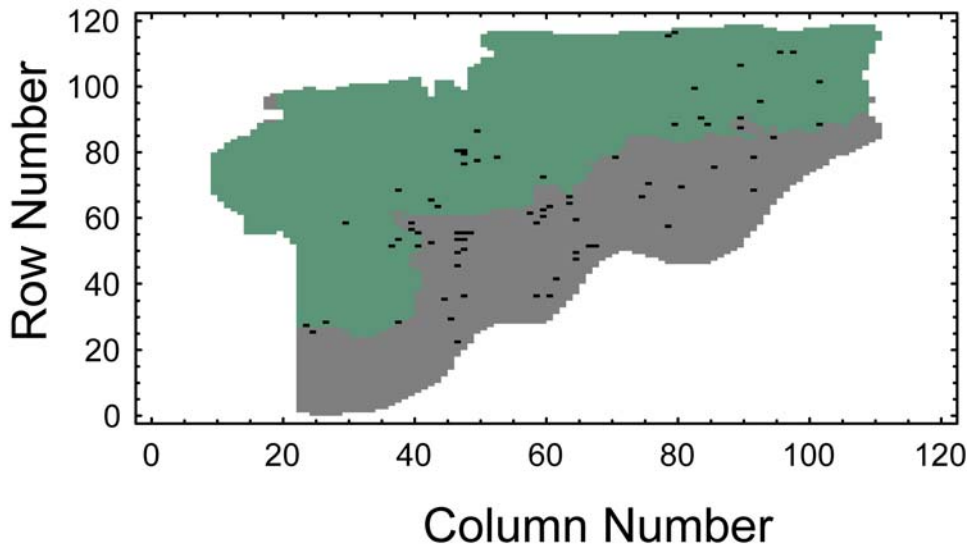


Figure 3.8 Locations of steady-state hydraulic head observations for calibrating the Barton Springs steady-state model are denoted with dots. Green shading denotes outcrop zone and gray shading denotes confined zone of the Edwards Aquifer.

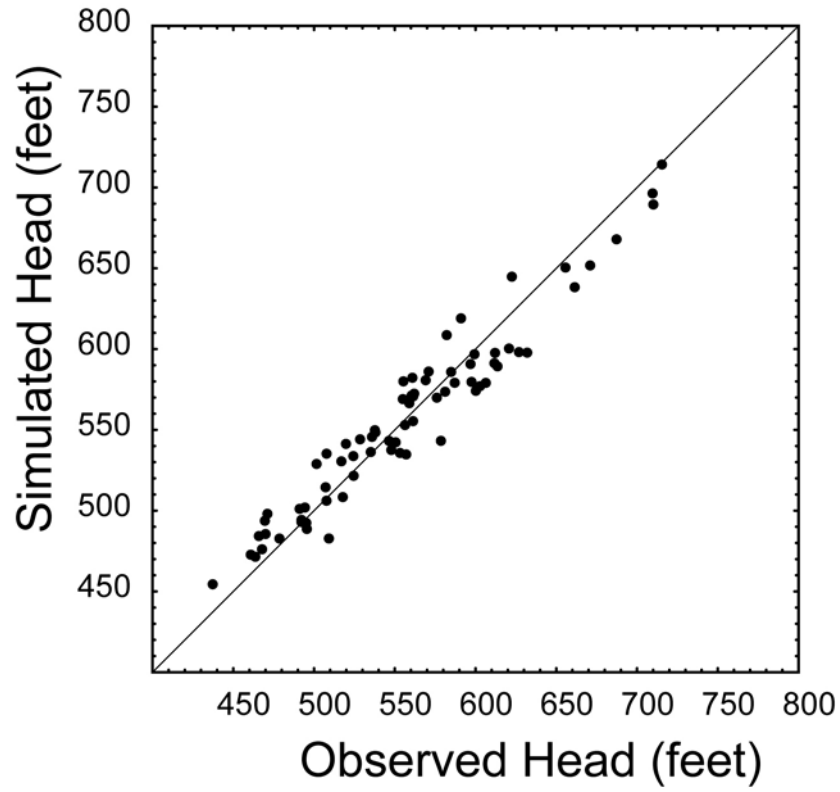


Figure 3.9 Crossplot of observed and simulated hydraulic heads for the Barton Springs steady-state model.

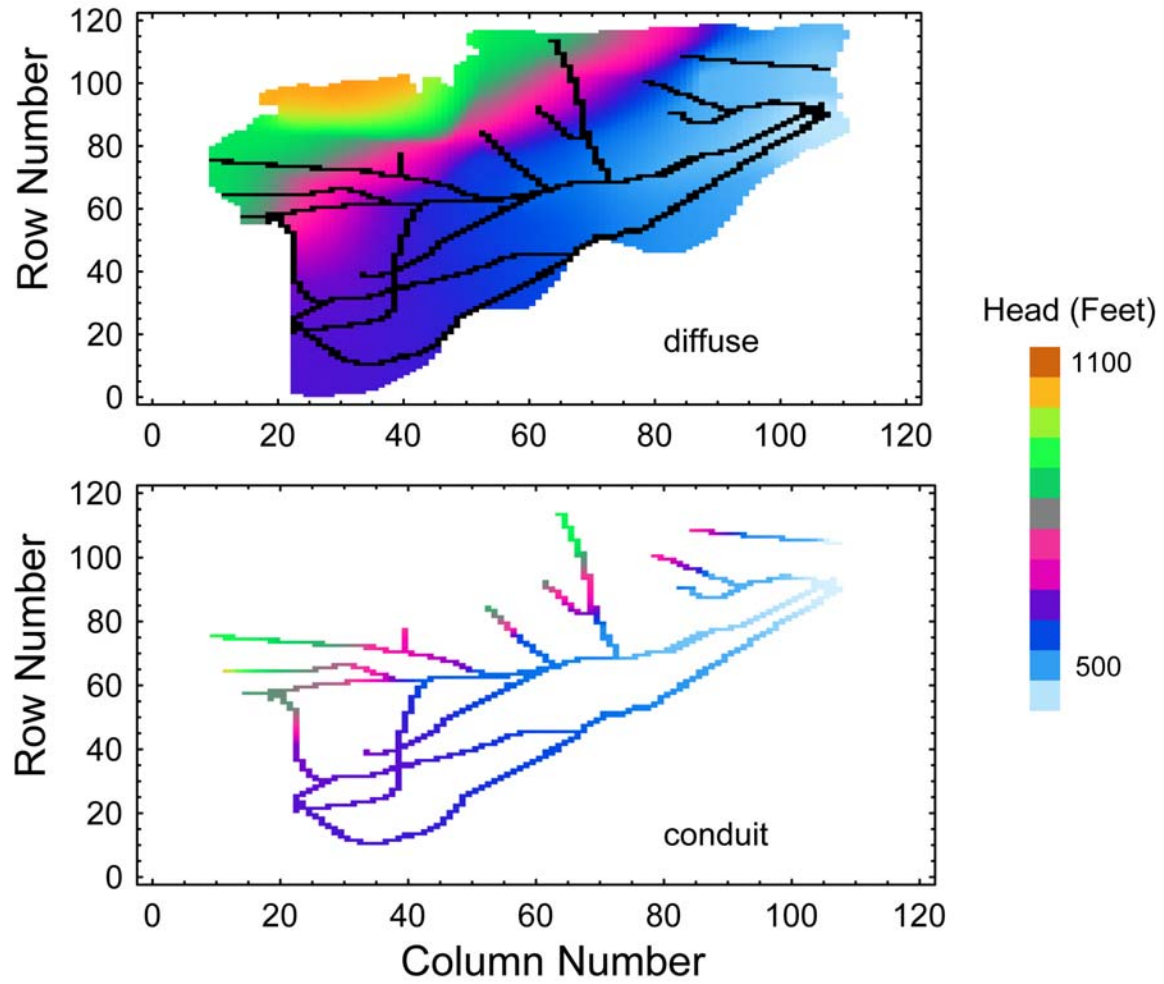


Figure 3.10 Diffuse and conduit hydraulic heads in the Barton Springs steady-state model.

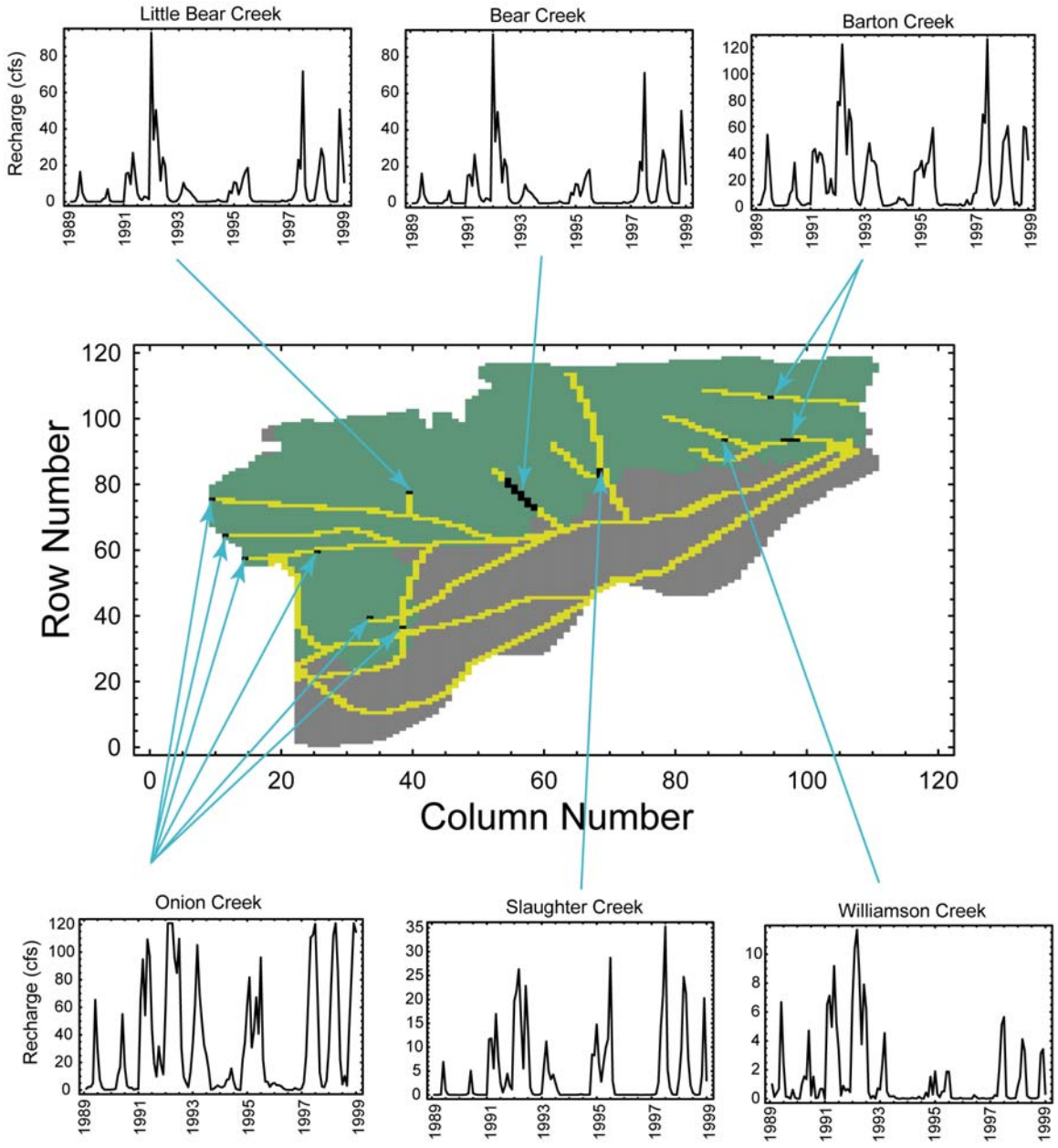


Figure 3.11 Recharge at selected locations for the period 1989–1998.

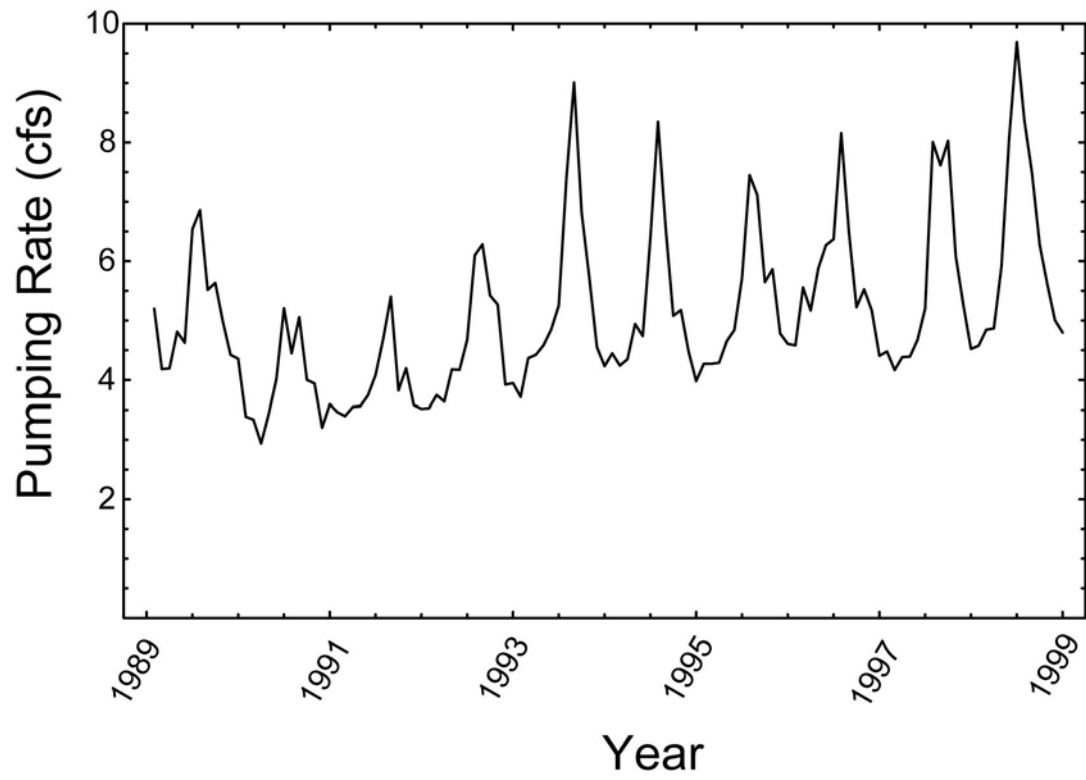


Figure 3.12 Pumping for the period 1989—1998.

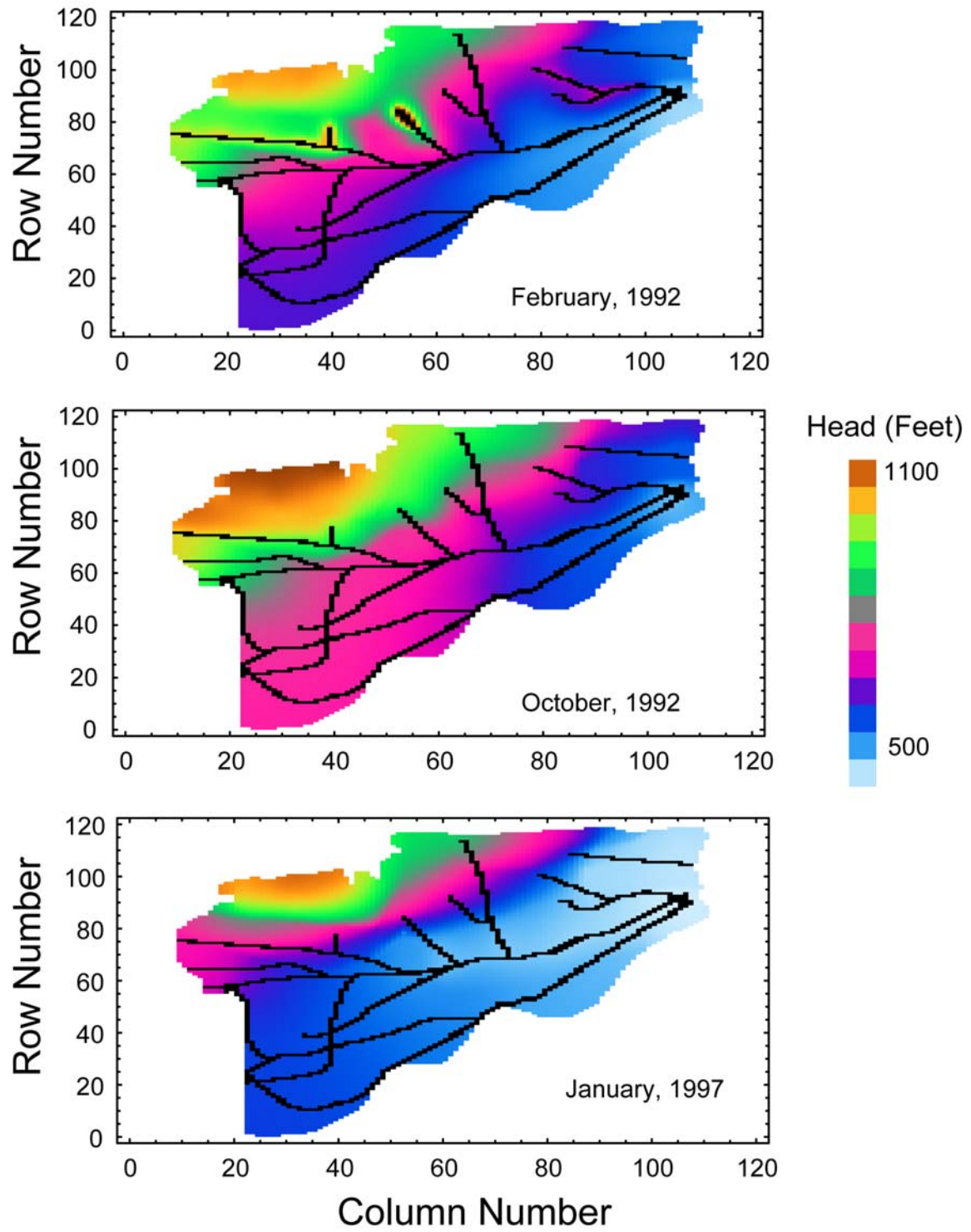


Figure 3.13 Water level at three selected times.

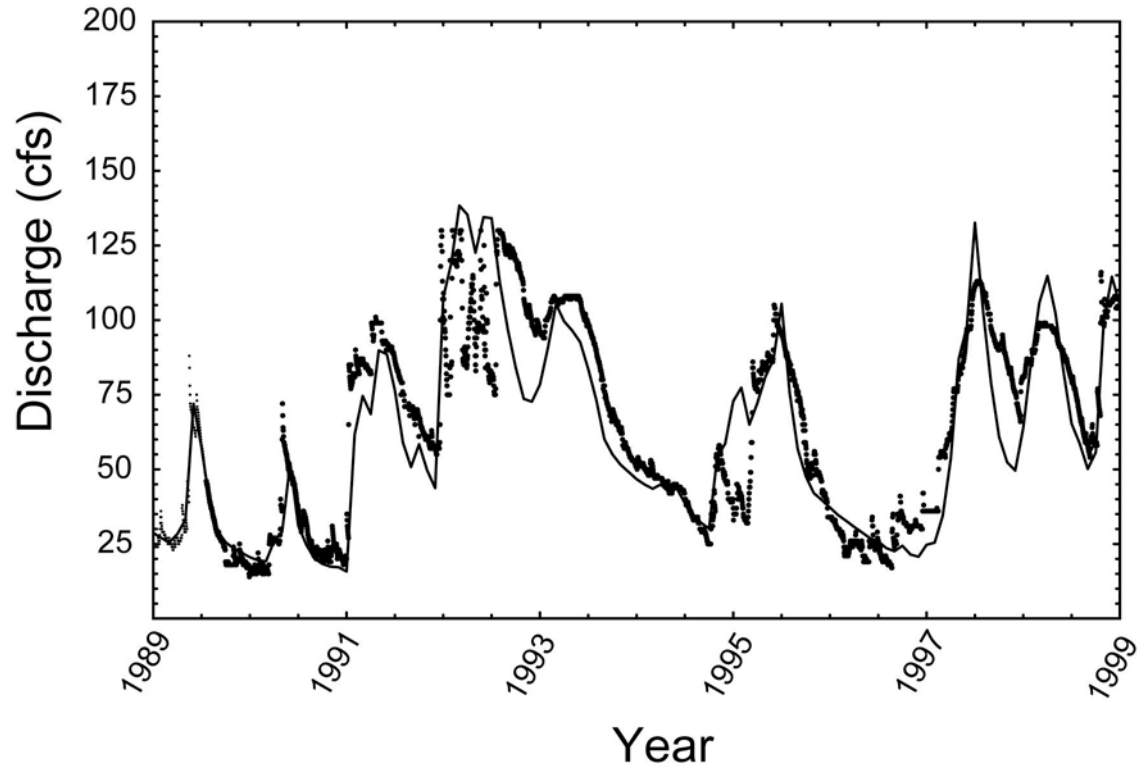


Figure 3.14 Barton Springs discharge versus time. Measured discharge indicated by dots and simulated discharge indicated by solid line.

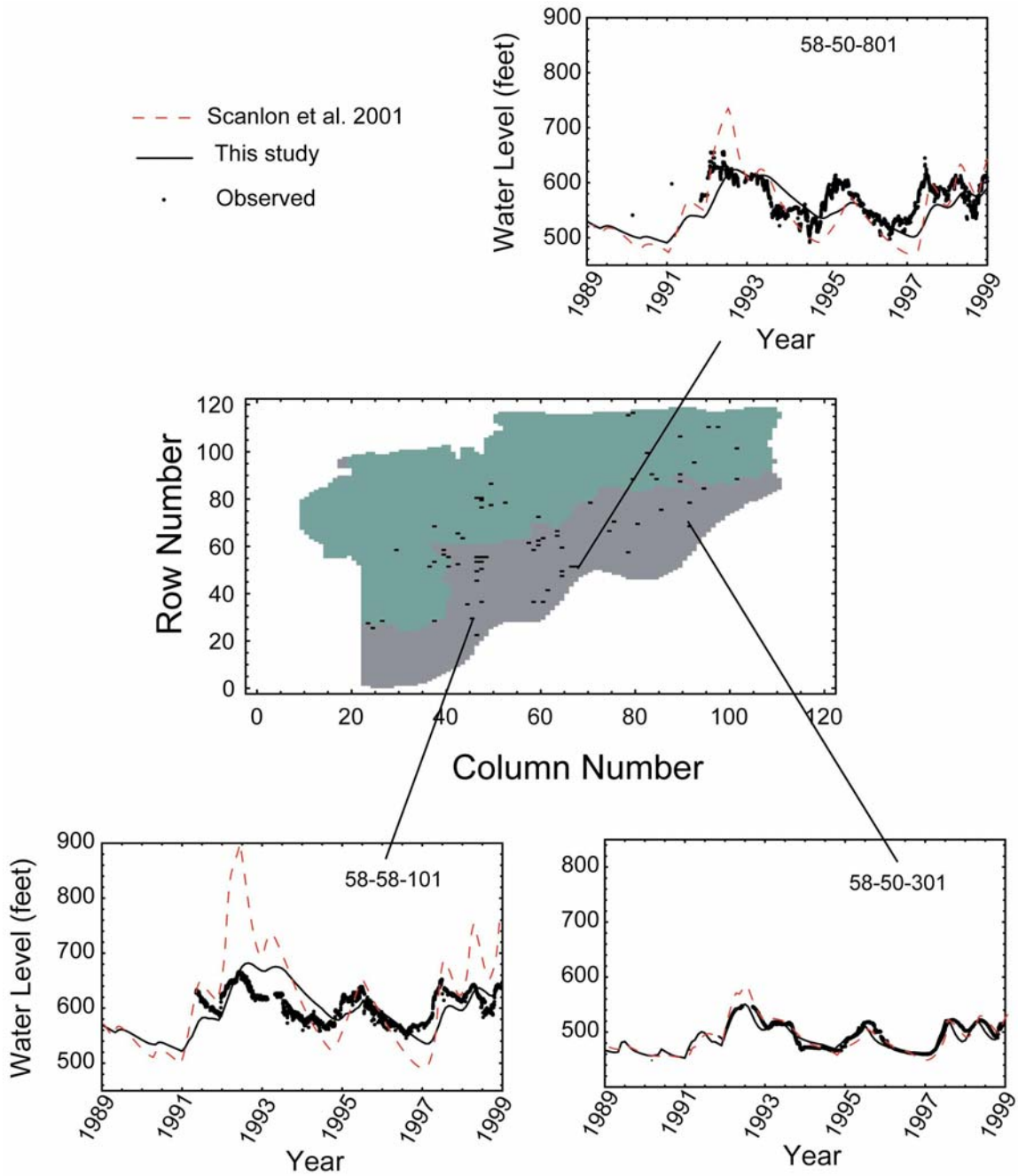


Figure 3.15 Groundwater elevation hydrographs for three wells.

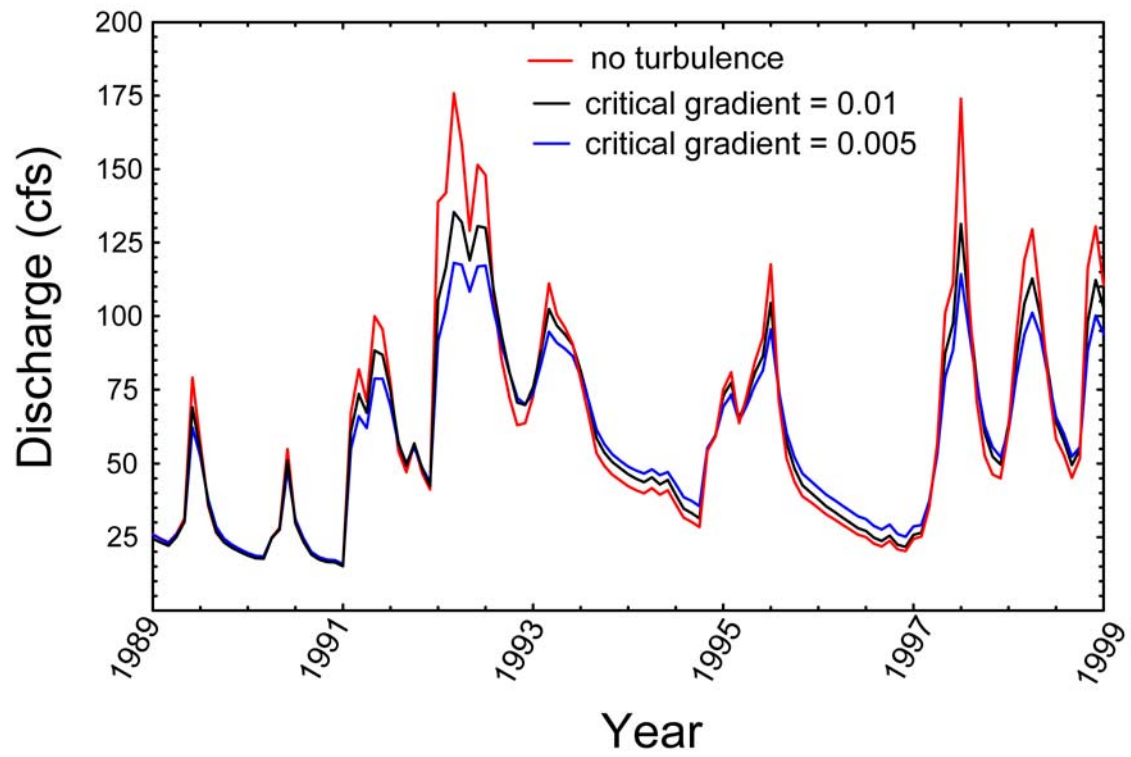


Figure 3.16 Barton Springs discharge for the period 1989 to 1998 for three values of the critical gradient.

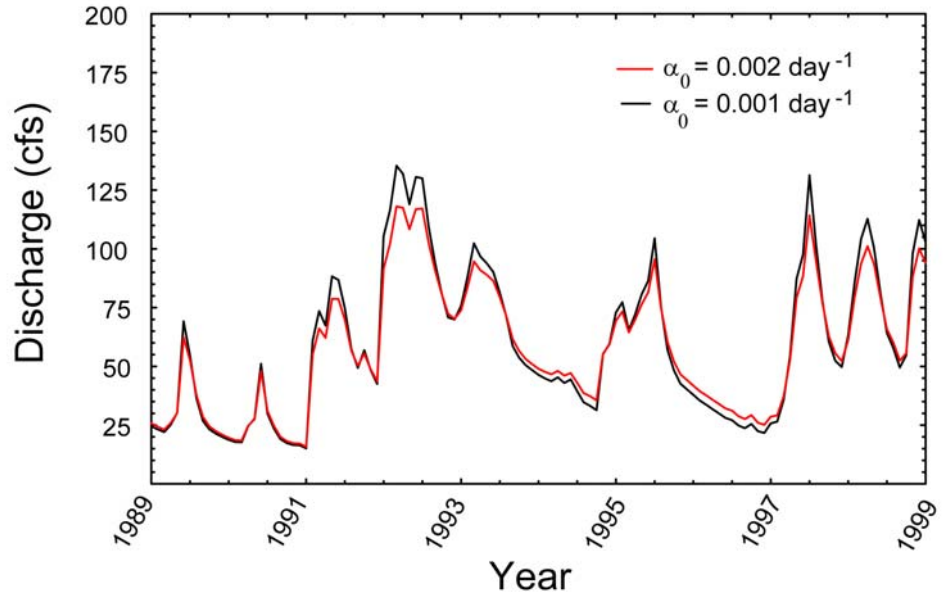


Figure 3.17 Barton Springs discharge for the period 1989 to 1998 for two different values of the exchange parameter.

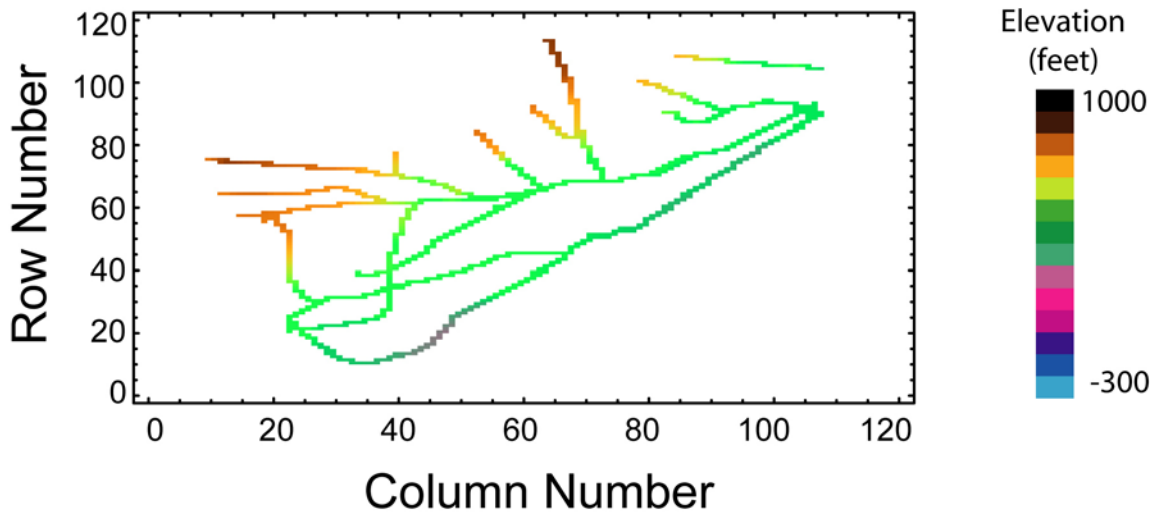


Figure 3.18 Revised conduit bottom elevation used in the drought-condition simulations.

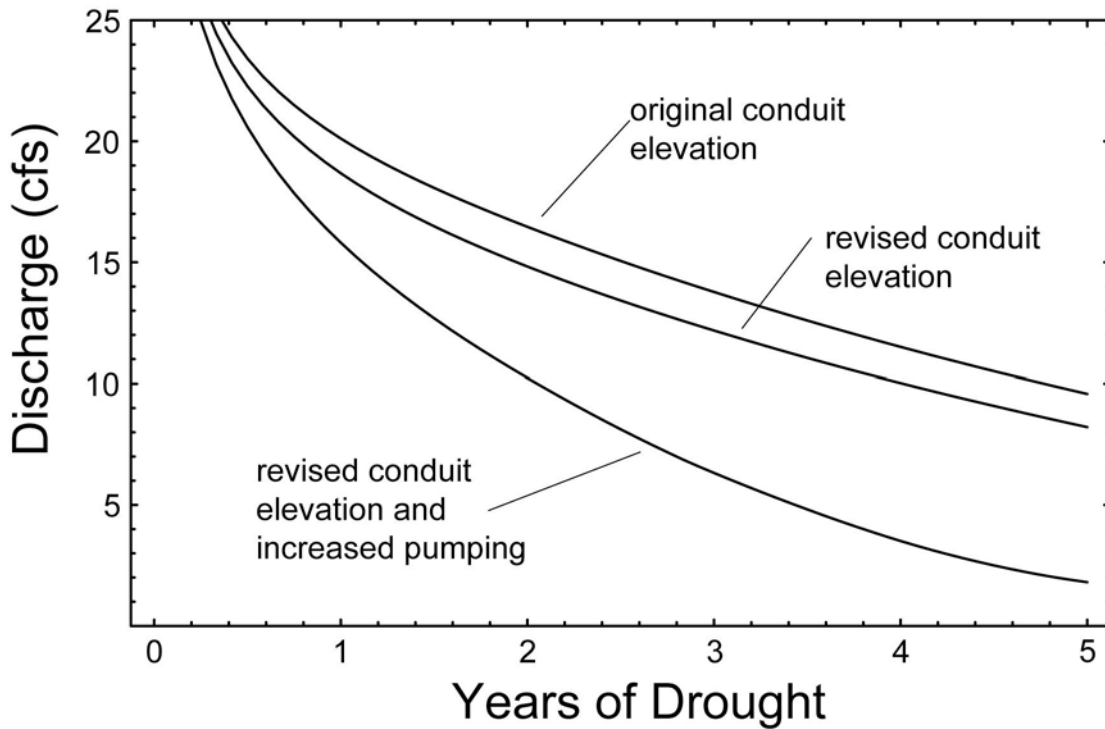


Figure 3.19 Barton Springs simulated discharge hydrographs for hypothetical drought conditions.

CHAPTER 4

DCM MODEL OF THE SANTA FE RIVER SINK/RISE SYSTEM OF THE FLORIDAN AQUIFER

BACKGROUND

The Santa Fe River Sink/Rise system was selected as the site to test MODFLOW-DCM to simulate conduit groundwater flow through the Floridan Aquifer because of the relatively extensive information available for the system. Although there is arguably more hydrogeological information available for the Santa Fe River Sink/Rise system compared with other Floridan Aquifer hydraulic systems in north-central Florida, key hydraulic and hydrogeological data are still lacking. However, it is important to remember that the motivation to model a Floridan Aquifer hydraulic system in this project is different from typical groundwater modeling motivation. The objective of this modeling exercise is to evaluate the ability of MODFLOW-DCM to capture the dynamic hydraulic response of a coupled conduit/diffuse flow regime representation of the relatively highly permeable Floridan Aquifer. This objective varies from a typical groundwater modeling objective, which would be to develop a comprehensive model representative for the Santa Fe River Sink/Rise system. The principal difference is that the modeling effort in this exercise does not set a high premium on replicating the entire hydraulic system, only the hydraulic dynamics of the Sink/Rise system.

The Santa Fe River is a tributary to the Suwannee River in north-central Florida. The confluence of the Santa Fe and Suwannee rivers is about 60 mi inland from the Gulf of Mexico (Figure 4.1). The Santa Fe River Sink/Rise system is a component of the Santa Fe River where a 4-mi-long reach of the river sinks below the surface at the River Sink and reappears at the River Rise. The “hidden” segment of the Santa Fe River is exposed at the surface at several karst windows and Sweetwater Lake.

A 60-day period from January 22, 2003 until late March 23, 2003 was selected as a stress period for the assessment of the Santa Fe River Sink/Rise system karst model. This timeframe was selected because it includes well-defined recharge events and because of the significant amount of data that documents the event. For this reason, the following sections in this chapter of the report focus on this time period.

CLIMATE

The mean annual precipitation recorded by the Southeast Regional Climate Center at the High Springs Station (083956) was 52.8 in for the period of 1948—2005 with a 72.04-in maximum in 1979 and a 32.90-in minimum in 1955 (<http://cirrus.dnr.state.sc.us/cgi-bin/sercc/cliMAIN.pl?fl3956>). This mean is similar to the mean annual precipitation of 53.9 in/yr recorded at Lake City, Florida (Hunn and Slack, 1983). Monthly precipitation measured at the High Springs Station for the time leading up to the 60-day stress period starting in early 2003 is presented in Table 4.1. As illustrated, precipitation during 2001 and 2002 did not significantly deviate from the long-term

monthly or annual averages. Daily precipitation measured at O'Leno State Park for the 60-day stress period is illustrated in Figure 4.2 (Martin, 2003).

GEOLOGY

The lithology of the Santa Fe River Sink/Rise system study site is comprised of carbonate rocks that range in age from Eocene to Pliocene with surficial sediments of Pliocene to Holocene age. The Eocene age Floridan unit is the oldest unit that crops out in the study area. The Floridan Aquifer is typically divided into the Upper Floridan Aquifer (UFA) and the Lower Floridan Aquifer (LFA). The UFA is separated from the LFA by a less permeable layer of carbonate rocks belonging to the lower Avon Park Formation (Bush and Johnston, 1988; Martin, 2003). The UFA is comprised of three highly permeable carbonate units: the Suwannee Limestone, Ocala Limestone, and the upper part of the Avon Park Formation (Bush and Johnson, 1988; Martin, 2003). The UFA is characterized as muddy, granular limestones (Sprouse, 2004). Although the UFA is approximately 900 ft thick near the Santa Fe River Rise (Hisert, 1994), only the upper 330 ft provides potable water. Water sampled from the deeper part of the UFA is typically brackish or saline. The LFA, which contains brackish or saline water, is largely undeveloped as a water supply in the study area (Martin, 2003), and is not within the scope of this assessment.

In the eastern portion of the study area, the UFA is overlain by a confining layer comprised of the Hawthorn Group sediments (Hunn and Slack, 1983). The Hawthorn Group is mainly comprised of interbedded clays, clayey sands, sandy clays, clays, and carbonates (Grozos *et al.*, 1992). A surficial aquifer overlies the Hawthorn Group in the eastern portion of the study area; is comprised of sands, sandy clays, and carbonates; and is the uppermost unit in the study area. The stratigraphic column representative of the study area is illustrated in Table 4.2.

PHYSIOGRAPHY

The catchment basin for the Santa Fe River covers about 1,350 mi² extending from Trail Ridge in the east to the confluence with the Suwannee River in the west (Martin, 2003). Within the basin, the Santa Fe River crosses three physiographic provinces: the Northern Highlands, the Central Highlands, and the Western Lowlands. The river originates in the east at Santa Fe Lake in the Northern Highlands plateau. From Santa Fe Lake, the Santa Fe River flows approximately 30 mi to the west into the Central Highlands until it reaches the Cody Scarp, an escarpment that bisects the Santa Fe River basin. The Cody Scarp is the erosional western edge of the Hawthorn Group-capped Central Highlands (Sprouse, 2004) and represents the physical divide between the confined and unconfined UFA (Martin, 2003). The Western Lowlands physiographic province extends west of Cody Scarp where the Hawthorn Group confining unit is absent (Hunn and Slack, 1983; Meyer, 1963; Martin, 2003; Sprouse, 2004). The Hawthorn Group confining unit thickens to the east away from Cody Scarp. Sinkholes have penetrated the confining unit near the Cody Scarp and some of the sinkholes serve as drains for streams and rivers (Hunn and Slack, 1983). The transition zone between the

Northern Highlands and the Western Lowlands is also referred to as the Marginal Zone (Martin, 2003).

The Santa Fe River Sink is an approximately 118-ft-deep sinkhole located at the edge of the Cody Scarp. The Santa Fe River flows into the sinkhole and reappears approximately 3 mi to the southwest in the Western Lowlands as a first magnitude spring at the Santa Fe River Rise. The 4-mi-long conduit connecting the River Sink and River Rise is breached at several karst windows and Sweetwater Lake. Most of the conduit has been physically mapped by cave divers (Old Bellamy Cave Exploration, unpublished report, 2001; Poucher¹) confirming earlier tracer test results using SF₆ (Hisert, 1994).

There are a limited number of known conduits that feed into the main conduit connecting the River Sink to the River Rise. The most extensive of these is the eastern conduit system that enters the main conduit north of Sweetwater Lake (Old Bellamy Cave Exploration, unpublished report, 2001; Poucher¹). This eastern conduit system does not appear to be sourced by a major stream as indicated by the absence of a significant recharge pulse. Sinkholes that connect to the eastern conduit system do not receive significant surface recharge. It is interpreted that this eastern conduit system is largely sourced by groundwater that enters the conduits from intergranular and fracture porosity (Martin and Dean, 2001).

RECHARGE

Recharge to the UFA in the study region varies significantly both spatially and temporally. The greatest variability in recharge of the UFA is between the confined and unconfined regions. Recharge to the unconfined portion of the UFA, where the Hawthorn Group confining layer is absent, is significantly greater than the confined portion of the UFA. Recharge to the unconfined portion of the UFA was estimated by Clark *et al.* (1964) to be 25.0 in. for 1959, which was considered a relatively wet year [64.08 in of precipitation was recorded at High Springs (Southeast Regional Climate Center, 2006)]. Hunn and Slack (1983) estimated the average annual recharge of the unconfined part of the UFA to be 18.1 in/yr using an analysis of recharge of the Ichetucknee Spring watershed, which is located immediately north of the Santa Fe River watershed. In their analysis, they assumed that the watershed of the Ichetucknee Springs covered 400 mi², of which 250 mi² are unconfined and 150 mi² are confined, and that spring discharge averaged 360 cfs. Inherent in this estimate is the assumption that recharge of the unconfined portion of the UFA is 2 in/yr. This assumption was presumably predicated on earlier work by Clark *et al.* (1964), who estimated recharge of the confined region of the UFA in eastern Aluchua County at 1.8 in/yr.

Martin (2003) evaluated potential evapotranspiration to assess the validity of the Hunn and Slack (1983) estimate for recharge. Martin (2003) calculated potential evapotranspiration at O'Leno State Park, located at the River Sink, to be 41.3 in/yr using the Thornthwaite method (Thornthwaite and Mather, 1957). This value for potential evapotranspiration was in agreement with Thornthwaite's (1948) estimate of 41.3—45.3

¹ Poucher, M. "Cave mapping" Personal communication. 2006.

in/yr for a region that included the Santa Fe River basin, Gordon's (1998) value of 42.1 in/yr for June 1996 through May 1997 for the Ichetucknee River basin, and Jacob and Satti's (2001) value of 43.7 in/yr for Gainesville, Florida, located 25 mi south of O'Leno State Park. Martin (2003) plotted estimates of monthly potential evapotranspiration versus precipitation (Figure 4.3) and recharge (Figure 4.4) from which the annual recharge was calculated to be 26.4 in/yr for April 2002 to May 2003, a period when precipitation totaled 67.7 in, and potential evapotranspiration totaled 41.3 in. Average annual precipitation for the study area is given as 52.8 in/yr (Southeast Regional Climate Center, 2006) to 53.9 in/yr (Hunn and Slack, 1983) suggesting that long-term recharge would be approximately 11.4 to 12.6 in/yr if actual transpiration were to equal potential evapotranspiration, somewhat less than the 18.1 in/yr estimate by Hunn and Slack (1983). The annual recharge value of 18.1 in/yr calculated using a water balance evaluation (Hunn and Slack, 1983) was believed to be more representative of the study area at the onset of this project because the Thornthwaite (Thornthwaite and Mather, 1957) method does not explicitly account for high infiltration rates appropriate for the highly developed karst geomorphology of the unconfined zone.

Recharge was also evaluated in terms of its percentage of precipitation. The amount of recharge realized from precipitation is a complex function of several factors, including sunlight, heat index, wind, and antecedent soil moisture. However, in the absence of these detailed data for the period of performance, the percentage of precipitation that eventually becomes recharge was directly calculated using existing measurements, calculations, and estimates for precipitation and recharge. Using this method, it was estimated that 39% of precipitation was recharged in 1959 based on the recharge estimate of 25.0 in by Clark *et al.* (1964) and precipitation of 64.2 in measured at High Springs. A value of approximately 34% was calculated for the percentage of precipitation that becomes recharge based an average annual precipitation of 52.8 to 53.9 in and a recharge estimate of 18.1 in (Hunn and Slack, 1983). This slightly lower percentage is believed to be more representative of long-term average conditions compared with the wet conditions of 1959. Precipitation and recharge values calculated for 34% for the period 2001 through 2003 are presented in Table 4.3. The percentage decreases to 21 to 24% if actual evapotranspiration approaches the estimates of potential evapotranspiration (41.3 to 45.3 in/yr) and if the annual precipitation is 52.8 to 53.9 in/yr. This analysis suggests that recharge of the unconfined zone would be somewhat lower at 11.1 to 12.9 in/yr.

HYDROLOGY

There are three fresh-water aquifers in north-central Florida. The UFA is the principal aquifer in the study area. The other two aquifers, the surficial aquifer in the surficial sediments and the intermediate aquifer in the carbonate beds of the Hawthorn Group, are minor (Hunn and Slack, 1983; Martin, 2003; Sprouse, 2004). Both minor aquifers, in localities where they exist, are found in the units above the UFA.

The surficial aquifer is only found where the Hawthorn Group confining unit overlies the UFA, which is limited to areas northeast of the Cody Scarp. The surficial

aquifer is recharged by local precipitation and by water discharged from water-bearing zones in those parts of the confining bed located upgradient from the surficial aquifer. Overlying the confined zone of the UFA is a significant river system that receives its base flow from the surficial aquifer and from other water-yielding zones in the confining bed (Hunn and Slack, 1983). In localities where the water-yielding units in the Hawthorn Group confining unit are sufficiently significant, these units are considered the intermediate aquifer. Typically, the intermediate aquifer is comprised of carbonate units of the Hawthorn Group (Sprouse, 2004).

The water table of the surficial aquifer is found at a depth of approximately 10 ft below ground surface near the Cody Scarp. This depth increases to 30 ft in the northeastern side of the study area (Sprouse, 2004). Because the surficial aquifer is about 16 ft thick in the Northern Highlands, parts of the surficial aquifer are entirely unsaturated, and the water table is found in the intermediate aquifer.

The surficial and intermediate aquifers are not hydraulically well connected with the UFA where the Hawthorn Group confining unit is substantial. However, since the water level in the surficial and intermediate aquifers is typically higher than in the UFA, there is the potential for recharge to the UFA by these aquifers. Regardless of this potential, actual recharge from the surficial and intermediate aquifers is minimal (estimated to be no more than 2 in/yr in localities away from Cody Scarp where the confining unit is relatively thick and has a low hydraulic conductivity).

Omission of the surficial or intermediate aquifers in the analysis of this report does not significantly compromise the representation of the Santa Fe River Sink/Rise System as a single unit aquifer. Any contribution of flow to the UFA hydrogeological regime by the surficial or the intermediate aquifers is accommodated by including their recharge contributions to the value assigned to distributed recharge of the UFA. There is insufficient understanding whether there is focused recharge from the river channels in the confined zone.

Because of the absence of a confining bed in the Western Lowlands physiographic province, the UFA is not confined to the southwest of Cody Scarp. It is noteworthy that there are limited tributaries to the Santa Fe River downstream from the Santa Fe River Rise (Martin, 2003). Rivers that are found over the unconfined portion of the UFA are typically surface expressions of the water table. Also within the unconfined zone of the UFA, there is considerable karst development as evidenced by numerous sinkholes and other karst features, including at least 22 springs within $\frac{1}{4}$ -mi downstream of the River Rise, indicating that the river is gaining along this reach (Hisert, 1994). Hisert (1994) indicated that river discharge increased from 966 to 1,691 cfs in the 2-mi reach downstream from the River Rise. Hunn and Slack (1983) estimated that during a period of low river stage on April 14, 1977, river discharge was 128 cfs at the River Sink and 275 cfs at a location $\frac{1}{4}$ -mi downstream of the River Rise. The 157 cfs gain in discharge along the $\frac{1}{4}$ -mi reach of the Santa Fe River was attributed to influx via storage water from the matrix in the conduit segment and via springs and influx from the riverbed in the $\frac{1}{4}$ -mile reach downstream from the River Rise. Precipitation in the months leading

up to April 1977 was similar to the long-term mean. The exception was 1.45 in recorded in March 1977, which was less than the long-term mean of 4.19 in for the month of March (Table 4.1).

Regional-scale hydrogeological investigations of north-central Florida provide consistent interpretations that the regional trend of groundwater flow in the UFA in the study area is to the southwest. The regional direction of groundwater flow in the UFA in the study area for predevelopment conditions was determined by Bush and Johnston (1988) to be southwest of a regional high in the water table near the intersection of Alachua, Bradford, Clay, and Putman counties toward a regional low in the water table in Levy County. Slightly different regional trends in flow were indicated by Fisk and Rosenau (1977) and Hunn and Slack (1983) for 1976; however, they also interpreted the direction of regional groundwater flow of the UFA to be to the southwest in the study area. In a recent analysis, Planert and Grubbs (2004) determined the potentiometric surface in 1990 to be to the southwest. Groundwater flow in 1993—1994 in the area that includes that study was also determined to be to the southwest by Sepúlveda (2002), although a significant depression in the potentiometric surface had developed in central Aluchua County near Gainesville.

The direction of groundwater flow at the relatively small-scale study site, however, is strongly influenced by local-scale variations in regional-scale physiographic features such as Cody Scarp, the extent of the confined and unconfined areas, the Santa Fe River, and topographic relief. Groundwater flow at the local scale is also influenced by the presence of sinkholes (focused recharge), springs (focused discharge), and the presence of surface water (rivers). Establishing the local direction of flow for the study area was problematic due to the lack of extensive local groundwater elevation data. The steady-state potentiometric surface of the study site was determined for use in this project using the current two-dimensional groundwater flow model under development (Schneider²). This model indicates that the greatest influences to the potentiometric surface at the scale of this study are the Santa Fe and Suwannee rivers. Their combined effect is to shift the local direction of groundwater to the west compared with regional models that indicate flow is to the southwest.

Water-level elevation measurements at wells and rivers that were collected by the SRWMD and the University of Florida (Martin, 2003; Martin *et al.*, 2006) are used in this study to evaluate the capability of the MODFLOW-DCM to replicate the conduit/diffuse groundwater flow regime at the Santa Fe River Sink/Rise system. The most useful data were collected at a relatively high frequency (i.e., 10-minute intervals) for a period of 15 weeks (December 13, 2002, to March 28, 2003)(Screaton³). These data included measurements taken at the River Sink, River Rise, Sweetwater Lake, and two nearby wells, referred to as Tower Well and Well 4 (Figure 4.5). Complete records for this 15-week period are only available for the River Sink, River Rise, Sweetwater Lake, and the Tower Well. Data from Well 4 were collected for the 9-week period of January 22, 2003, to March 28, 2003. Data for the High Springs well (081703001) were provided

² Schneider, J. "Draft groundwater model" Personal communication. 2006.

³ Screaton, L. "Hydrogeological data" Personal communication. 2006.

by the SRWMD (Wetherington⁴) (Figure 4.6). Several other wells mentioned in the University of Florida study (Wells 3, 5, and 6) were located close to Well 4, and the water levels in those wells can be effectively represented by Well 4. Only a partial record was available for Well 1 and Well 2. The Sweetwater Lake is halfway between the River Sink and River Rise, and the High Springs well is located approximately 6 mi south of the River Sink.

Water-level elevations recorded in a well in High Springs and from the Santa Fe River at the Highway 441 bridge during this period also proved to be useful. The High Springs well is located about 2.4 mi east from where the river crosses under Highway 441. Water-level elevations recorded at these two monitoring locations for the period including December 13, 2002, to March 28, 2003, are illustrated in Figure 4.7. Hourly water-level elevation measurements collected during the recharge event in mid-March 2003 indicate that the time lag between peak water-level elevations at the river and 2.4 mi from the river was about 23 hrs (Figure 4.8). The peak river water elevation of 38.57 ft mean sea level (msl) exceeded the peak well water-level elevation of 36.74 ft msl by 1.83 ft indicating the modulating effect of the karst matrix on pressure waves.

HYDRAULIC RELATIONSHIP BETWEEN THE CONDUIT AND THE MATRIX

Significant hydrogeological investigations have been performed at the Santa Fe River system, and although not all aspects of the complex hydraulic system are well understood, it is recognized that both conduits and the matrix contribute to conveyance of water through the Santa Fe River Sink/Rise system (Martin and Sreaton, 2001). The hydraulic relationship between matrix and conduit flow in the reach between the River Sink and the River Rise has been evaluated in terms of temperature (Martin and Dean, 1999; Sreaton *et al.*, 2004), chemistry (Martin and Dean, 2001), and well hydraulics (Martin, 2003; Martin and Sreaton, 2003; Sreaton *et al.*, 2004; Martin *et al.*, 2006).

Martin and Dean (1999) measured temporal variations in temperature at the River Sink, Sweetwater Lake (a karst window approximately midway between the River Sink and River Rise), and River Rise to provide insight on the residence time of water flowing through the Santa Fe River Sink/Rise system. Their observations indicate that water travel times vary with river stage and range from 12 hours to more than 4 days between the River Sink and Sweetwater Lake at high and low stage and range from about 6 hours to almost 2 days between Sweetwater Lake and the River Rise at high and low stage.

Martin and Dean (2001) evaluated the exchange of water between conduits and diffuse system in the Santa Fe River Sink/Rise system using chemical analyses of water collected at the River Sink and River Rise, wells located near both of these features, and Sweetwater Lake. Martin and Dean (2001) used available discharge measurements to show that more water discharges from the River Rise than enters the River Sink at low to intermediate discharge rates. Sulfate measurements indicated that a probable source for this additional water is the eastern conduit system.

⁴ Wetherington, M. "Groundwater elevation data" Personal communication. 2006.

Martin and Dean (2001) also interpreted that the fraction of water discharged at the River Rise contributed by the River Sink increases with increased discharge. This means that a greater portion of the water discharged at the River Rise during high flow comes from the River Sink. This interpretation is supported by the observations that water at the River Sink has similar concentrations of Cl^- and Na^+ during flooding as water at the River Rise. During low flow periods, these concentrations more closely reflect the chemistry of matrix water.

Concentrations of Cl^- and Na^+ from water sampled from an observation well located approximately 1.2 mi downgradient from the River Rise decreased with time after flooding. Because these two constituents are conservative, there is no geologic contribution, and their only source is marine aerosols (Martin and Dean, 2001). Their decreased concentrations observed after flooding suggest that floodwater that originally flowed into the rock matrix was slowly discharged back into the conduits as stage level decreased. Martin and Dean (2001) also noted that floodwaters that enter the rock matrix during high stage are typically undersaturated with respect to calcite, thereby leading to continued dissolution of limestone and development of solution cavities.

The respective contributions of conduits and matrix to groundwater flow are reflected in spring discharge measurements at high and low stage. During flood events and high stage, water recharging the River Sink typically exceeds spring discharge at the River Rise indicating that excess water is being stored in the matrix (Martin and Sreaton, 2001; Martin *et al.*, 2006). This relationship was observed by Hisert (1994), who recorded recharge at the River Sink at 1,105 cfs during a flood event compared with a spring discharge at the River Rise of 967 cfs. Subsequent studies by Martin and Dean (2001) supported this observation. At low river stage, discharge at the River Rise typically exceeds recharge at the River Sink (Martin and Dean, 2001; Sreaton *et al.*, 2004). Martin and Dean (2001) and Sreaton *et al.* (2004) suspect the largest source for this excess discharge is the eastern conduit system northeast of Sweetwater Lake and mapped by cave divers (Old Bellamy Cave Exploration Team, unpublished report, 2001; Michael Poucher, personal communication). No well-developed surface recharge feature similar to the River Sink has been associated with the eastern conduit system. Another source for the excess discharge observed at the River Rise is matrix water draining into the conduit system.

The Santa Fe River Sink/Rise system is potentially more complicated than suggested by these straightforward data and observations. Sreaton *et al.* (2004) noted that during a small precipitation event on March 7, 2002, 162 cfs of recharge was recorded at the River Sink, at the same time 55 cfs of discharge was recorded at the River Rise. Contrary to the prevailing conceptual model, however, specific conductance increased from 74 $\mu\text{S}/\text{cm}$ to 170 $\mu\text{S}/\text{cm}$ to 188 $\mu\text{S}/\text{cm}$ from the River Sink to Sweetwater Lake to the River Rise, respectively. The prevailing conceptual model in which the matrix is being recharged would have predicted a decrease, not an increase, in specific conductance. The increase in specific conductance suggests that water with higher concentrations in specific conductance is, in fact, coming out of storage from the matrix rather than going into storage in the matrix as suggested by recharge and discharge

volumes. Screamton *et al.* (2004) noted, however, that the potential range in variability in specific conductance measurements may have exceeded the range in recorded measurements raising doubts as to their significance. The availability of additional specific conductance data would allow closer examination of the relative contributions by the matrix and conduits to flow.

Analysis of discharge volumes indicated that if there as a single main conduit between the River Sink and the River Rise, it would have a diameter of 72 ft (Screamton *et al.*, 2004). If there were two similarly sized conduits, their diameters would be 52.5 ft (Hisert, 1994). These analyses are predicated on the assumption that the conduits are fully saturated. The assumption of full saturation is supported in observations by cave divers that the conduits were typically 100—130 ft below the water table (Old Bellamy Cave Exploration Team, unpublished report, 2001), with the exception of karst windows where the conduit roof has collapsed, exposing the conduit to the surface.

Passive assessment of hydraulic head values measured in conduits and in the matrix adjoining the conduit system can provide a quantitative measure of the hydraulic relationship between conduits and matrix, which in turn allows for evaluation of fluid exchange. Martin (2003) and Martin *et al.* (2006) used frequent (i.e., 10-minute interval) water-level elevation measurements to determine the transmissivity of the host limestone rock in which the Santa Fe River Sink/Rise system is found.

An analytical solution by Pinder *et al.* (1969) relates fluctuations in river stage to transmissivity and storativity

$$\Delta h_m = \Delta H_m \operatorname{erfc}\left(\frac{x}{2\sqrt{tT/S}}\right) \quad (4-1)$$

where Δh_m is the incremental change in hydraulic head at the well in the m^{th} timestep, ΔH_m is the incremental change in the hydraulic head in the conduit in the m^{th} timestep, x is the distance between the well and the conduit, t is the timestep size, T is transmissivity, and S is storativity. Diffusivity is defined as the transmissivity divided by storativity. Transmissivity, in turn, is defined as the hydraulic conductivity times the aquifer thickness. Therefore, transmissivity can be determined from diffusivity for an assumed value of storativity from whence hydraulic conductivity can be determined for an assigned aquifer thickness. This solution assumes the aquifer is homogeneous and semi-infinite.

Martin (2003) and Martin *et al.* (2006) used hydrographs recorded at three wells (Tower Well, Well 1, and Well 4) over a two-month period in early 2003 to calculate transmissivity. The analytical solution by Pinder *et al.* (1969) was incrementally applied to segments of the hydrographs to calculate transmissivities of 1,722,000 ft²/day (Tower Well) 1,044,000 ft²/day (Well 1) and 10,200 ft²/day (Well 4).

NUMERICAL MODEL

Existing numerical groundwater flow models that included the Santa Fe River Sink/Rise system area were regional in extent. Although the resolution of these models was too coarse to allow their use in evaluating the Sink/Rise system, parameter property characterization, boundary conditions, and input and output fluxes from these regional models were useful in developing the model used in this assessment. The U.S. Geological Survey (USGS) regional groundwater flow model of the Florida peninsula by Sepúlveda (2002) provided property values for the UFA and hydrogeologic information from which boundary conditions for a local-scale model could be extracted. Of the numerous preexisting groundwater flow models that were subsumed by the Sepúlveda model, only a model by Motz (1995) extended into the Santa Fe River Sink/Rise system area, but even the Motz model did not cover the entire study area.

The Sepúlveda model had four layers of which the UFA was the third layer. The top two layers represented surficial and the intermediate aquifers. A uniformly spaced grid of 5,000-ft cells was used to discretize this larger model domain (Sepúlveda, 2002). Given the coarseness of the Sepúlveda (2002) model, only approximate values of the media properties and boundary conditions could be extracted.

Additional insight on groundwater flow in the study area was gained through inspection of two draft groundwater models. The first is an SRWMD groundwater model, a DRAFT-INTERIM Version dated September 2005, calibrated to the September 1990 time period (Good⁵). This model is three dimensional and regional in extent. The second draft model is two dimensional and is being developed by SDII-Global (Schneider⁶). The SDII-Global model is also regional in extent and is anticipated to eventually have extended boundaries compared with the SRWMD model (Good⁵). Results from these draft models have not been explicitly used in this analysis; however, input data (i.e., property values) and hydraulic head distributions were inspected to help identify no-flow and hydraulic head boundaries.

Hisert (1994) noted that the ground and surface water basins for the Santa Fe River do not have the same boundaries. This complexity raises questions regarding the amount of autogenic and allogenic recharge realized by the Santa Fe River basin. This uncertainty in the total volume of recharge of the Santa Fe River basin was taken into consideration, but was not resolved as part of the groundwater modeling exercises of this project.

Conduit-Flow Groundwater Flow Model

A new numerical groundwater model had to be developed for the Santa Fe River Sink/Rise system because existing models were either too coarse or covered too large of an area, thereby precluding sufficient resolution to assess the hydraulics of the Santa Fe

⁵ Good, J. "Groundwater data". Personal communication, 2006.

⁶ Schneider, J. "Draft groundwater model" Personal communication. 2006.

River Sink/Rise system in appropriate detail. The MODFLOW-DCM model of the Santa Fe River Sink/Rise system was developed based upon the two-dimensional regional SRWMD model developed by SDII-Global (Schneider⁷). This regional model was originally developed in GMS[®] (Environmental Modeling Research Laboratory, 2006). The MODFLOW-DCM model domain has approximate dimensions of 45,000 ft by 45,000 ft and is centered over the Santa Fe River Sink/Rise system. Figure 4.5 illustrates the extent of the Santa Fe River Sink/Rise model, in which the locations of the Santa Fe River, River Sink, River Rise, Cody Scarp, and the conduit network mapped by the cave divers (Old Bellamy Cave Exploration, unpublished report, 2001; Poucher⁸) are labeled.

Development of the local-scale Santa Fe River Sink/Rise system model was necessary because the main objective of this project was studying the local impact of the Santa Fe River Sink/Rise system on aquifer dynamics. The area of the local model covers the Santa Fe River Sink/Rise system, a significant portion of the Santa Fe River, and all wells monitored in the University of Florida 2002—2003 studies (Martin, 2003; Sprouse, 2004; Martin *et al.*, 2006). The origin of the Santa Fe River Sink/Rise model is (2550000 ft, 300440 ft) in the State Plane HPGN (Florida North) coordinate system. The model cell dimension is 300 ft by 300 ft.

Late 2002 until early 2003 University of Florida studies yielded a set of water-level and discharge measurements that were collected at relatively high frequency (i.e., 10-minute intervals) for 15 weeks (December 13, 2002, to March 28, 2003) as described before. The relatively comprehensive data set was used to evaluate the capability of MODFLOW-DCM to replicate the conduit/matrix groundwater interactions at and around the Santa Fe River Sink/Rise system (Figure 4.5).

A steady-state model was developed first to provide the initial-head distribution required by the transient-state simulation. The standard steps for creating DCM models were followed. All parameters and boundary conditions were interpolated from the regional model in the first version of the steady-state model. Because the resolution of the Santa Fe River Sink/Rise model is higher than the regional model, a number of refinements were performed to improve the model quality. These refinements included regenerating the top elevation of the model using a more refined 5-ft digital elevation map of the model area and adjusting locations of river cells to match the diffuse map discretization.

The hidden river segment between the River Sink and the River Rise and the exposed segment downstream from the River Rise are represented as conduits. Based on the development of conduit networks into the structure of MODFLOW-DCM, it is understandable that the 4-mi-long underground segment of the Santa Fe River would be represented as a conduit. It is not as intuitive that the Santa Fe River segment downstream from the River Rise would also be represented as a conduit. However, it is important to understand that the river is merely a surface expression of the water table along this reach. The hydraulic relationship between the rock matrix and the conduit in the hidden

⁷ Schneider, J. “Draft groundwater model” Personal communication. 2006.

⁸ Poucher, M. “Cave mapping” Personal communication, 2006.

river segment and between the rock matrix and the surface-flow river segment should be essentially the same; however, the potential for this relationship to be different in the two river segments is evaluated in this study.

Chemical analyses by Martin and Dean (2001) of water collected at River Sink, Sweetwater Lake, and the River Rise support the representation of the hidden segment of river as a conduit. Their analyses indicated that water collected during periods of low flow is near full saturation in terms of calcite. In contrast, during periods of high flow, water sampled from these locations is strongly undersaturated with respect to calcite. This inverse correlation between river stage and calcite concentration is consistent with karst conduit water in which calcite-saturated matrix water contributes to conduit flow during periods of low flow.

Analyses of water collected from the Santa Fe River at Worthington, Florida, and at High Springs, Florida, corroborate the designation of the downstream reach of the Santa Fe River as a conduit (Clark *et al.*, 1964). The Worthington sample point is located in the confined zone approximately 9 mi upstream of the River Sink. The High Springs sample point is located in the unconfined zone approximately 3 mi downstream of the River Rise. Water samples were analyzed for calcium, bicarbonate, and pH. Calcite saturation indices were calculated from these chemical analysis results using PHREEQCI Version 2.8 with an assumed temperature of 20 °C. Calcite saturation and river discharge are plotted versus time for a three-year period from mid-1957 to late 1960 (Figure 4.9). Although data density is sparse at times, two trends are apparent in the plotted results. First, in general, Santa Fe River water was undersaturated with respect to calcite prior to the river entering the River Sink and oversaturated downstream from the River Rise. Second, the degree of calcite saturation of water from both locations decreased during high discharge (i.e., flood) events.

This interpretation of the hydrogeology near Cody Scarp is partially supported by Upchurch (2002), who recognized that surface water from the upper Santa Fe River is undersaturated with respect to calcite. He specifies the area near the Cody Scarp as the Scarp Domain — an area where the sinking streams increases saturation with respect to calcite. Upchurch extends his interpretation by noting that surface water sampled from sinkholes and other karst features in the unconfined portion of the UFA are undersaturated with respect to calcite due to the contribution by rainwaters undersaturated with respect to calcite. Upchurch (2002) notes that it is this undersaturated rainwater that continues to promote the dissolution of limestone and the development of karst features in this area.

Water chemistry analysis results combined with river discharge measurements support an interpretation that the Santa Fe River gains water downstream from the River Rise that is oversaturated with calcite. This oversaturation indicates that the water discharging into the river had been in contact with the limestone matrix long enough to become oversaturated with respect to calcite and that the water was not provided by an overland source that had not spent time in contact with the rock matrix. Water discharge assessments made by Hisert (1994) for the 2-mi-long reach downstream from the River

Rise indicated that this segment of the river gains significant water during both low and high stage. The source of the water along this 2-mi-long reach is presumed to be limestone matrix water based on its high calcite saturation index. The contribution of water from the River Rise during high stage is mostly surface flow as indicated by its low calcite index.

The 4-mi-long underground segment of the Santa Fe River is represented as a conduit with a siphon. The siphon segment is represented as a 118-ft tall vertical conduit at the River Sink connected to a 4-mi-long mostly horizontal segment which terminates with a 115-ft-tall vertical conduit at the River Rise. There is an approximate 3-ft reduction in surface elevation between the River Sink and the River Rise. The conduit has a constant diameter of 72 ft. The dimensions of the siphon segment of the Santa Fe River and a shape file for the actual conduit location were taken from cave diving survey results (Old Bellamy Cave Expedition, unpublished report, 2001; Poucher⁹).

The locations and parameter values of the relevant MODFLOW source/sink packages (i.e., well, drain, and river) were largely extracted from the SDII-Global model, except for the segment of the Santa Fe River downstream from the River Rise (Lower Santa Fe River hereafter), which was modeled as a conduit. Modeling the river as a conduit allows the river stage to vary during the transient simulation. The standard MODFLOW river package assumes constant river stage in each stress period. The exchange parameter (α_0) in the DCM package can be calibrated to function in a similar fashion as the river conductance parameter in the river package. The calibrated value of α_0 is 1.0 day⁻¹ for the Lower Santa Fe River in the steady-state model.

Cody Scarp represents the physical divide between the unconfined and confined aquifer in the study area (Hunn and Slack, 1983; Martin, 2003). Recharge to the two aquifers was calibrated to match the low-flow period in late January 2003, which is the starting time of the transient model. The calibrated recharge values for the confined and unconfined aquifers were 2.0 in/yr and 18.0 in/yr, respectively. These values are consistent with recharge estimates by Hunn and Slack (1983).

The conductivity of the diffusive (i.e., matrix) layer was interpolated from the regional SDII-Global model. The conduit network and the Lower Santa Fe River were treated as two uniform zones. High conductivity values were assigned to the conduit network zone (10^8 ft/day) and to the Lower Santa Fe River zone (2×10^8 ft/d). The exchange parameter (α_0) used for the conduit network was 1.0 day⁻¹. The turbulence mode of the DCM was used (see Chapter 2), and the critical gradient for the onset of the turbulence mode was set to 0.1 ft/ft. The River Sink was modeled as a well with specified discharge (i.e., recharge). River Sink discharge values are from Martin (2003) (Figure 4.10). The estimated sink elevation is 31.2 ft.

Establishing the model boundary conditions was difficult given the limited amount of hydrogeological data available within the limits of this local-scale model. All

⁹ Poucher, M. "Cave mapping" Personal communication, 2006.

boundaries were specified as constant head because of the lack of sufficient natural boundary information in the area of study. This assumption is justified for steady-state and limited (i.e., short term) simulations. Figure 4.11 illustrates the steady-state diffuse continuum hydraulic heads calculated with MODFLOW-DCM. The general groundwater flow direction in the model area is from east to west. The River Rise flux at steady state was estimated to be 170 cfs based on observed discharge measurements on February 1, 2003, a time which was assumed to reflect base-flow conditions during the period of simulation. Calculated heads in several wells were compared to the water-level elevation measurements (Martin 2003; Wetherington¹⁰), and the results are listed in Table 4.4. Note that the calculated heads are in good agreement with the measured heads (the first timestep).

Characterization and location of conduits in a MODFLOW-DCM model are obviously problematic because all conduit locations will never be completely known even in well-characterized conduit systems. The Santa Fe River Sink/Rise system was selected as a test site in this project because the main conduit connecting the River Rise to the River Sink is relatively well characterized. Other features, such as the eastern conduit system, are also relatively well characterized (Old Bellamy Cave Expedition, unpublished report, 2001; Poucher¹¹).

However, much about the Sink/Rise system remains unknown. Quantification and detection of water influxing via the springs and the riverbeds is difficult due to the depth of the river and the dark color of the tannic water (Hisert, 1994; Hunn and Slack, 1983). Because of this difficulty in characterizing flux rates, it is not known whether water entering the Santa Fe River downstream from the River Rise is conveyed as conduit flow or as matrix flow. If the water is indeed conveyed as conduit flow, it is unknown whether this conduit flow should be characterized as part of the main Santa Fe River conduit or whether it should be represented as a separate conduit system with characteristics distinct from the main conduit.

Transient-State Model

As mentioned previously, the purpose of the transient-state simulation was to assess the capability of the MODFLOW-DCM model to replicate karst aquifer interactions. The steady-state simulation provided initial conditions required by the transient-state simulation. Recorded precipitation, spring discharge, and surface and groundwater elevation data were compiled to establish a stress period to evaluate the ability of MODFLOW-DCM to replicate the dynamic hydraulics of the Santa Fe River Sink/Rise system. A stress period covering 60 days from January 22, 2003 until March 23, 2003, was used in the evaluation. Data for the stress period were based on work by Martin (2003) and Martin *et al.* (2006) and augmented by the SRWMD (Wetherington⁴). Monthly precipitation data were recorded by the Southeast Regional Climate Center at the High Springs Station (083956), located approximately 3 mi south of the River Rise. Precipitation data are graphically illustrated in Figures 4.2 and 4.3 and numerically

¹⁰ Wetherington, M. "Groundwater elevation data" Personal communication. 2006.

¹¹ Poucher, M. "Cave mapping" Personal communication, 2006.

presented in Table 4.1. These data provide the most comprehensive compilation of hydraulic head, recharge rates, and discharge rates for the Santa Fe River Sink/Rise system.

The total time period was divided into six stress periods, and each stress period was subsequently divided into multiples of 5-day intervals for reporting purposes (e.g., 25, 15, 5, 5, 5, and 5 days). Table 4.5 lists stress periods used in the transient simulations. Table 4.6 lists the stress periods and timesteps used in the transient simulations. Table 4.7 lists the average water levels during each timestep, which were calculated based on the daily observation data (Martin, 2003; Screamon¹²).

Base Case

A base case model was developed to calibrate the MODFLOW-DCM model parameters so that the simulated discharge rates and hydraulic head values were consistent with observed values. The model was mostly calibrated manually, that is, each variable was changed by trial and error. Given data limitations and uncertainties at this time, a fully calibrated model was beyond the scope of this analysis. Rather, the objective was to establish a base case model so that the relative impact of various parameters on the Santa Fe River Sink/Rise system could be assessed. Therefore, the model was calibrated for the 60-day period of investigation. The diffuse continuum hydraulic head distribution for steady-state conditions is illustrated in Figure 4.11. The predicted head distribution clearly illustrates the effect of the prescribed boundary conditions (i.e., constant head). The prescribed boundary conditions are consistent with hydraulic head values taken from the regional groundwater model (Schneider¹³).

Results for the transient base case are illustrated as diffuse continuum head distribution (Figure 4.12) and observed versus calculated water elevation at the River Sink and the River Rise (Figure 4.13), discharge rates at the River Rise (Figure 4.14), and water elevations at the Tower Well, Sweetwater Lake, High Springs Well, and Well 4 (Figure 4.15). The peak discharge rate corresponds with the March 2003 flood event. The model results indicated that water elevations at the River Sink and River Rise were reproduced well. General trends at the four wells were also captured, but simulated water levels at Tower Well were less responsive than the observed. The inability to capture the minor increase in water elevation near day 30 of the simulation was mostly a reflection of the 5-day long time steps used in the model runs. Discharge rates at the River Rise were also reproduced well in the base case, although once again the event at day 30 was not discernable in the predictions and the peak discharge at day 51 was slightly overpredicted. Comparison of simulated with observed heads at the four calibration wells indicated that head at the Tower Well, located west of the River Sink within the confined zone, was underpredicted during the major discharge event and the head at Well 4, located near the River Rise, was underpredicted during low flow conditions.

¹² Screamon, L. "Hydrogeological data" Personal communication. 2006.

¹³ Schneider, J. "Draft groundwater model!" Personal communication. 2006.

To investigate the sensitivity of the system to different model parameters, additional tests were performed. Three of these cases are reported here: (i) Case I — reduction of the conductivity of the hidden conduit from 1×10^8 to 5×10^7 ft/day; (ii) Case II — reduction of the diffuse conductivity by a factor of five; and (iii) Case III — reduction of the matrix/conduit calibration factor, α_0 , from 1.0 to 0.01. Discharge simulated at the River Rise for all sensitivity cases was essentially the same as in the base case. Head elevations simulated at the Tower Well were below the observed head values during peak flow conditions for all simulations suggesting that the model does not currently capture the flashy response of the Floridan Aquifer near the Tower Well. This may be an indication of conduit flow near the Tower Well that is not currently represented in the model. However, the simulated head at the Tower Well was consistent with observed head values during low flow conditions indicating that local recharge conditions (i.e., thickness and extent of the Hawthorn confining layer) were reasonably well represented in the model. The predicted head at Well 4 was less than the observed head at low flow conditions, but reasonably matched peak flow. Following are discussions of the sensitivity simulation results in terms of calculated diffuse hydraulic head distributions and comparison of predicted heads with observed heads at the four calibration wells.

Case I: Effect of Conduit Conductivity

Case I was developed to investigate the effect of reducing the hydraulic conductivity of the hidden conduit from 1×10^8 to 5×10^7 ft/day. Simulated heads at the calibration wells were not significantly different from the base case. However, the simulated conduit head at the sink was significantly higher. Specifically, the conduit head at the sink peaked at 52.8 feet compared with 47.4 feet for the base case. The simulated value 52.8 feet is significantly higher than the observed water levels. This demonstrates the sensitivity of discharge to the value assigned to the conduit hydraulic conductivity.

Case II: Effect of Matrix Conductivity

Case II was developed to investigate the effect of reducing the diffuse conductivity by a factor of five. Results from Case II were similar to those of Case I. Inspection of the heads simulated at the calibration wells suggests that reducing the conductivity of the diffuse continuum had minimal impact on the model performance.

Case III: Effect of Matrix/Conduit Exchange Parameter

Case III was developed to investigate the effect of reducing the matrix/conduit exchange parameter, α_0 , from 1.0 to 0.01. The calculated hydraulic head distribution for Case III is illustrated in Figure 4.17 and the heads predicted at the four calibration wells are compared with observed values in Figure 4.18. As illustrated in Figure 4-17, the reduction in the exchange parameter had the expected effect of decreasing the rate at which conduit water entered the diffuse continuum. This decrease resulted in less mounding of water in the diffuse continuum in the area near the River Sink, which suggests that observations of transient head near the sink could be used to constrain the

matrix/conduit exchange parameter. Unfortunately, none of the calibration wells was located sufficiently close to the River Sink to constrain the matrix/conduit calibration factor. Inspection of heads predicted at the four calibration wells (Figure 4.18) suggests a slight increase in the flashiness observed at Well 4 when compared with the base case and Cases I and II. This outcome is consistent with the fact that Well 4 is located close to the conduit near the River Rise. The performance at the other three calibration wells was not as good in Case III when compared with the base case, suggesting that a matrix/conduit exchange parameter greater than 0.01 is probably more representative of the modeled domain.

CONCLUSIONS

The matrix/conduit network in the Santa Fe River Sink/Rise system was modeled using the MODFLOW-DCM variant. The model was calibrated for a 60-day period lasting from January 22, 2003, until March 23, 2003. Data for this period were provided by the University of Florida (Martin, 2003) and the SRWMD (Wetherington¹⁴). The model was relatively easily calibrated to the observed data set. This was achieved because water elevations at the River Sink, which were relatively well known, are sensitive to conduit hydraulic conductivity. Secondly, hydraulic head of the diffuse continuum near the conduit is sensitive to the matrix/conduit exchange parameter. Having information on the diffuse head relative to conduit head during significant discharge events would allow for better resolution of the matrix/conduit exchange parameter. Limited diffuse head data near the conduit near the upgradient end of the hidden conduit in the Santa Fe River, however, precluded full evaluation of this relationship.

In general, the MODFLOW-DCM base case model performed well in simulating the dynamic hydraulic system observed at the Santa Fe River Sink/Rise system, although there were secondary features in the simulation results with subtle differences when compared to observed data. Model performance was judged using head values and discharge rates observed during the 60-day study period.

The MODFLOW-DCM model analysis process led to an in-depth evaluation of the hydraulic dynamics of the Santa Fe River Sink/Rise system. Insight on a region greater than the modeled area would be possible with a larger model, obviously, and a longer simulation period. As previously discussed, the scope of this exercise was to model this relatively well-documented system as representative of the Floridan Aquifer to allow assessment of the capability and limitations of MODFLOW-DCM to simulate the flow dynamics of an aquifer with relatively high matrix permeability and large spring systems.

Further improvement in the Santa Fe River Sink/Rise model can be made by:

- Coupling or linking the local Santa Fe River Sink/Rise model with the regional SRWMD model so that the heads and fluxes across the shared boundaries are consistent. This enhancement would minimize the negative impact of prescribing

¹⁴ Wetherington, M. "Groundwater elevation data" Personal communication. 2006.

the model boundaries as constant head, if the regional model accurately represents recharge in the confined zone of the UFA.

- Validating the model outputs with historical data collected from longer periods. When combined with more realistic boundary conditions, this enhancement would make the model more representative of the local hydraulic system, rather than being limited to representing the hydraulic response of the Sink/Rise system.
- Improving the model reliability by calibrating it with data from other locations within the model area, especially with respect to areas near the River Sink to allow refinement and greater evaluation of the matrix/conduit exchange parameter.

Table 4.1 Monthly precipitation values (inches) for 2001—2003 and the mean precipitation values for 1948—2005 at High Springs, Florida (083956) (Southeast Regional Climate Center, 2006)

| Year | Jan | Feb | Mar | Apr | May | Jun | Jul | Aug | Sep | Oct | Nov | Dec | Ann |
|------|------|------|------|------|------|------|-------|------|------|------|------|------|-------|
| 2001 | 1.94 | 0.62 | 6.6 | 0.45 | 1.91 | 7.75 | 13.15 | 3.5 | 7.69 | 0.12 | 0.72 | 0.79 | 45.24 |
| 2002 | 3.88 | 1.46 | 3.82 | 2.96 | 1.27 | 7.45 | 8.5 | 9.41 | 2.68 | 4.05 | 5.57 | 6.92 | 57.97 |
| 2003 | 1.95 | 7.52 | 6.03 | 3.39 | 4.27 | 8.9 | 4.29 | 9.83 | 3.78 | 4 | 1.56 | 1.02 | 56.54 |
| Mean | 3.41 | 3.77 | 4.19 | 3.03 | 3.50 | 6.87 | 7.29 | 7.87 | 4.89 | 2.93 | 2.21 | 2.86 | 52.77 |

Table 4.2 Stratigraphic and hydrostratigraphic units of the Santa Fe River Basin (modified from Sprouse, 2004)

| Series | Stratigraphic Unit | Hydrostratigraphic Unit | | Lithology | Thickness (m) |
|-------------------------------------|---|------------------------------------|-----|---|---------------|
| Holocene Pleistocene Pliocene | Undifferentiated sediments | surficial aquifer | | fine sands and gravel | 0-25 |
| Pliocene to Miocene Miocene | Hawthorn Group sediments | intermediate aquifer/confining bed | | interbedded sands and clays carbonates | 0-45 |
| Oligocene Eocene | Suwannee Limestone Ocala, Avon Park and Oldsmar Formations | Floridan Aquifer System | UFA | porous limestone and dolomite | 325-425 |
| | | | LFA | | |
| Paleocene | Cedar Keys Formation | sub-Floridan Confining Unit | | limestone with some clay and evaporites | ? |

Table 4.3 Recharge (in) estimated as a percentage (34%) of precipitation measured at High Springs, Florida

| Year | Jan | Feb | Mar | April | May | June | July | Aug | Sept | Oct | Nov | Dec |
|------|------|------|------|-------|------|------|------|------|------|------|------|------|
| 2001 | 0.66 | 0.21 | 2.24 | 0.15 | 0.65 | 2.64 | 4.47 | 1.19 | 2.61 | 0.04 | 0.24 | 0.27 |
| 2002 | 1.32 | 0.50 | 1.30 | 1.01 | 0.43 | 2.53 | 2.89 | 3.20 | 0.91 | 1.38 | 1.89 | 2.35 |
| 2003 | 0.66 | 2.56 | 2.05 | 1.15 | 1.45 | 3.03 | 1.46 | 3.34 | 1.29 | 1.36 | 0.53 | 0.35 |

Table 4.4 Simulated and measured steady-state water levels in the wells used for calibration. The steady-state model was calibrated to provide initial conditions for the transient simulation. [Data are feet above NGVD29.]

| Well | Simulated water level (ft) | Measured water level (ft) |
|-------------------|----------------------------|---------------------------|
| Well 4 | 33.0 | 34.7 |
| Sweetwater Lake | 33.0 | 32.6 |
| High Springs Well | 32.7 | 32.0 |
| Tower Well | 33.4 | 33.4 |

Table 4.5 Stress periods used in transient simulation

| Stress Period | Period |
|---------------|-------------------|
| 1 | 1/22/03 – 2/11/03 |
| 2 | 2/11/03 – 2/26/03 |
| 3 | 2/26/03 – 3/3/03 |
| 4 | 3/3/03 – 3/8/03 |
| 5 | 3/8/03 – 3/13/03 |
| 6 | 3/13/03 -3/8/03 |
| 7 | 3/18/03 – 3/23/03 |

Table 4.6 Stress periods and timesteps used in transient simulation

| No. | Stress Period | Simulation Step End Date |
|-----|---------------|--------------------------|
| 1 | 1 | 1/27/03 |
| 2 | 1 | 2/1/03 |
| 3 | 1 | 2/6/03 |
| 4 | 1 | 2/11/03 |
| 5 | 2 | 2/16/03 |
| 6 | 2 | 2/21/03 |
| 7 | 2 | 2/26/03 |
| 8 | 3 | 3/3/03 |
| 9 | 4 | 3/8/03 |
| 10 | 5 | 3/13/03 |
| 11 | 6 | 3/18/03 |
| 12 | 7 | 3/23/03 |

Table 4.7 Averaged water levels for Well 4, Tower Well, and Sweetwater Lake (Martin, 2003) and High Springs well (SRWMD). [Data are feet above NGVD29.]

| No. | Well 4 (ft) | Tower Well (ft) | Sweetwater Lake (ft) | High Springs Well (ft) |
|-----|-------------|-----------------|----------------------|------------------------|
| 1 | 34.74 | 33.40 | 32.55 | 31.95 |
| 2 | 34.55 | 33.17 | 32.41 | 31.87 |
| 3 | 34.38 | 32.97 | 32.28 | 31.80 |
| 4 | 34.55 | 33.07 | 33.10 | 32.17 |
| 5 | 34.88 | 33.37 | 33.56 | 32.41 |
| 6 | 35.96 | 33.92 | 36.12 | 33.45 |
| 7 | 36.55 | 34.65 | 35.37 | 33.24 |
| 8 | 36.91 | 35.17 | 36.38 | 33.59 |
| 9 | 38.35 | 36.09 | 38.91 | 35.02 |
| 10 | 40.42 | 37.30 | 43.14 | 38.27 |
| 11 | 40.91 | 38.71 | 39.86 | 36.26 |
| 12 | 39.73 | 38.78 | 37.17 | 34.47 |

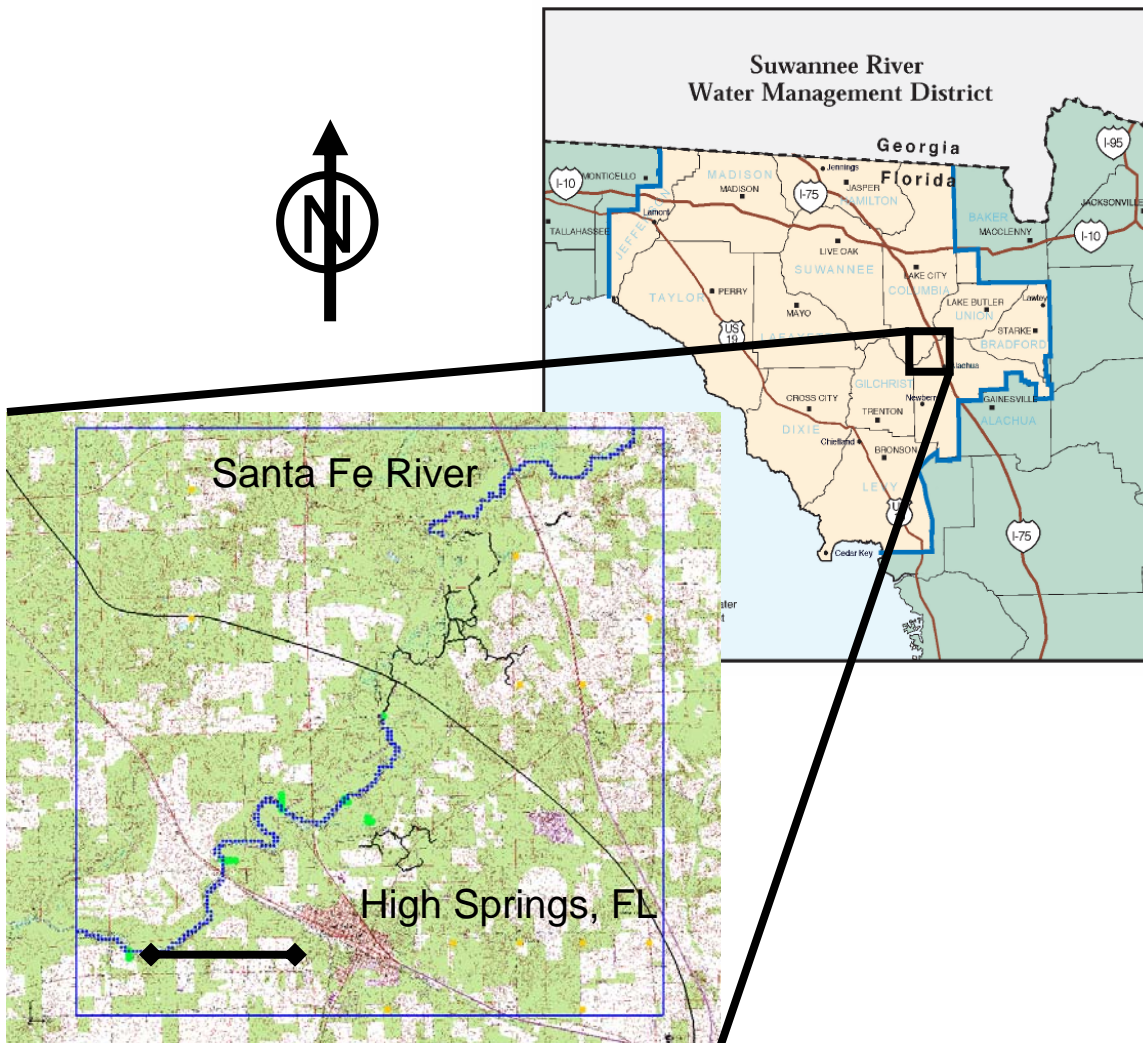


Figure 4.1 Study area of the Santa Fe River Sink/Rise system.

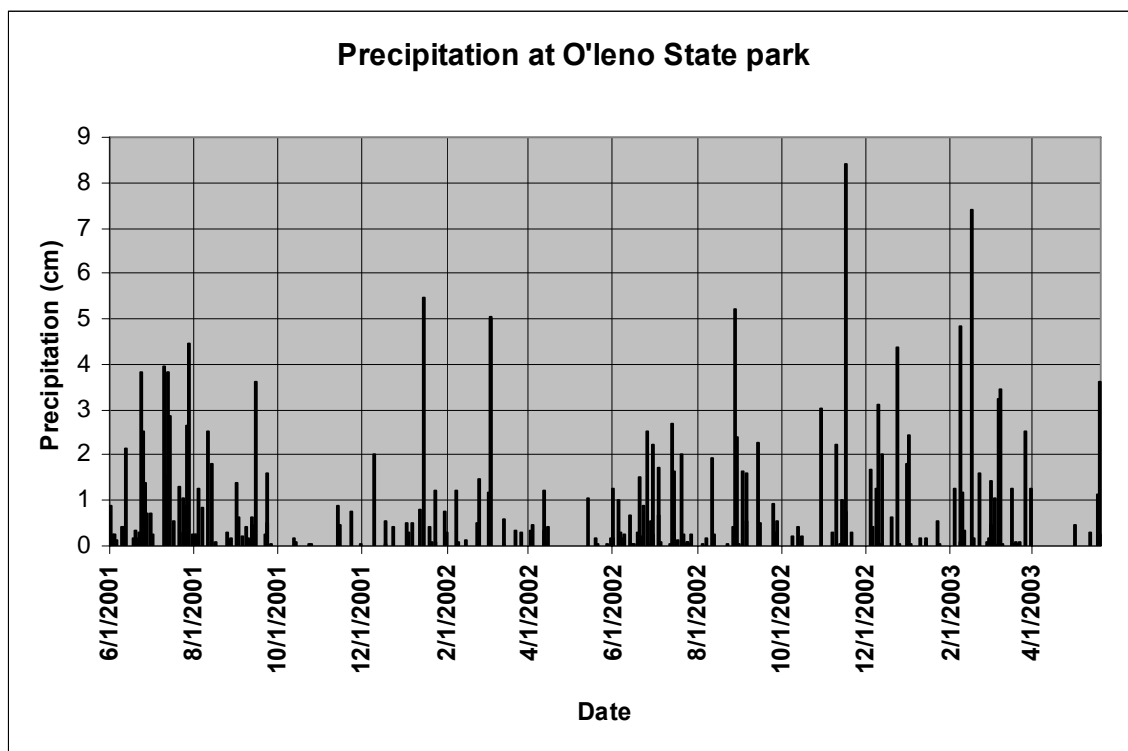


Figure 4.2 Precipitation measured at O’Leno State Park (cm) for the period June 2001 until June 2003 (Martin, 2003; Screamon, personal communication, 2006).

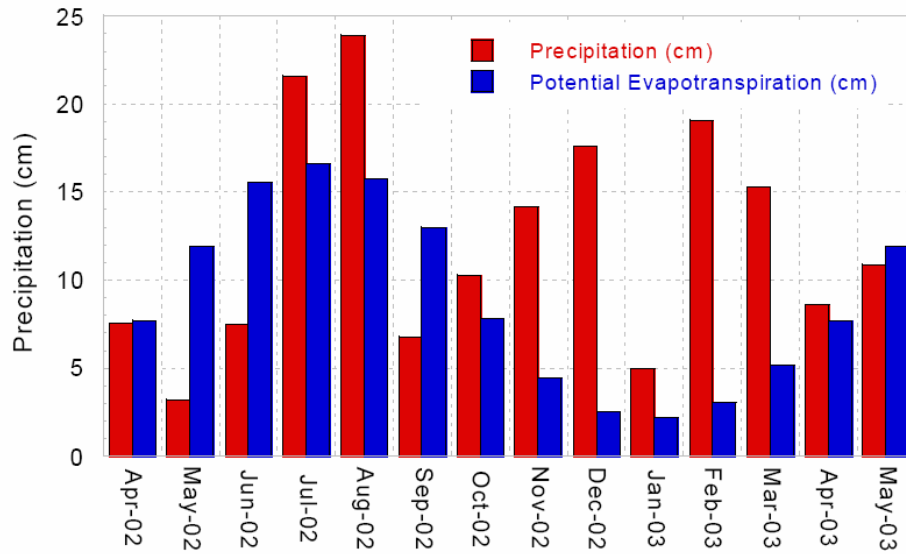


Figure 4.3 Estimates of monthly potential evapotranspiration (cm) versus precipitation (cm) for the period of April 2002 to May 2003 (Martin, 2003). [1 cm = 0.39 inch].

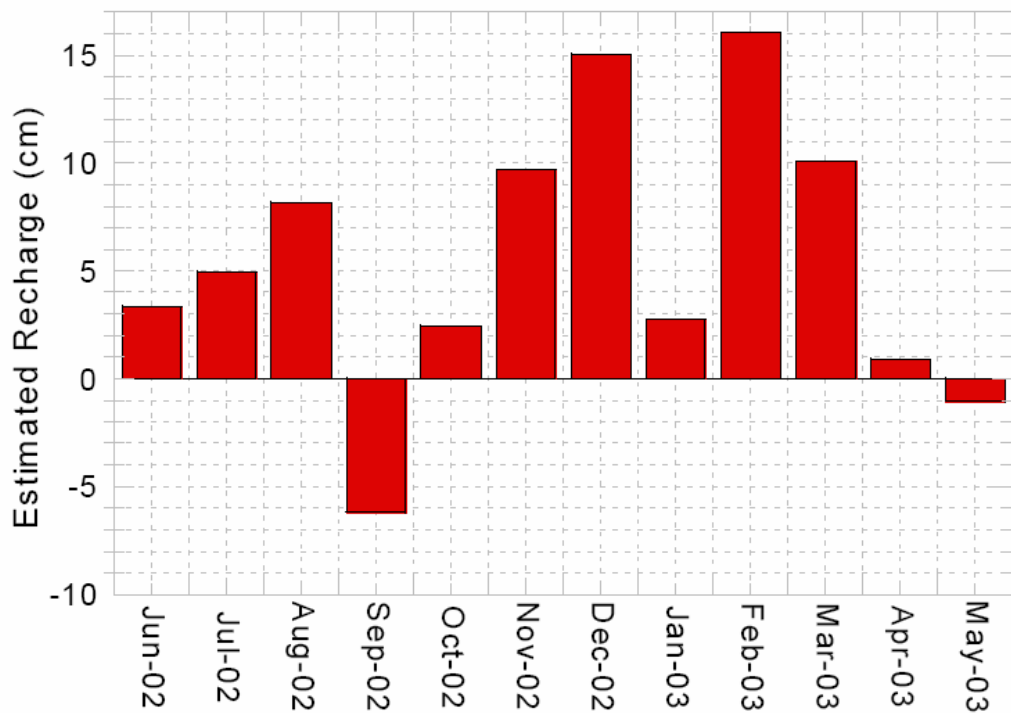


Figure 4.4 Estimates of monthly recharge (cm) for the period of April 2002 to May 2003 (Martin, 2003). [1 cm = 0.39 inch].

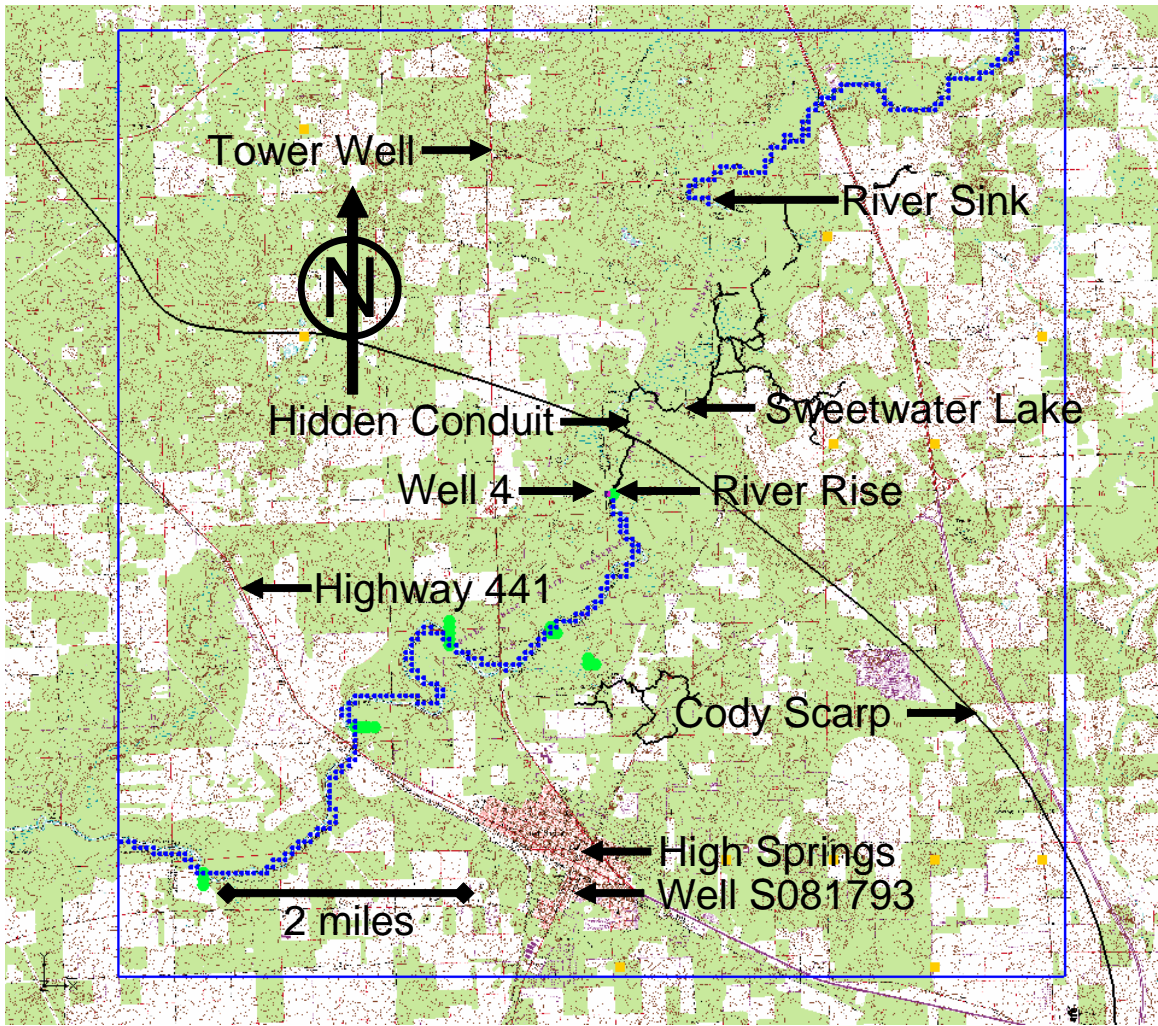


Figure 4.5 Model extent of the Santa Fe River Sink/Rise system. The locations of the Santa Fe River, Sink and Rise, Cody Scarp, conduit network (black lines), and monitoring wells are labeled on the map.

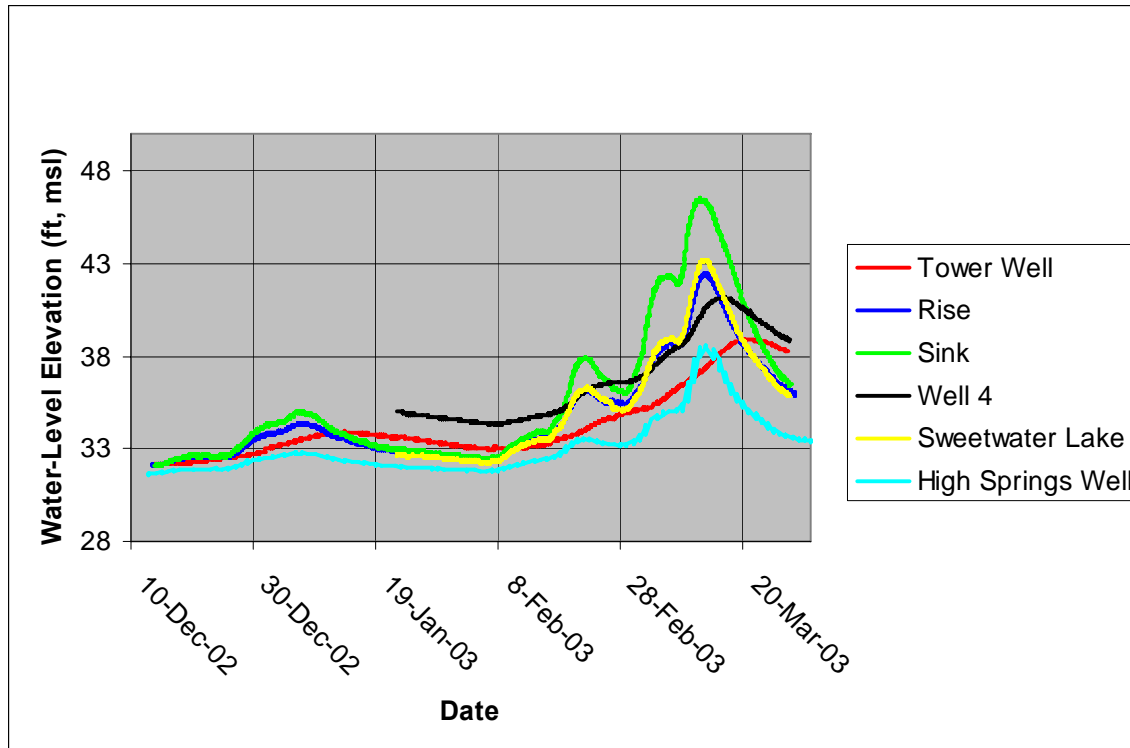


Figure 4.6 Water-level elevations (ft, msl) measured at the River Sink and River Rise, and at the Tower, and 4, and High Springs wells, and at Sweetwater Lake from December 2002 through March 2003.

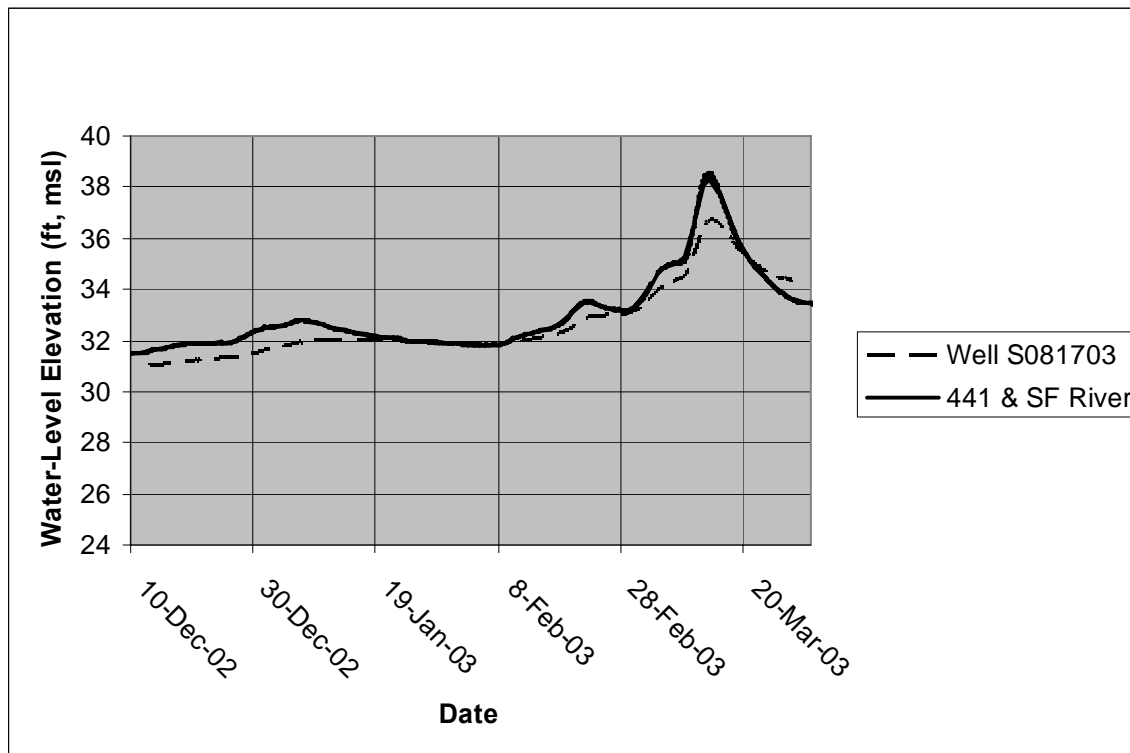


Figure 4.7 Water-level elevations (ft, msl) measured in the Santa Fe River at the Highway 441 Bridge and at well S081703 from December 13, 2002, to March 31, 2003.

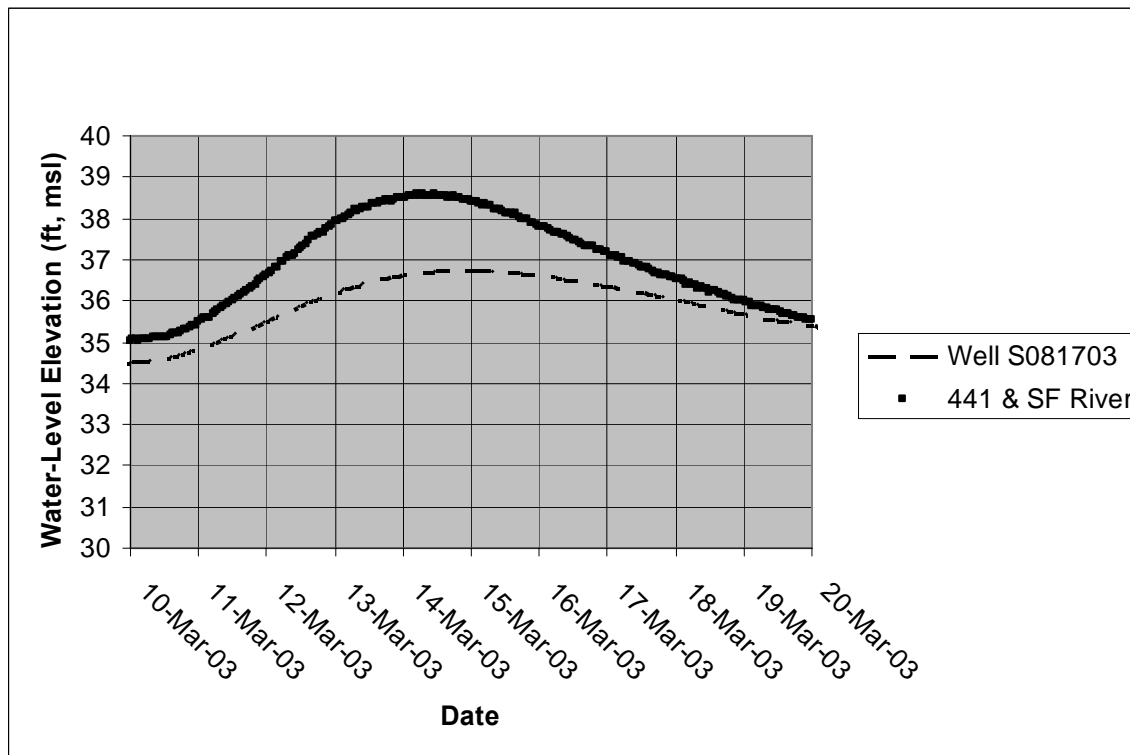


Figure 4.8 Water-level elevations (ft, msl) measured in the Santa Fe River at the Highway 441 Bridge and at Well S081703 from March 10, 2003, to March 20, 2003.

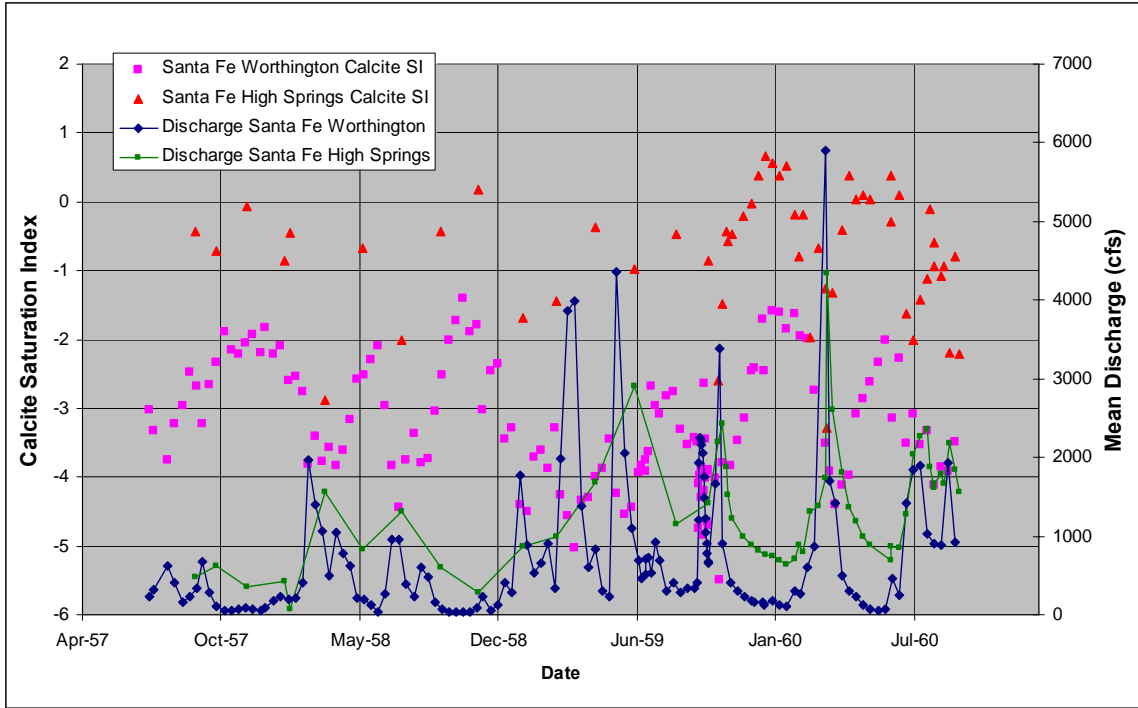


Figure 4.9 Calcite saturation index and river discharge measurements for the Santa Fe River at Worthington, Florida, and High Springs, Florida.

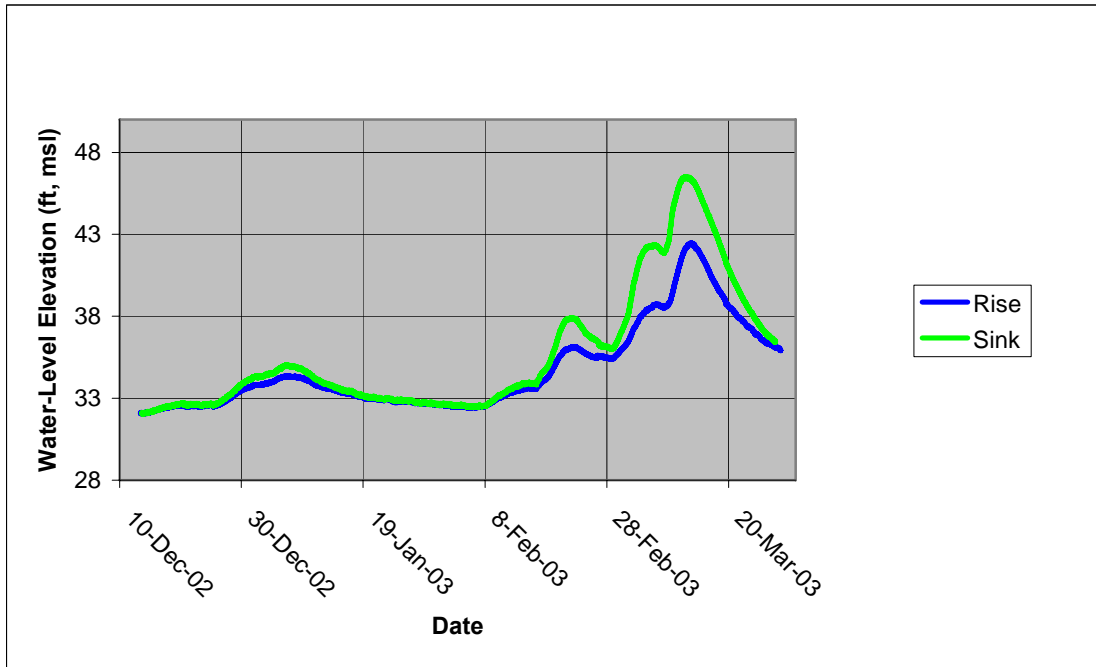


Figure 4.10 Water-level elevations at the River Sink and River Rise (after Martin, 2003).

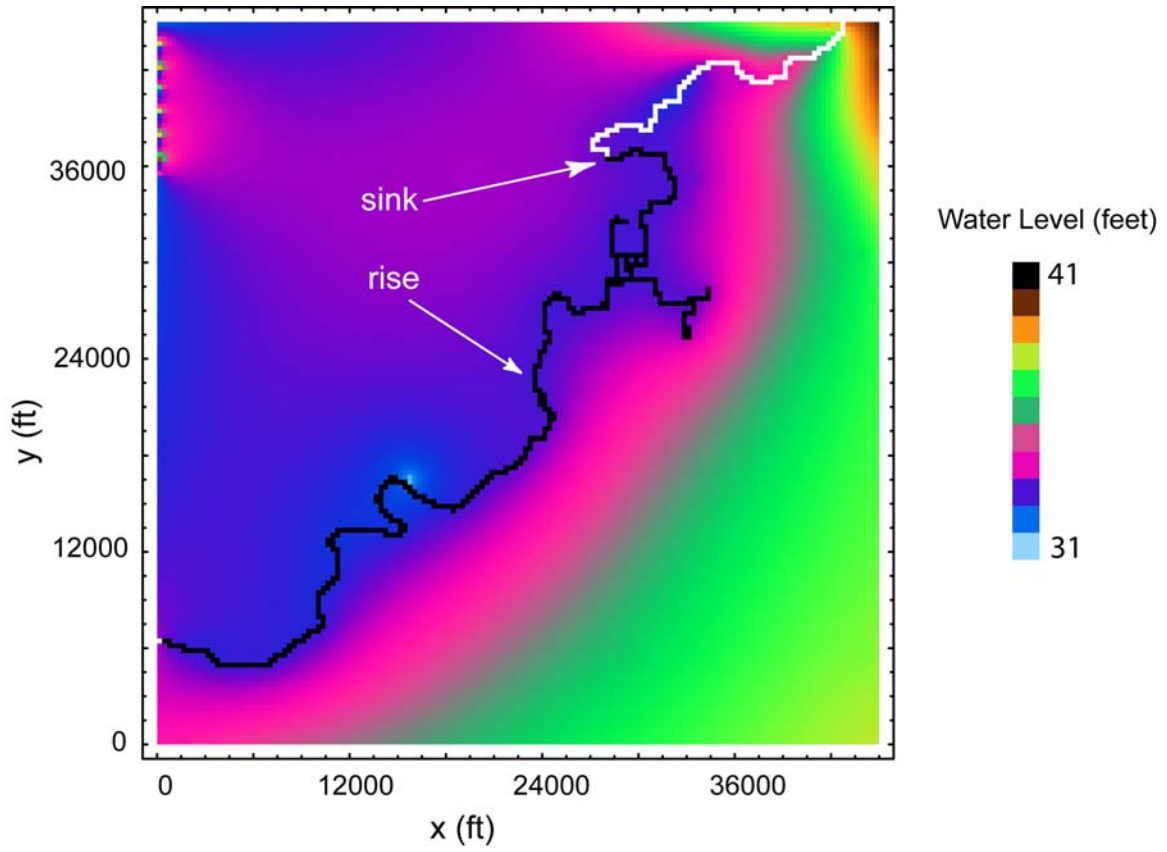


Figure 4.11 Steady-state base case diffuse continuum hydraulic head distribution.
[Data are feet above NGVD29.]

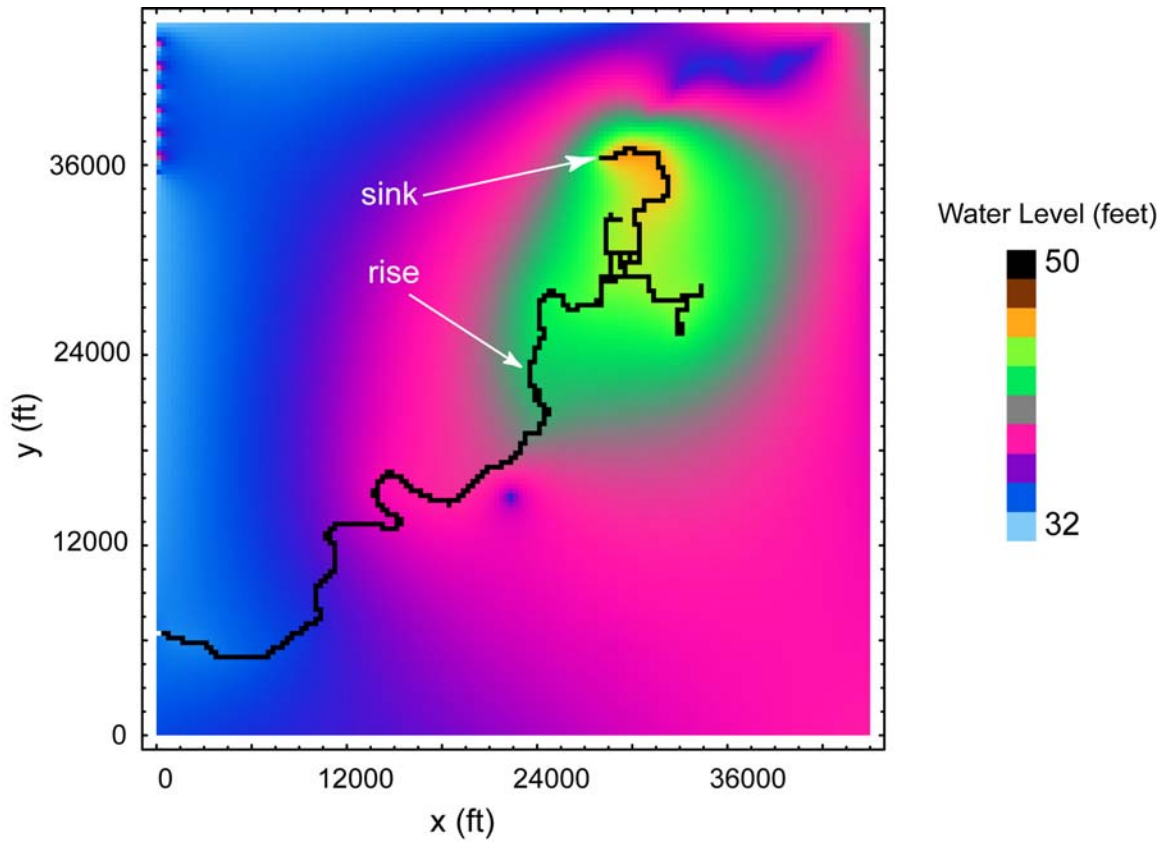


Figure 4.12 Transient base case diffuse continuum hydraulic head distribution during peak discharge. [Data are feet above NGVD29.]

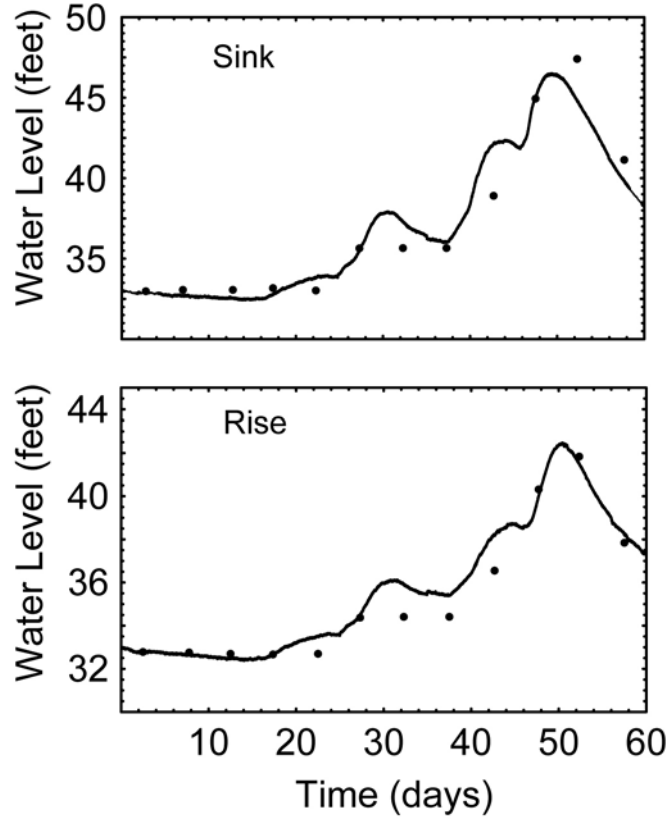


Figure 4.13 Transient River Sink (a) and River Rise (b) elevation for days after start of stress periods (January 22, 2003). The solid lines denote observed water-level elevation and the dots denote simulated water elevation. [Data are feet above NGVD29.]

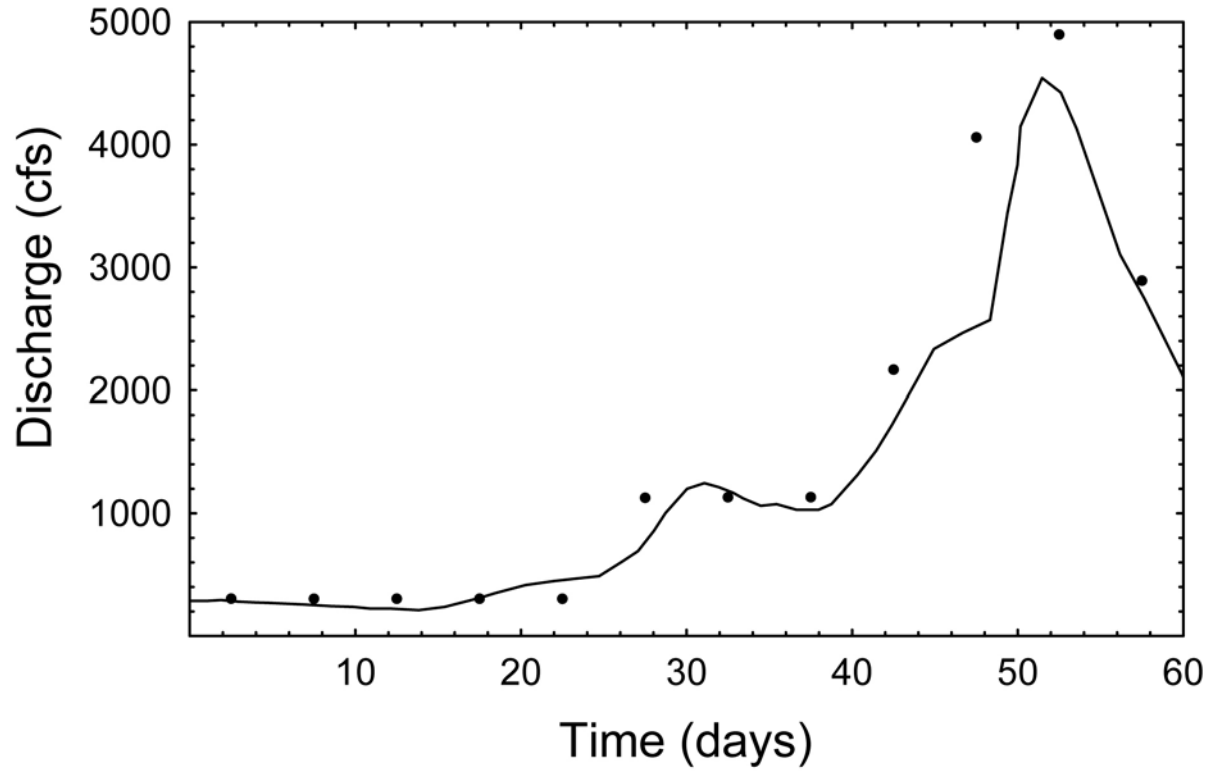


Figure 4.14 River Rise discharge after start of stress periods (January 22, 2003) for the transient base case simulation. The solid line denotes observed discharge and the dots denote simulated discharge.

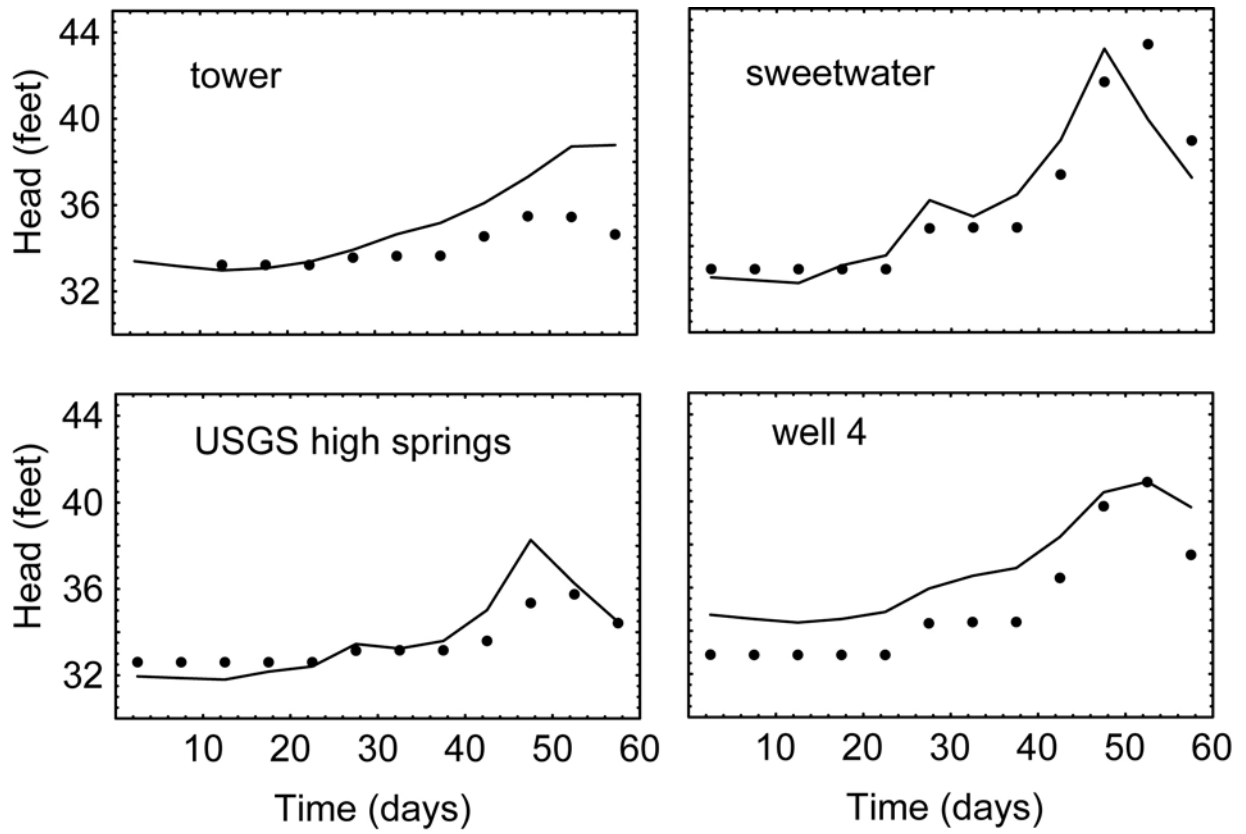


Figure 4.15 Transient base case: simulated versus measured heads (ft) in the calibration wells. The solid line denotes observed discharge and the dots denote simulated discharge. [Data are feet above NGVD29.]

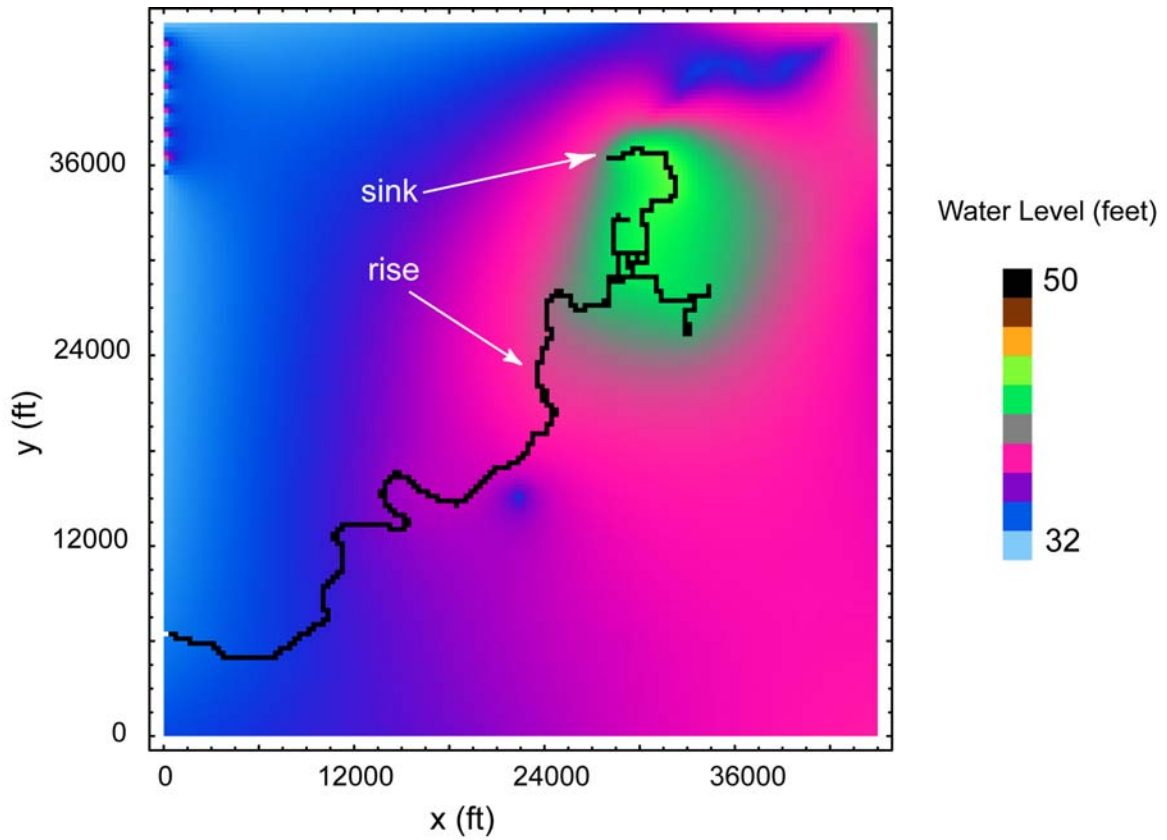


Figure 4.16 Case III. Contour map of the transient head distribution during peak discharge in the diffuse continuum with a reduction in the matrix/conduit exchange parameter α_0 from 1.0 to 0.01. [Data are feet above NGVD29.]

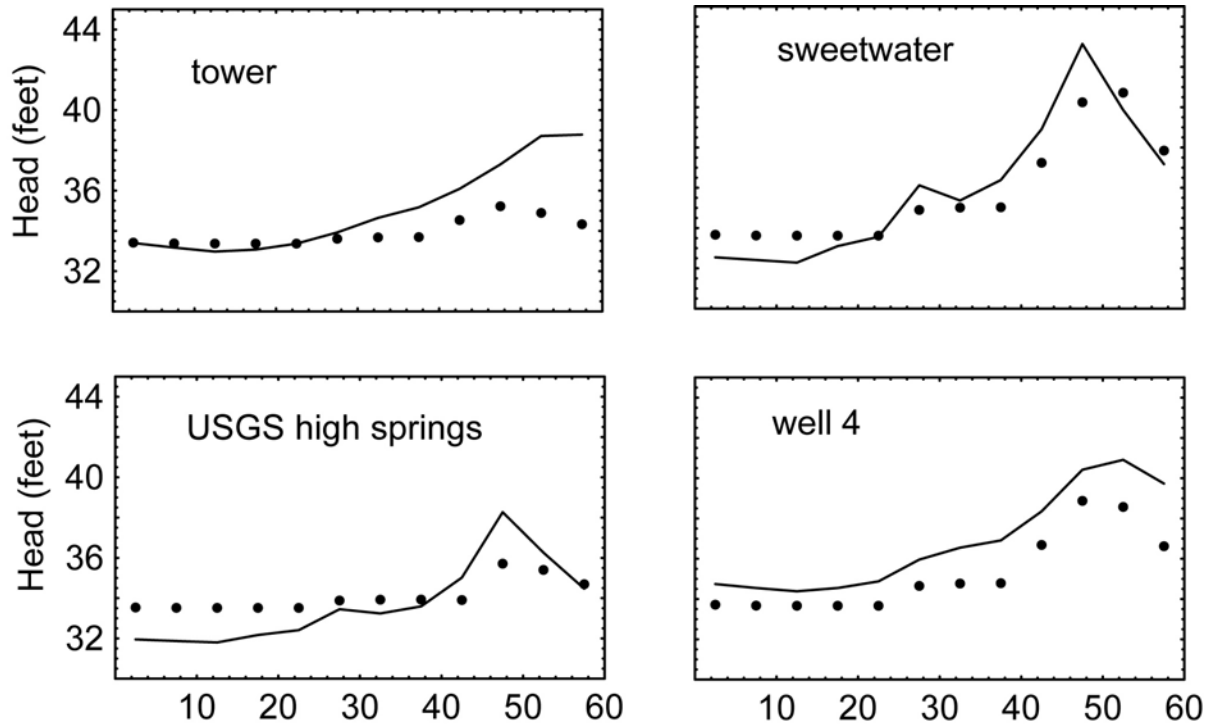


Figure 4.17 Case III. Simulated versus measured heads (ft) in the calibration wells for reduction in the matrix/conduit exchange parameter α_0 from 1.0 to 0.01. The solid lines denote observed water-level elevation and the dots denote simulated water elevation. [Data are feet above NGVD29.]

CHAPTER 5 CONCLUSIONS

DEVELOPMENT OF MODELING TOOL FOR KARST AQUIFERS —PHASE II

The long-term objective of the karst modeling project is to develop new modeling approaches and tools to address applications involving karst aquifers with significant conduit flow. The objective of Phase II was to enhance the karst modeling approach that was developed during the first phase of the karst modeling project. The principal product of Phase II was the development of the conduit modeling variant, MODFLOW-DCM, intended for karst aquifers, but also applicable to other aquifer systems that exhibit strongly preferential flow. As described, the model package is appropriate for two-dimensional karst aquifers, although information in the vertical dimension, namely aquifer and conduit top and bottom elevations, is incorporated. The MODFLOW-DCM variant promises to significantly improve modeling of groundwater flow through conduits located within porous media.

The capability and limitations of the MODFLOW-DCM were assessed by applying it to two karst aquifers that exhibit contrasting hydrogeologic characteristics: the Barton Springs segment of the Edwards Aquifer in south-central Texas and the Santa Fe River Sink/Rise system of the Floridan Aquifer in north-central Florida.

Three primary tasks and two secondary subtasks were implemented to accomplish the objectives of Phase II. Following are summaries of these accomplished tasks.

Task 1. Code Refinement.

DCM Version 1.0, a dual-conductivity model for MODFLOW, was developed in Phase I of the karst modeling project. Version 1.0 was implemented as a self-contained module (“package” in the MODFLOW terminology). Numerical experiments undertaken as part of Phase I revealed poor numerical performance and even convergence failures for DCM Version 1.0. During Phase II, it was discovered that the current solver routines in the standard MODFLOW package are inadequate to support the DCM approach.

A new solver capable of solving the highly nonlinear systems associated with the conduit/matrix flow regime under confined/unconfined conditions was developed. The new solver, NR1, is based on the Newton-Raphson method and requires derivative information from active MODFLOW packages. The derivative information is beyond that currently provided by the MODFLOW groundwater flow packages. Because of this new data requirement from the packages, NR1 and DCM could not be implemented as a self-contained package, and it was necessary to modify multiple packages. Therefore, a new MODFLOW variant, MODFLOW-DCM Version 2.0, was created.

The improved robustness of the new solver made it unnecessary to consider adaptive timestepping, which was originally in the Phase II project plan. In addition to the new solver and more robust formulation, MODFLOW-DCM Version 2.0 also

represents transition between turbulent and laminar flow. DCM Version 1.0 could only accommodate one flow regime or the other without providing for a transition between the two.

A new algorithm for simulation of dry cells was developed for DCM Version 1.0 and further refined in MODFLOW-DCM Version 2.0. The algorithm combines a new updating procedure for potentially dry cells with an upstream-weighted calculation of intercell conductances. In the new updating procedure, hydraulic head is never allowed to drop below the bottom elevation of a cell. If an outer iteration calculates a hydraulic head that is below the bottom elevation of a cell, the updated head for that cell is set equal to the arithmetic average of the previous head and the cell bottom. This procedure allows the head in a cell to become arbitrarily close to the cell bottom over the course of several iterations. However, the head will always be greater than the cell bottom, thus allowing the cell to remain active in the calculation.

It should be noted that MODFLOW-DCM Version 2.0 is currently limited to single-layer aquifers. A three-dimensional version of the MODFLOW-DCM would be required to model an aquifer with multiple layers with disparate properties.

Task 2. Barton Springs Demonstration Simulations.

The application of DCM to the Barton Springs segment of the Edwards Aquifer was initiated during Phase I of the karst modeling project. The Barton Springs model was completely revised in Phase II by incorporating site-specific groundwater hydraulic data and more detailed conduit characterization information. The model was successfully calibrated to hydraulic head and spring flows for steady and transient conditions. Sensitivities to major parameters were identified.

The Barton Springs segment of the Edwards Aquifer proved to be a challenging test site because of the large elevation changes and complex topography of the recharge zone. Accurate representation of the Edwards Aquifer recharge zone has proved to be problematic in past MODFLOW models because upgradient cells tend to dry out during periods of limited recharge. This tendency provided added motivation to resolving the dry-cell problem inherent in MODFLOW. As illustrated in the Barton Springs model results, MODFLOW-DCM successfully simulated the drying and rewetting of cells in the unconfined recharge zone.

Sensitivity analyses were performed to test the laminar/turbulent flow transition and the sensitivity to the exchange parameter. During periods of low flow, the turbulence model has only a minor effect on the simulated discharge. In periods of high discharge, the turbulence model reduces the peak discharge significantly. Model results indicate that the addition of the turbulence model results in an improved match to the dynamic spring hydrograph for Barton Springs. Sensitivity analysis indicated that the matrix/conduit exchange parameter α_0 was more important to transient simulations. Modeling results demonstrated that the exchange parameter α_0 can be tuned to better match dynamic spring flow.

Limited recharge during the 1950s led to the drought of record for south-central Texas. It was not possible to simulate this period because there is insufficient information on the recharge rates for that time. Therefore, for the purposes of this evaluation, hypothetical drought conditions were simulated for three test cases by starting with the calibrated steady-state model and then eliminating recharge for a 5-year period. Conduit elevation and pump rates were adjusted in the test cases.

Model results for the drought-period analysis highlighted the relative sensitivity of spring discharge to conduit elevation. This important outcome confirms that conduit elevations influence flow during low-flow conditions and suggests that the conduit elevations may be determined by model calibration during low-flow periods. Model results also indicated that spring discharge of less than 2 cfs would be realized for drought conditions when the aggregate pumping rate was increased by a factor of 4 to 20 cfs.

Although these simulations do not specifically represent the drought of the 1950s, they do accurately represent drought conditions with severity comparable to the record drought in terms of suspected recharge rates and spring discharge. The MODFLOW-DCM simulation of drought conditions appeared to better match hydraulic head and spring discharge rates than the existing BSEACD MODFLOW model, which is predicated on porous media flow concepts. As evidence of this capability, the BSEACD MODFLOW-DCM model was capable of simulating recharge/discharge for periods of both normal recharge and drought. This is an improvement over existing BSEACD models, which do not perform as well when attempting to match hydraulic head and spring discharge for both normal recharge and drought conditions with the same calibrated values.

Task 3. Floridan Aquifer Demonstration Simulations.

MODFLOW-DCM was applied to a site in the Floridan Aquifer to test the ability of MODFLOW-DCM to simulate large-flow karst systems with relatively high-matrix permeability. The Santa Fe River Sink/Rise system was selected as the Floridan Aquifer model site because there is extensive site characterization, tracer tests, and hydraulic testing data available. Although the scope of this task was predicated on the assumption that there was a viable MODFLOW model for the Floridan Aquifer demonstration site, it became apparent that the scale and resolution of existing MODFLOW models were inappropriate to evaluate MODFLOW-DCM. It was decided to retain the Santa Fe River Sink/Rise system as the Floridan Aquifer test site and develop a new MODFLOW model, however, because of the extensive hydrogeological information available. Similar to the BSEACD demonstration simulation, matching of model results to the physical system was evaluated in terms of hydraulic head, recharge rates, and spring discharge.

A base case model was developed to calibrate the MODFLOW-DCM model parameters so that the simulated discharge rates and hydraulic head values were consistent with observed values. The objective was to establish a base case model so that

the relative impact of various parameters on the Santa Fe River Sink/Rise system could be assessed using the MODFLOW-DCM package. The model was relatively easily calibrated to the observed data set. In general, the MODFLOW-DCM base case model performed well in simulating the dynamic hydraulic system observed at the Santa Fe River Sink/Rise system. Model performance was judged using head values and discharge rates observed during the 60-day study period. Calibration was easily achieved because conduit hydraulic conductivity is sensitive to the River Sink discharge rates, which were relatively well known. Secondly, hydraulic head of the diffuse continuum near the conduit is sensitive to the matrix/conduit exchange parameter. Having information of the diffuse head relative to conduit head during significant discharge events would allow for better resolution of the matrix/conduit exchange parameter. Limited diffuse head data near the conduit near the upgradient end of the hidden conduit in the Santa Fe River, however, precluded full evaluation of this relationship.

To investigate the sensitivity of the system to different model parameters, additional tests were performed. Three of these cases are reported here: (i) Case I — reduction of the conductivity of the hidden conduit from 1×10^8 to 5×10^7 ft/day; (ii) Case II — reduction of the diffuse conductivity by a factor of five; and (iii) Case III — reduction of the matrix/conduit exchange parameter, α_0 , from 1.0 to 0.01. Discharge simulated at the River Rise for all sensitivity cases was essentially the same as in the base case. Head elevations simulated in the confined zone were comparable to observed head values during low flow conditions for all simulations suggesting that local recharge conditions (i.e., thickness and extent of the Hawthorn confining layer) were well represented in the model. The head predicted near the River Rise was less than the observed head during low flow conditions, but reasonably matched peak flow.

Case I was developed to investigate the effect of reducing the hydraulic conductivity of the hidden conduit from 1×10^8 to 5×10^7 ft/day. Simulated heads at the calibration wells were not significantly different from the base case, however, simulated conduit head at the sink was significantly higher than the observed water levels.

Case III was developed to investigate the effect of reducing the matrix/conduit exchange parameter, α_0 , from 1.0 to 0.01. The reduction in the exchange parameter had the expected effect of decreasing the rate at which conduit water entered the diffuse continuum. This decrease resulted in less mounding of water in the diffuse continuum in the area proximal to the River Sink. Unfortunately, none of the calibration wells was located sufficiently close to the River Sink to allow refinement in prescribing the matrix/conduit exchange parameter most appropriate for the model. The performance at the other three calibration wells was not as good in Case III when compared with the base case, suggesting that a matrix/conduit exchange parameter greater than 0.01 is probably more representative of the modeled domain.

Modeling the Santa Fe River Sink/Rise system in the Floridan Aquifer demonstrated that MODFLOW-DCM reasonably replicated the hydraulic dynamic response of a karst aquifer with large spring discharge rates and high matrix permeability. In particular, it was shown that it is possible to infer conduit conductance by calibrating

to the water level elevation at the River Sink during intense recharge events. Similarly, it was demonstrated that it is reasonable to calibrate the matrix/conduit exchange parameter by observing diffuse head near the River Sink during intense recharge events.

Insight on a region greater than the Santa Fe River Sink/Rise system modeled area would be possible with a larger model, obviously, and a longer simulation period. Further improvement in the Santa Fe River Sink/Rise model can be made by:

- Coupling the local Santa Fe River Sink/Rise model with the regional SRWMD model so that the heads and fluxes across the shared boundaries are consistent. This enhancement would minimize the negative impact of prescribing the model boundaries as constant head, if the regional model accurately represents recharge in the confined zone of the UFA.
- Validating the model outputs with historical data collected from longer periods. When combined with more realistic boundary conditions, this enhancement would make the model more representative of the local hydraulic system, rather than being limited to representing the hydraulic response of the Sink/Rise system.
- Improving the model reliability by calibrating it with data from other locations within the model area, especially with respect to areas near the River Sink to allow refinement and greater evaluation of the matrix/conduit exchange parameter.

Subtask 4.1. Preparation of a GUI with Environmental Simulations International

The addition of a Groundwater Vistas GUI for MODFLOW-DCM was coordinated with Environmental Simulations, Inc. (ESI). SwRI provided specifications for the additional input data sets required for MODFLOW-DCM to ESI. Because of the necessity to develop a solver routine external to the standard MODFLOW package, it was not possible to strictly adhere to U.S. Geological Survey guidance standards that seek to retain all modifications to singular packages. The final product is a MODFLOW variant that includes modifications to all packages that incorporated nonlinear dependence on hydraulic head. Final implementation of the GUI was completed as part of a separate karst modeling project with the University of Florida (Hatfield¹⁵).

Subtask 4.2. Evaluation of the Costs and Benefits of Developing a Three-Dimensional MODFLOW-DCM.

The potential future development of a three-dimensional version of MODFLOW-DCM was assessed. It was decided that additional validation of the two-dimensional MODFLOW-DCM is needed before a decision on the development of a three-dimensional version should be considered. Additional validation of MODFLOW-DCM will be provided as the code is used after its release at the conclusion of Phase II. It was

¹⁵ Hatfield, K., "Model calibration" Personal communication, 2007.

therefore decided to not initiate development of a three-dimensional version of a conduit model during this phase of the karst modeling effort.

FUTURE DEVELOPMENT OF KARST MODELING TOOLS

Specification of model parameters is a challenging aspect of any groundwater modeling study. Explicit conduit models require additional parameters compared with conventional porous media groundwater models. Understanding conduit data requirements and methods for estimating conduit parameters from field data is one of the long-term (future) goals of the karst modeling project. Detailed case studies of multiple sites will be required to fully develop this topic. However, some preliminary understanding has emerged based on the numerical experiments and the initial experience with the MODFLOW-DCM variant applied to the Barton Springs segment of the Edwards Aquifer and the Santa Fe River Sink/Rise system of the Floridan Aquifer.

Interest has shifted from model development to model calibration and model parameter estimation. Identifying the backbone of the conduit network remains an important karst aquifer characterization requirement. Absence of this information is the most significant limitation in successfully applying the DCM model. Tracer tests provide a well-established method for identifying connectivity between recharge features and springs and are extremely valuable in developing a conceptual model for the conduit network. Major flow paths to springs corresponding to main conduits can often be identified from troughs in the potentiometric surface or from variations in water chemistry. The accuracy of this approach is sensitive to the density of monitoring wells in the vicinity of the conduit. If global quantities such as spring flows and large-scale averages of water levels are the only quantities of interest, then it may not be necessary to know the locations of conduits with high accuracy.

It is clear that the efficient and effective application of MODFLOW-DCM to karst aquifers will hinge on using better methods to calibrate karst aquifer models and estimate parameter values. Calibration is expected to be important for determining conduit properties such as conduit hydraulic conductivity, matrix/conduit exchange parameters, and the top and bottom elevations of conduits. For calibration to be effective, accurate records of recharge and spring flows are necessary. At the conclusion of Phase II of the karst modeling project, model calibration and parameter estimation are the most important factors for advancing the MODFLOW-DCM modeling approach. Development of advanced calibration and parameter estimation tools and techniques will allow for quicker and better focused karst aquifer characterization.

REFERENCES

- Banta, E.R. 2000. MODFLOW-2000, the U.S. Geological Survey Modular Ground-Water Model - Documentation of Packages for Simulating Evapotranspiration with a Segmented Function (ETS1) and Drains with Return Flow (DRT1): U.S. Geological Survey Open-File Report 00-466, 127 p.
- Bush, P.W. and R.H. Johnston. 1988. Ground-water hydraulics, regional flow, and ground-water development of the Floridan aquifer system in Florida and in parts of Georgia, South Carolina, and Alabama. USGS Professional Paper. Report P 1403-C. pp. C1-C80.
- Clark, W.E., R.H. Musgrave, C.G. Menke, and J.W. Cagle Jr. 1964. Water resources of Alachua, Bradford, Clay, and Union Counties, Florida. Florida Geological Survey Report of Investigation 35. 170p.
- Cooley, R.L. 1983. Some new procedures for numerical-solution of variably saturated flow problems. *Water Resources Research*, 19(5):1271–1285.
- Environmental Modeling Research Laboratory. 2006. GMS Version 6.0. Salt Lake City, Utah: Environmental Modeling Research Laboratory, Brigham Young University.
- Fisk, D.W. and J.C. Rosenau. 1977. Potentiometric surface of the Floridan aquifer in the Suwanee River Water Management District, north Florida, May, 1976. U.S. Geological Survey Water-Resources Investigations Open-File Report 77-1, 1 sheet.
- Ford, D.C. and P.W. Williams. 1989. Karst Geomorphology and Hydrology. Chapman and Hall. New York, NY. 601 p.
- Gale, S.J. 1984. The Hydraulics of Conduit Flow in Carbonate Aquifers. *Journal of Hydrology*, 70:309–327.
- Gordon, S.L. 1998. Surface and groundwater mixing in an unconfined karst aquifer, Ichetucknee River ground water basin, Florida. PhD dissertation. University of Florida.
- Grozos, M., R. Ceryak, D. Allison, R. Cooper, M. Weinberg, M. Macesich, M.M. Enright, and F. Rupert. 1992. Carbonate Units of the intermediate aquifer system in the Suwanee River Water Management District, Florida. Florida Geological Survey Open File Report No. 54.
- Halihan, T., J.M. Sharp, and R.E. Mace. 2000. Flow in the San Antonio Segment of the Edwards Aquifer: Matrix, Fractures, or Conduits? In *Groundwater Flow and Contaminant Transport in Carbonate Aquifers*. Edited by I.D. Sasowsky and C.M. Wicks. Rotterdam: Balkema.

- Hauwert, N.M., D.A. Johns, J.W. Sansom, and T.J. Aley. 2002. Groundwater tracking of the Barton Springs Edwards Aquifer, Travis and Hays Counties, Texas. *Gulf Coast Association of Geological Societies Transactions* 52. pp. 377—384.
- Hisert, R.A. 1994. A multiple tracer approach to determine the ground and surface water relationships in the western Santa Fe River, Columbia County, Florida. PhD Dissertation. University of Florida, Gainesville, Florida. 211 p.
- Hunn, J.D. and L.J. Slack. 1983. Water resources of the Santa Fe River basin, Florida. USGS Water-Resources Investigations Report 83-4075. 105 p.
- Hunt, B.B., B.A. Smith, J. Beery, D. Johns, and N. Hauwert. 2006. Summary of 2005 Groundwater Dye Tracing, Barton Springs Segment of the Edwards Aquifer, Hays and Travis Counties, Central Texas. BSEACD Report of Investigations 2006-0530. Barton Springs/Edwards Aquifer Conservation District. Austin, Texas.
- Jacobs, J.M. and S.R. Satti. 2001. Evaluation of reference crop evapotranspiration methodologies and AFSIRS crop water use simulation model. SJRWMD SJ2001-SP8. University of Florida. 122p.
- Jeannin, P.-Y. 2001. Modeling Flow in the Phreatic and Epiphreatic Karst Conduits in the Holloch Cave (Muotatal, Switzerland). *Water Resources Research*, 37:191—200.
- Martin, J.M. 2003. Quantification of the matrix hydraulic conductivity in the Santa Fe River Sink/Rise system with implications for the exchange of water between the matrix and conduits. MS Thesis. University of Florida. 80 p.
- Martin, J.B. and R.A. Dean. 1999. Temperature as a natural tracer of short residence times for ground water in karst aquifers. In: Palmer, A.N., M.V. Palmer, and I.D. Sasowsky Eds., *Karst Modeling*. Karst Waters Institute Special Publication. Vol. 5. pp 236—242.
- Martin, J.B. and R.A. Dean. 2001. Exchange of water between conduits and matrix in the Floridan Aquifer. *Chemical Geology*. Vol. 179. pp. 145—166.
- Martin, J.B. and E.J. Sreaton. 2001. Exchange of matrix and conduit water with examples from the Floridan Aquifer. In E.L. Kuniansky, Ed. USGS Karst Interest Group Proceedings. Water-Resources Investigations Report 01-4011. p. 38—44.
- Martin, J.M., E.J. Sreaton, and J.B. Martin. 2006. Monitoring well responses to karst conduit head fluctuations: Implications for fluid exchange and matrix transmissivity in the Floridan Aquifer. *Geological Society America Special Paper* 404. pp 209—217.
- McDonald, M.G., A.W. Harbaugh, B.R. Orr, and D.J. Ackerman. 1991. A method for converting no-flow cells to variable head cells for the U.S. Geological Survey modular

finite-difference ground-water flow model. U.S. Geological Survey Open File Report 91-536.

Mehl, S.W. and M.C. Hill. 2005. MODFLOW-2005, the U.S. Geological Survey modular ground-water model – documentation of shared node local grid refinement (LGR) and the Boundary Flow and Head (BFH) Package: U.S. Geological Survey Techniques and Methods 6-A16. 68 p.

Meyer, F.W. 1963. Reconnaissance of the geology and ground water resources of Columbia County, Florida. Florida Geological Survey. Report of Investigations No. 30.

Motz, L.H. 1995. North-central Florida regional ground-water investigation and flow model: Palatka, St. Johns River Water Management District Special Publication SJ95-Sp7. 255p.

Murdoch, J.W. 1996. Mechanics of Fluids. In *Marks' Standard Handbook for Mechanical Engineers, 10th Edition*. Edited by E.A. Avallone, and T. Baumeister III. New York: McGraw Hill.

Painter, S.L., A. Sun, and R.T. Green. 2006. Enhanced Characterization and Representation of Flow through Karst Aquifers. Final Report. Awwa Research Foundation. Project 2987.

Painter, S., J. Yefang, and A. Woodbury. 2006. Transmissivity estimation for highly heterogeneous aquifers: comparison of three methods applied to the Edwards Aquifer, Texas, USA. *Hydrology Journal*. July 29, 2006. DOI: 10.1007/s10040-006-0071-y.

Pinder, G.F., J.D. Bredehoeft, and H.H. Cooper, Jr. 1969. Determination of aquifer diffusivity from aquifer response to fluctuations in river stage: Water Resources Research. Vol. 5. pp. 850—855.

Planert, M. and J.W. Grubbs. 2004. Simulation of regional ground-water flow in the Suwannee River Basin, north-central Florida and south-central Georgia. USGS Open-File Report 2004-xxxx. 34 p. + attachments.

Puente, C. 1976. Statistical analysis of water-level, springflow, and streamflow data for the Edwards Aquifer in south-central Texas. U.S. Geological Survey Report. 58 p.

Puente, C. 1978. Method of estimating natural recharge to the Edwards Aquifer in the San Antonio area, Texas. U.S. Geological Survey Water Resources Investigations 78-10. 34 p.

Quinlan, J.F., and R.O. Ewers. 1989. Subsurface drainage in the Mammoth Cave area, in White, W.B., and White, E.L., eds., *Karst hydrology: Concepts from the Mammoth Cave area*: New York, Van Nostrand Reinhold, p. 65–103.

Saad, Y. 2003. Iterative Methods for Sparse Linear Systems. 2nd Edition. Society of Industrial and Applied Mathematics. Philadelphia, PA.

Scanlon, B.R., R.E. Mace, B. Smith, S. Hovorka, A.R. Dutton, and R. Reedy, 2001. *Groundwater Availability Modeling of the Barton Springs Segment of the Edwards Aquifer, Texas: Numerical Simulations Through 2050*. Austin, Texas. Bureau of Economic Geology.

Scanlon, B.R., R.E. Mace, M.E. Barrett, and B. Smith. 2003. Can We Simulate Regional Groundwater Flow in a Karst System Using Equivalent Porous Media Models? Case study, Barton Springs Edwards Aquifer, USA. *Journal of Hydrology*, 276:137–158.

Screaton, E., J.B. Martin, B. Ginn, and L. Smith. 2004. Conduit properties and karstification in the unconfined Floridan Aquifer. *Ground Water* 24(3). Pp. 338-346.

Sepúlveda, N. 2002. Simulation of ground-water flow in the intermediate and Floridan Aquifer systems in Peninsular Florida. USGS Water-Resources Investigations Report 02-4009. 130p.

Smith, B. and B. Hunt. 2004. Evaluation of the sustainable yield of the Barton Springs Segment of the Edwards Aquifer, Hays and Travis Counties, Central Texas. Barton Springs/Edwards Aquifer Conservation District. Austin, Texas.

Southeast Regional Climate Center, 2006. (<http://cirrus.dnr.state.sc.us/cgi-bin/serce/cliMAIN.pl?fl3956>).

Springer, G.S. 2004. A Pipe-Based, First Approach to Modeling Closed Conduit Flow in Caves. *Journal of Hydrology*. 289(1-4). Pp 178-189.

Sprouse, B.E. 2004. Chemical and isotopic evidence for exchange of water between conduit and matrix in a karst aquifer: an example from the Santa Fe River Sink/Rise System. MS Thesis. University of Florida. Gainesville, Florida. 75p.

Thorntwaite, C.W. 1948. An approach toward a rational classification of climate. *Geographical Review*. Vol. 38. pp. 53-94.

Thorntwaite, C.W. and J.R. Mather. 1957. Instructions and tables for computing potential evapotranspiration and the water balance. Drexel Institute of Technology. *Publications in Climatology*. Vol. X. No. 3. Centerton, New Jersey. 311 p.

Upchurch, S.B. 2002. Hydrogeochemistry of a karst escarpment. J.B. Martin, C.M. Wicks, and I.D. Sasowsky, Eds. Proceedings of the symposium Karst Frontiers Florida and Related Environments. Karst Waters Institute. Special Publication 7. pp. 73-75.

Wolfram Research, Inc. 2005. Mathematica, Version 5.2. Champaign, IL.

APPENDIX A: INPUT INSTRUCTIONS FOR THE MODFLOW-DCM PACKAGE

A.1 Name File

To activate the DCM package, the following line needs to be added to a MODFLOW name file

```
DCM Nunit Fname
```

where Nunit is the Fortran unit to be used for file I/O and Fname is the name of the I/O file. Note that LPF, DCM, and BCF are all flow solvers and thus cannot be used simultaneously.

DCM is designed to work with a new Newton-Raphson solver NR1. The NR1 solver will be activated automatically. Other MODFLOW solvers (i.e., PCG2, GMG, DE4, SIP, etc) should not be included in the name file.

A.2 DCM Input Parameters

The structure of the DCM input file follows that of LPF. Because DCM only allows one diffuse layer and one conduit layer, vertical conductivity and vertical anisotropy parameters are not needed and are not recognized. In addition, LPF parameters related to drying and rewetting are not needed in DCM and should not be entered. DCM requires one additional global variable and two additional layer variables that are not required for LPF.

Many instructions that appear below are copied from the LPF instruction. The changes and instructions specific to DCM are highlighted in blue. Note that DCM requires input for two layers. Layer 1 represents the conduit and Layer 2 the diffuse (matrix) system.

0. [#Text]

Item 0 is optional—“#” must be in Column 1. Item 0 can be repeated multiple times.

1. ILPFCB HDRY NPDCM
2. LAYTYP(NLAY)
3. LAYAVG(NLAY)
4. CHANI(NLAY)
5. FLOWLAW
6. [PARNAM PARTY Parval NCLU]
7. [Layer Mltarr Zonarr IZ]

Each repetition of Item 7 is called a parameter cluster. Repeat Item 7 NCLU times.

Repeat Items 6—7 for each parameter to be defined (that is, NPDCM times).

A subset of the following two-dimensional variables is used to describe each layer. All the variables that apply to Layer 1 are read first, followed by Layer 2. If a variable is not required due to simulation options (for example, SS and SY for a completely steady-state simulation), then it must be omitted from the input file.

These variables are either read by the array-reading utility module, U2DREL, or they are defined through parameters. If a variable is defined through parameters, then the variable itself is not read; however, a single record containing a print code is read in place of the array control record. The print code determines the format for printing the values of the variable as defined by parameters. The print codes are the same as those used in an array control record. If any parameters of a given type are used, parameters must be used to define the corresponding variable for all layers in the model.

- | | |
|-----------------------|--|
| 8. HK(NCOL,NROW) | If there are any HK parameters, read only a print code. |
| 9. [HANI(NCOL,NROW)] | Include Item 9 only if CHANI is less than or equal to 0. If there are any HANI parameters, read only a print code. |
| 10. [CRTG(NCOL,NROW)] | Include Item 10 only for Layer 1 when FLOWLAW is equal to 1. If there are no CRTG parameters, read only a print code. |
| 11 [SS(NCOL,NROW)] | Include Item 11 only if at least one stress period is transient. If there are any SS parameters, read only a print code. |
| 12. [SY(NCOL,NROW)] | Include Item 12 only if at least one stress period is transient and LAYTYP is not 0. If there are any SY parameters, read only a print code. |
| 13. CDEX(NCOL,NROW) | Read Item 13 only for Layer 1. If there are any CDEX parameters, read only a print code. |

ILPFCB – is a flag and a unit number.

If $ILPFCB > 0$, it is the unit number to which cell-by-cell flow terms will be written when “SAVE BUDGET” or a nonzero value for ICBCFL is specified in Output Control. The terms that are saved are storage, constant-head flow, and flow between adjacent cells.

If $ILPFCB = 0$, cell-by-cell flow terms will not be written.

If $ILPFCB < 0$, cell-by-cell flow for constant-head cells will be written in the listing file when “SAVE BUDGET” or a nonzero value for ICBCFL is specified in Output Control. Cell-by-cell flow to storage and between adjacent cells will not be written to any file.

HDRY – is not used in DCM, but should be present in the input.

NPDCM – is the number of parameters.

LAYTYP – indicates the layer type. Enter one value for each layer. Value 0 represents confined layer type, and nonzero value represents unconfined layer type.

LAYAVG – indicates the method for calculating intercell conductances. One value is needed for each layer.

0 – harmonic mean

1 – logarithmic mean

For a detailed description of the averaging methods, please refer to the User's Manual for MODFLOW2000. [In DCM, these averaging methods apply only to the hydraulic conductivity. Upstream weighting of the saturated thickness is used in DCM to calculate the intercell conductances.](#)

CHANI – contains a value for each layer that is a flag or the horizontal anisotropy. If CHANI is less than or equal to 0, then variable HANI defines horizontal anisotropy. If CHANI is greater than 0, then CHANI is the horizontal anisotropy for the entire layer, and HANI is not read. If any HANI parameters are used, CHANI for all layers must be less than or equal to 0.

[FLOWLAW – indicates the governing flow equation for conduits. Enter 0 for laminar flow \(Darcy's equation\) and 1 for turbulent flow \(Darcy-Weisbach equation\). The diffuse system is always modeled with Darcy's equation.](#)

PARNAM – is the name of a parameter to be defined. This name can consist of 1 to 10 characters and is not case sensitive. That is, any combination of the same characters with different case will be equivalent.

PARTYP – is the type of parameter to be defined. For the DCM Package, the allowed parameter types are

HK – defines variable HK, horizontal hydraulic conductivity

HANI – defines variable HANI, horizontal anisotropy

SS – defines variable Ss, the specific storage

SY – defines variable Sy, the specific yield

[CDEX – defines variable \$\alpha\$, the linear exchange term between the conduit layer and the diffuse matrix layer. Enter for Layer 1.](#)

[CRTG – defines the critical gradient for the onset of turbulent flow in the conduit. Enter for Layer 1 if the turbulent flow law is chosen.](#)

PARVAL – is the parameter value.

NCLU – is the number of clusters required to define the parameter. Each repetition of Item 7 is a cluster (variables Layer, Mltarr, Zonarr, and IZ). There is usually only one cluster for each layer that is associated with a parameter.

LAYER – is the layer number to which a cluster definition applies.

MLTARR – is the name of the multiplier array to be used to define variable values that are associated with a parameter. The name “NONE” means that there is no multiplier array, and the variable values will be set equal to PARVAL.

ZONARR – is the name of the zone array to be used to define the cells that are associated with a parameter. The name “ALL” means that there is no zone array, and all cells in the specified layer are part of the parameter.

IZ – is up to 10 zone numbers (separated by spaces) that define the cells that are associated with a parameter. These values are not used if ZONARR is specified as “ALL”. Values can be positive or negative, but 0 is not allowed. The end of the line, a zero value, or a nonnumeric entry terminates the list of values.

HK– is the hydraulic conductivity along rows. HK is multiplied by horizontal anisotropy (see CHANI and HANI) to obtain hydraulic conductivity along columns.

HANI – is the ratio of hydraulic conductivity along columns to hydraulic conductivity along rows, where HK of Item 10 specifies the hydraulic conductivity along rows. Thus, the hydraulic conductivity along columns is the product of the values in HK and HANI. Read only if CHANI is not equal to 0.

CRTG – is the critical gradient for the onset of turbulence. Read only for Layer 1 and only if FLOWLAW > 1.

SS – is specific storage. Read only for a transient simulation (at least one transient stress period).

SY – is specific yield. Read only for a transient simulation (at least one transient stress period) and if the layer is convertible (LAYTYP is not 0).

CDEX – is the exchange term for flow between conduit and matrix system (α_0). Enter for Layer 1 only.

A.3 Example Input File

The following shows an example of DCM input file, DCM File,

```
#Example1 DCM package
50 -1E+30 3 Item 1: ILPFCB HDRY NPLPF
00 Item 2: LAYTYP
00 Item 3: LAYAVG
11 Item 4: CHANI
0 Item 5: FLOWLAW
HK_0 HK 1 2 Item 6: PARNAM PARTY PARVAL NCLU
1 HK1 ZHK1 999 Item 7: LAYER MARRAY ZARRAY [zones]
2 HK2 ZHK2 999
SS_0 SS 1 2 Item 6: PARNAM PARTY PARVAL NCLU
1 SS1 ZSS1 999 Item 7: LAYER MARRAY ZARRAY [zones]
2 SS2 ZSS2 999
CDEX_0 CDEX 1 1 Item 6: PARNAM PARTY PARVAL NCLU
1 CDEX1 ZCDEX1 999 Item 7: LAYER MARRAY ZARRAY [zones]
31 1(20G14.0) -1 10: HK of layer 1
31 1(20G14.0) -1 11: HANI of layer 1
31 1(20G14.0) -1 12: Ss of layer 1
31 1(20G14.0) -1 13: CDEX of layer 1
31 1(20G14.0) -1 10: HK of layer 2
31 1(20G14.0) -1 11: HANI of layer 2
31 1(20G14.0) -1 12: Ss of layer 2
```

The values of parameters are defined in the associated multiplier file and zone file, respectively.

Multiplier file,

```
#Example1 Multiplier file
5
HK1
Constant 0.50 4: HK Multiplier array for layer 1
HK2
Constant 0.10 4: HK Multiplier array for layer 2
SS1
Constant .0005 4: Ss Multiplier array for layer 1
SS2
Constant .0001 4: Ss Multiplier array for layer 2
CDEX1
Constant 0.0001 4: CDEX Multiplier array for layer 1
```

Zone file,

```
#Example1 Zone file
7
ZHK1
Constant 999 HK zone array for layer 1
ZHK2
Constant 999 HK zone array for layer 2
ZSS1
```

| | | |
|--------------------|-----|-----------------------------|
| Constant ZSS2 | 999 | SS zone array for layer 1 |
| Constant ZSY1 | 999 | SS zone array for layer 2 |
| Constant ZSY2 | 999 | SY zone array for layer 1 |
| Constant ZCDEX1 | 999 | SY zone array for layer 2 |
| Constant | 999 | CDEX zone array for layer 1 |

A.4 NR1 Solver Input

The NR1 solver input is read from a file called nr1in.dat. The file must be named nr1in.dat. If the file is not present, default values will be used for all input parameters. The NR1 input is given below.

1. ITMXO HTOL
2. ATYPE LEVEL NVECTORS DETAIL
3. ITMAXI R2TOL RXTOL SXTOL

Definitions for the input parameters follow.

ITMAX0 – is the maximum number of outer iterations.

HTOL – is the head tolerance used to define convergence in the outer iterations.

ATYPE – is an integer-controlling selection of accelerator in a preconditioned conjugate gradient linear solver. Currently, the only allowed value is 4, which corresponds to the bi-conjugate gradient stabilized method. Alternative values may be available in future versions.

LEVEL – is the level of infill allowed in the incomplete lower-upper decomposition used for preconditioning. Recommended values are 1 or 0.

NVECTORS – is read but not currently used.

DETAIL – is an integer controlling output from the linear solver. Enter 0 for no output, 1 for summary output, and 2 for residual information at each inner iteration. Output is written to the file NR1OUT.DAT.

ITMAXI – is the maximum number of inner iterations.

R2TOL – is a convergence criterion based on the Euclidian norm of the residual.

RXTOL – is a convergence criterion based on the maximum residual.

SXTOL – is a convergence criterion based on the maximum scaled solution update.